A TWO-PHASE CLOSED THERMOSYPHON AT LOW TEMPERATURE

by

Syed Hasan Zahir

A thesis submitted to the
Faculty of Science and Engineering
of the University of Ottawa
in partial fulfilment of the requirements for
the degree of
MASTER OF APPLIED SCIENCE
in Mechanical Engineering

November, 1972

ABSTRACT

A two-phase closed thermosyphon which consists of a sealed tube enclosing a certain amount of fluid, transfers thermal energy from one place to another by means of boiling and condensation phenomena. The heated section is located below the cooled section to utilize gravity for condensate return. Other body force fields may also be used, such as centrifugal force in the case of rotating thermosyphons. The two-phase system provides a very high thermal conductivity several orders of magnitude higher than that of a solid conductor. The two-phase system being almost unidirectional can achieve a negative thermal storage in permafrost over a one-year cycle. For the stability of structure foundations in permafrost regions, it is essential to maintain the ground in a frozen state. Attempts have been made previously to use such a device but the effects of various parameters on the behaviour of this system around freezing conditions have not yet been studied.

In the present study an experimental investigation into the performance of a two-phase closed thermosyphon with particular attention to low temperature operation ($20^{o}F$ to $40^{o}F$) was made. Freon-11 was used as the working fluid. The effects of heat flux, quantity of fluid, mean operating pressure, and heated length-cooled length ratio on heat transfer coefficient were studied. An increase in pressure gave significant rise to the heat transfer coefficient, whereas

the increase in heated length-cooled length ratio had the reverse effect. The effect of quantity of working fluid, beyond a certain minimum amount, was insignificant. Within the required range of operating temperature, no other experimental results were available with which the present findings could be compared. A theoretical relationship for heat transfer rate was found to be in good agreement.

ACKNOWLEDGMENT

My sincere gratitude is due to Dr. Y. Lee, under whose supervision this project was carried out. His constant encouragement, critical discussions and valuable suggestions at every stage of the work are highly appreciated.

The partial financial support of the Defence Research Board of Canada under Grant No. 951196 is gratefully acknowledged.

Many thanks to the technical staff, Department of Mechanical Engineering, who helped for the completion of this project. Special thanks are due to Mrs. W. Storto for typing this thesis.

The author would not forget to acknowledge his wife, Shahnaz Zahir, for her great perseverance and encouragement at all steps.

CONTENTS

LIST OF TABLES

LIST OF FIGURES

NOMENCLATURE

A,B	defined quantities (Eqn. 4.1)
C_p	specific heat at constant pressure, of the working fluid in the liquid phase
D	inside diameter of the thermosyphon tube
g	gravitational acceleration
h	heat transfer coefficient
h_{fg}	latent heat of evaporation of the working fluid
k	thermal conductivity of the working fluid in the liquid phase
L	length
L^+	heated length-cooled length ratio, (L_h/L_c)
p	saturation pressure inside thermosyphon tube
q	heat flux
R	inner radius of thermosyphon tube
S	entropy
T	temperature
V^+	dimensionless volume of the working fluid in the thermosyphon (fluid volume/total volume)
Y_i'	dimensionless thickness of condensate film
Nu	Nusselt number $(h.D/k)$
Pr	Prandtl number $(C_p.\mu/k)$
Gr	Grashof number $(\rho^2 g\theta\beta D^3/\mu^2)$
Ra	Rayleigh number $(Gr.Pr)$

Greek Letter Symbols

β	coefficient of thermal expansion
δ	liquid film thickness at the lower end of the condensing section
μ	viscosity of the working fluid in liquid phase
ρ	density of the working fluid in liquid phase
θ	overall temperature difference ($T_h - T_c$)

Subscripts

b	boiling
c	cooled, condensing or average temperature in condensing section
d	diameter
h	heated or average temperature in heated section
s	saturation
v	vapor core
w	wall
NU	Nusselt

CHAPTER I

INTRODUCTION

Heat transfer processes play an important role in modern engineering achievements. For over a half century, serious and systematic investigations have been carried out to search for the most efficient, economical, and suitable system of transferring thermal energy from one place to another, and much progress has been made. 'Thermosyphons' and 'heat pipes' have come up as devices for such purposes. Their major applications are in various fields. Some relevant and possible applications are:

to transfer the heat energy from the core of the reactor of a nuclear power station for producing electrical power,

to solve the problem of cooling the gas turbine rotor blades,

to preserve permafrost under building foundations in such places as the Canadian North,

to decrease the heat sink temperature of a heat engine, producing a significant thermal efficiency gain,

to serve as a thermal rectifier for maintaining a desired temperature at a particular place,

to connect the hot gas exhaust manifold of an automobile engine to heat rejection fins inside the car, thus avoiding a water circulation pump,

to prevent icing on navigation buoys, using the heat of the sea to de-ice the superstructure, and similar other utilizations.

A tube partially filled with a working fluid, used for transporting thermal energy from one end to another, can prove to be several hundred times more effective than the best metallic conductor of the same geometry. Both devices, 'Thermosyphons' and 'Heat pipes', have taken advantage of the above mentioned fact.

A 'Thermosyphon' is a simple and inexpensive device which can transfer heat, mass, and momentum by utilizing buoyancy forces on a fluid contained in a vessel. For the circulation of fluid it is essential to have a force field, which may be gravitational or centrifugal, acting on the fluid of variable density. The density-change is caused by heat transfer alone, without the use of any mechanical power. Under steady state conditions, the potential and kinetic energies within the thermosyphons remain constant.

A 'Heat pipe', on the other hand, consists of a closed outer shell, a porous wick and a working fluid. It transfers thermal energy, relying on evaporation, condensation and surface tension characteristics of the working fluid. The internal wick brings the condensate back to the evaporator section by capillary action, while in a thermosyphon, there is no other component inside the tube and the condensate comes back to the evaporator under the gravitational or centrifugal forces.

The practical application of a thermosyphon was first made by Schmidt (1), for cooling down the rotor blades of a gas turbine. Later on, this system was found suitable for various applications and a detailed study was carried out by Davies and Morris (2,3), followed by Mital (4). It can be classified, depending on certain characteristics, as outlined below:

1. The nature of boundaries
    a) Open thermosyphon
    b) Closed thermosyphon
2. The nature of force field
    a) Gravitational
    b) Centrifugal
3. The number of phases present
    a) Single phase
    b) Two phase
4. The regime of heat transfer
    a) Free convection
    b) Mixed convection

An open thermosyphon (Fig. 1.1a) consists of a tube, having one end sealed and the other opening into a reservoir of the coolant, from which the heat is removed. It exactly resembles the fins provided for cooling down an I.C. engine. Circulation of the fluid in the tube and the reservoir maintain the heat transfer.

A closed thermosyphon consists of a sealed tube, enclosing a fixed quantity of fluid which plays the predominant role in transporting thermal energy from one end to another. In both the open and closed systems, the tube axis is parallel to the direction of the acting body force, which is earth's gravitational field if used in static form. When the system is part of a rotating body, as for instance in the turbine rotor application, the centrifugal body force predominates and it is generally several thousand times that of the static gravitational field. If the fluid used remains either in liquid or gaseous form during the operation, the system is called a single-phase closed thermosyphon and promotes the pure free convection mode of heat transfer. Fig. 1.1b shows the direction of circulation of the fluid.

A two-phase closed thermosyphon (Fig. 1.1c) works on the principle of boiling and condensing phenomena and the tube is partially filled with the working fluid. The heat transfer along the thermosyphon tube takes place by the process of boiling, vapor flow and condensation. It employs the gravity or centrifugal force for bringing the condensate back to the heat input section. In an open or single-phase closed thermosyphon the mixing of opposite streams of fluid restricts the flow and reduces the rate of heat transfer, as reported by Martin and Cohen (5); whereas this deleterious effect of the opposing circulation in the cold end of the free convection system is replaced by the very high heat transfer rates possible with condensing vapors.

This two-phase system does not require any pump or compressor and can work as a thermal rectifier due to its unidirectional high heat transfer capability. The pressure inside the thermosyphon tube corresponds to the saturation temperature of fluid which in turn depends on the condensing and boiling temperatures. The tube has to be perfectly leak proof and be able to maintain the purity of the fluid used. The boiling, vapor formation and condensation phenomena in a thermosyphon are highly complex, and the only acceptable theoretical correlation available is that given by Mital (4). Still due to its simple structure, easy installation and highly efficient heat transporting quality, the two-phase closed thermosyphon may have a wide range of applications. Currently more attention is being paid towards this device. The complications with the investigations are chiefly due to the large number of independent variables.

The objective of the present study was to carry out an experimental investigation into the performance of a two-phase closed thermosyphon, operated in low temperature range (of the order of 20° to 40°F). The main aim is to achieve an optimum practical solution to the problem of preserving permafrost in the Canadian northland. A laboratory apparatus was used to investigate the effects of the following parameters on the heat transfer coefficient: a) heat flux; b) quantity of working fluid (Freon-11); c) heated length-cooled length ratio; d) variable operating pressure and e) constant operating pressure.

CHAPTER II

LITERATURE SURVEY

From the basic concept of natural convection, the idea of transporting a large amount of thermal energy from one location to another was first applied by Schmidt (1) during the Second World War. He applied this idea for cooling down gas turbine rotor blades, having inside radial holes, closed at one end and opened at the other forming an open thermosyphon. Since that time the thermosyphon system has been a subject of great interest and many investigators (2-11) have worked on open and closed thermosyphons, utilizing single-phase of fluid. But very little progress has been achieved regarding two-phase closed thermosyphon, probably due to great complications in its analysis, whereas extensive research work has been carried out on the system known as 'Heat pipes' (12-19) which were mainly developed for use in zero gravity.

To earlier investigators, the open system had been more attractive, because it was generally capable of producing relatively high heat transfer rates, as for example, to expel large amounts of energy quickly from a nuclear reactor in case of emergency. Lighthill (6) theoretically examined the flow regimes existing in an open thermosyphon. Martin and Cohen (5) have reported that the interface between the hot and cold fluid streams moving in opposite directions, decreases the heat transfer rate significantly.

Bayley and Lock (7) conducted a theoretical and experimental investigation dealing with the general study of the behavior of a single-phase closed thermosyphon for various flow regimes. Air, water, ethylene glycol, and glycerine were used as the working fluids to find the effect of physical properties of the convecting medium. They studied the effects of various parameters and observed that the effect of tube geometry (length-diameter ratio L_h/D) was very little for $L_h/D < 7.5$, but was significantly higher for $L_h/D > 11.25$ in reducing the value of $(t_d)_C^H$ (as defined by Bayley and Lock (7)) due to change from laminar to turbulent flow. Japikse, Jallouk and Winter (9), and Evarrat (10) also carried out similar investigations and reported that their results were in good agreement with that of Bayley and Lock (7). In a recent study of heat transfer characteristics of a liquid-metal filled closed thermosyphon, Pucci and Gerretsen (11) used two geometrically similar apparatuses. Experiments on both were conducted with water, mercury and sodium-potassium eutectic (NaK 56/44) as the working fluids. The energy and temperature distribution, while using water, were quite similar for the constant hot wall temperature as well as uniform heat flux cases, whereas they were different in case of liquid metals. Their results, giving the variation of Nu_d versus $t_d = Ra \times D/L_h$, were in good agreement with those of Bayley and Lock (7).

Cohen and Bayley (20) in pursuance to achieve a better solution of the heat transfer problems of liquid cooled

gas turbine blades, came out with the two-phase closed thermosyphon as the most suitable system. They performed a number of experiments using both static and rotating tubes. With water as the enclosed coolant, they noted that the heat transfer from the heated to the cooled end was independent of the quantity of fluid inside the thermosyphon, until this quantity was reduced to one percent. From the static rig experiment they observed very little difference in heat flow rate whether the heated surface was submerged or merely covered by a film of liquid, and a criterion for the maximum rate of heat flow was determined. The effect of increase in tube diameter and saturation pressure was to raise the heat transfer coefficient. In addition to distilled water they also used the organic liquids, butyl alcohol and chlorobenzene, but found them quite unsuitable due to their low latent heats and low thermal conductivities.

Schmidt (21) in a similar approach towards the problem of cooling the gas turbine blades, experimented with the fluids near their critical states. At this state, the coefficient of thermal expansion increases considerably while the viscosity of all liquids has its lowest possible value, both resulting in high convection currents and high Rayleigh number. For studying the behavior of such an application he used a vertical tube with critical quantity of fluid, heated below and cooled above, at the critical operating temperature and found that the apparent heat conductivity of

the fluid reaches values of 4,000 times that of a solid copper rod of the same outer diameter. Bewilogua and Knoner (22) used this two-phase system as a nitrogen cryostat for operation in the horizontal reaction channel and found it very suitable. Bewilogua, Knoner and Kappler (23) utilized this system for pre-cooling an apparatus, which conventionally would have required a very large quantity of liquid refrigerant in reducing the temperature of the apparatus down to about $4^{o}K$.

Long (24) used this system to preserve the permafrost under building foundations in Alaska, but did not pay much attention to the effect of various parameters governing the heat transfer characteristics of the system. Koh, Sparrow and Hartnett (25) found that in laminar film condensation of the two-phase flow, shear at the liquid-vapor interface is negligible for Prandtl numbers of ten and higher and is quite small even for Pr = 1.

Recently the literature (26-29) reported the effects of various parameters of the performance of two-phase closed thermosyphons. Larkin (28) observed that the overall heat transfer coefficient increased with tube diameter but was not very sensitive to heat flux, heated length-cooled length ratio and the depth of working fluid. Using Freon-11, he expected better heat transfer results than water, if operated at temperatures below $80^{o}F$. Lee and Mital (29) found good agreement between their theoretical analysis and the experimental

results. In their investigations, they observed that the heat transfer coefficient was independent of the quantity of working fluid above a certain amount, increased with pressure, but had a reverse trend with increase in heated length-cooled length ratio.

It may be noted from the above review that the effects of various parameters on the performance of a two-phase closed thermosyphon at low operating temperature have not yet been studied, which might be very helpful in finding a suitable means of preserving permafrost in the Arctic region.

CHAPTER III

EXPERIMENTAL STUDIES

Experimental details for the investigation of the heat transfer characteristics of two-phase closed thermosyphon at low temperatures are described through the following:

3.1 General set-up

3.2 Test section - the thermosyphon

3.3 Cooling system

3.4 Instrumentation and control

3.5 Choice of a working fluid

3.6 Procedure

3.7 Data reduction

3.1 General set-up

The test thermosyphon was designed for a maximum of 10 kw thermal energy transfer. It consisted of three sections; the lower, as heated length, comprising of five coiled heaters in series, the middle as an adiabatic length, and the upper as cooled length having five cooling jackets.

The heated section was supplied with electrical power from 208 V, 70 A main, through a powerstat rated at 13.4 KVA at 240 V. A current transformer (General Electric Co., type JP 1, with ratio provisions 10:5 to 1000:5) was

used in line and the power was measured by means of an ammeter (0-5 amps) and a voltmeter (0-10, 25, 100, 250, 1000 V ranges). Two switch boxes (Hampden Ltd., 600 V - 3Ø - 70A) were used to serve as six terminals of the heaters. This facilitated the changing of the heated length, simply by plugging in the required terminals. Fig. 3.1 illustrates the overall set-up and Fig. 3.2 shows the circuit diagram for the heating unit.

In addition to the main heaters, a guard heater (Fig.3.3) was provided to minimize the heat loss, if any, through the insulation.

The cooled section consisted of five cooling jackets. Each jacket was separately connected to the main supply from the cooling system, through an orifice meter for flow measurement and a control valve to maintain a uniform temperature throughout the cooled length. Coolant used was a mixture of ethylene glycol and water, with 1:1 ratio, decreasing the freezing point to $-30^{\circ}F$. The cooling system is described later in Section 3.3. The five calibrated orifice meters were connected to respective U-tube mercury manometers. Fig. 3.4 is a typical calibration chart for the measuring orifice.

The exit pipe carrying the coolant, before going to the cooling system, was connected to a steel tank containing four immersion heaters of 10 kw capacity. These heaters served dual purposes. One, as a stand-by for the cooling

system, in case the hot gas bypass arrangement of the cooling system failed, and the second to control the coolant temperature. The heaters were separately connected through variacs to 208 V main. This provided controlled variation of the coolant temperature in the test section, required for constant pressure operation of the thermosyphon.

All the Iron-Constanton thermocouples connected to the thermosyphon tube were recorded by the Data Acquisition System (Hewlett Packard 2010 K), while a potentiometer (Leeds and Northrup 8686 millivolt potentiometer) measured the Copper-Constanton thermocouples.

3.2 Test section - the test thermosyphon

The test thermosyphon was made of copper tube 1-1/4" nominal size, 72" in length with O.D. 1.66" and wall thickness 0.194". Twelve grooves were made longitudinally to accommodate Iron-Constanton thermocouples for the measurement of wall temperatures. The grooves were spaced uniformly around the circumference as shown in Fig. 3.5. The thermocouples, insulated with magnesia and sheathed in stainless steel tube of 0.032" O.D., had on one end a male connection and the other grounded. They were embedded in the grooves with the help of copper strips and white babbit metal solder. A finished copper tube sample is shown in Fig. 3.6.

At the top end, the thermocouples were sheathed in teflon spaghetti tubing, 0.053" I.D., 0.012" wall thickness,

and supported on a brass disc (Fig. 3.7), covered under plexiglass to hold them in position and to avoid sharp bends. All the thermocouples with their extension were carried in a plexiglass pipe to the Data Acquisition System.

The thermosyphon was connected to a vacuum pump, pressure gauge, manometer, and the charging funnel, through a 1/2" O.D. copper tube protruding out of the top end. Swagelok fittings, Whitey valves, and Vacuum Tygon tubing with inserts were used, so as to provide good vacuum connections. A thermocouple probe, to measure the vapor core temperatures, was made of a stainless steel tubing (AISI Type 304) O.D. 1/4" and I.D. 0.18". It consisted of eight thermocouple junctions at 6" apart. One end of the tubing was vacuum sealed and all the thermocouple wires were taken out from the other end as shown in Fig. 3.8. This probe was inserted up to 42" from the top end, inside the thermosyphon tube. It was held vertical with the help of a reducing union whose one end gripped the probe tightly and the other was connected to the protruding copper tube. The annular space (1/16") between the probe and the protruding copper tube was sufficient for charging the fluid.

The thermosyphon tube had heat input in the lower 30" of length, heat output in the upper 30" of length, and the middle 12" was an adiabatic section.

The heat output section consisted of five cooling jackets. Each one was 6" in length and made from 3-1/2" N.S. copper pipe of O.D. 3.63" and wall thickness 0.1", with ends

closed by welding 1/4" thick brass sheet. The end walls of the jackets contained n-butane O'rings to prevent leakage. After fixing the thermocouples of the thermosyphon tube on the brass disc, as described earlier, an asbestos disc was placed and the jackets were slid over the main tube. The O'rings provided tight seal compartments. The whole assembly of cooling jackets were insulated by 1-1/2" fiberglas and held in position by clamps.

The 12" adiabatic section was insulted by 2" thick fiberglas. This section was provided with a view to keeping the heated and cooled zones apart, maintaining 1:1 ratio between the heated length and the cooled length, and to give a close similarity to the practical applications of the thermosyphon.

The heat input section consisted of five coiled heaters, each 6" in axial length. 10 AWG Chromel-A-Nichrome wire insulated with ceramic beads (Leeds and Northrup No. STD-715 Fish-Spine Insulators, 0.26" O.D., 0.152" I.D.) was wound around the main tube to form coiled heaters. Each heater was of resistance 0.8 ohms and could generate thermal energy of 2 kw at 208 V. The heaters were connected in series and the six terminals were lead to the switch boxes (Fig. 3.2). The heaters were held in the required position by two asbestos discs at both ends and an asbestos tape of 0.25" thickness was wound over the heaters. Further a 3-1/2" thick pipe insulation (2" asbestos and 1-1/2" Newtherm insulations) covered the wrapped heaters. A ceramic insulated 15 AWG Chromel 'A' wire was wound over this assembly to form a guard heater, which was finally insulated with a 2" thick fiberglas,

resulting in a heated length assembly of 12" dia. and 30" length, Fig. 3.9. Two Iron-Constanton thermocouples were embedded in the inner insulation, to sense the temperature difference and actuate the Achromag relay (Model 370) connecting the guard heater to the 115 V main supply. An Iron-Constanton thermocouple, to measure the boiling liquid temperature at the bottom of the main tube, was soldered to the screw fitting at the bottom plug end.

3.3 Cooling system

A 5 H.P. refrigeration unit, with F-12 as refrigerant, was used as a cooling system. If operated at low load it could result in coil icing and compressor tripping. This can be explained by the T-S diagram as shown in Fig. 3.10(a). Let 'm' be the mass of refrigerant flowing in the circuit. As the load in the evaporator decreases, only a fraction m_1 of $m(=m_1 + m_2)$ enters the compressor in gaseous state while m_2 remains as liquid in the suction accumulation. This results in a reduced load on the condenser, consequently lowering down the refrigerant's temperature at the outlet of the condenser. The expansion valve being fixed for a particular pressure ratio will reduce the pressure of refrigerant in the evaporator, that is, the suction pressure (Fig. 3.10(a)). A continuation of the above, results in lowering the suction pressure below the recommended value (5 psi for this compressor) and ultimately trips off the compressor.

This system was redesigned to work continuously, Fig. 3.10(b), irrespective of the heating load from the test section. This was accomplished by providing (1) a hot gas discharge bypass in the refrigerant circuit and (2) a 1.5 kw immersion heater in the heating load circuit. The bypass valve was set to operate as the suction pressure dropped below 10 psi, a sufficiently safe limit to keep it more than the short cycling condition (5 psi). Fig. 3.11 illustrates the system circuit diagram.

From the compressor discharge line hot gas was tapped out to pass through the Sporlan discharge bypass valve and was allowed to mix with the liquid-vapor mixture tapped through the desuperheating thermostatic expansion valve. Both the fluids were admitted, through a Tee connection, to flow against the flow direction of the suction gas before going to the suction accumulator. The thermostatic expansion valve bulb was fixed downstream of the accumulator, which was placed on the suction side just before the compressor. The external equalizer connecting the suction line to the discharge bypass valve, the desuperheating valve, and the main thermostatic expansion valve, maintained the suction pressure almost constant to the set value (10 psi) for any load variation as stated earlier. The 1.5 kw heater provided the heating load for the initial starting of the system and was also set to operate whenever the temperature of the coolant dropped down to $40^{\circ}F$.

The following describes the working procedure of the control circuit (Fig. 3.12) for the cooling system. As the pump starts circulation of the coolant, a pressure difference is established between the evaporator ends, and the 'Hi-Lo', differential pressure control switch energizes the relay, putting the three parallel circuits, cooling, heating, and compressor, across the 115 V main. The time delay relay, 'RI', takes three minutes to energize and close the contact of the auxiliary compressor starter. This delay period allows sufficient time for the coolant to pick up the initial heating load given by the additional heater. The compressor starts working and it takes 90 secs. to build up the required pressure. Fuses were used to take care of any overload.

3.4 Instrumentation and control

3.4.1 Temperature measurement

The thermosyphon wall temperatures at different points and the bottom liquid temperature were measured by calibrated Iron-Constanton thermocouples. They were of Thermo Electric make with one end grounded and the other having male connector. Further calibration up to 100°C was carried out using an oil bath maintained at constant temperature and measured by a Fisher, N.B.S. certified precision thermometer (-1°C to 101°C range with subdivision of 1/10°). The calibration curve is given in Fig. 3.13.

The stainless steel thermocouple probe carried eight 30-gauge Honeywell Copper-Constanton thermocouple

junctions, to measure the vapor core temperatures. Twenty-gauge Copper-Constanton thermocouples measured the inlet and outlet temperatures of the cooling jackets and outer surface temperatures of the cooled and adiabatic sections. All were connected to a 16 point rotary switch and measured by a Leeds and Northrup potentiometer No. 8686 having an accuracy of ±.03% of reading + 3 μV. The evaporator of the cooling system was equipped with thermocouple wells on both ends. Twenty-gauge Iron Constanton thermocouples sensed the respective temperatures. Calibration for all these thermocouples was done using the same oil bath procedure as explained above and the curve is given in Fig. 3.14.

The Iron-Constanton thermocouples were recorded by a self calibrated Hewlett Packard 2010 K Data Acquisition System, measuring up to 1 μV with an accuracy of 0.01% of the reading for 100 mV range. The cold junctions for both types, i.e., Iron-Constanton and Copper-Constanton thermocouples were separately made of a mixture of crushed ice and distilled water and were maintained at the melting point of ice. Ambient temperature was recorded by an Iron-Constanton thermocouple.

3.4.2 Power measurement

The heat input to the test section, in the form of electrical energy, was determined by measuring the voltage drop across the heaters using a voltmeter and the current by an ammeter. The ammeter was used in conjunction with a

current transformer. Power was controlled through the powerstat (Superior Electric Co., 13.4 KVA, 240 V). An Amprobe (RS-1000) was also used for a quick check of current flow.

Heat input to the guard heater was periodically checked. It functioned on the signal given by the two thermocouples to the Achromag relay (Fig. 3.3). Power was supplied from 115 V main through a variable autotransformer (0-140 V, 22 Amps, 3.1 KVA). An electric lamp was put in the circuit to indicate whether the heater was on or not.

Power to the cooling system was supplied through a 15 KVA single-phase 600 V/240 V step down Marcus transformer. The control devices have already been described in the previous section (3.3). The 2 H.P. coolant circulation pump was connected to 208 V main supply. Auxiliary immersion heaters of total 10 kw capacity were used for coolant temperature control and were placed inside the tank connected to the exit line from the test section. These heaters were connected to 115 V supply through a step-up (120 V/240 V) transformer and the power was controlled by a variac (General Radio Co., Type W20M, 0-140 V, 20A).

3.4.3 Pressure measurement

Air and other non-condensible gases were removed from the thermosyphon tube using the Teltron Vacuum System. Both, the Forevac unit (TEL 505B), and the Highvac unit (TEL 506B), were used in conjunction to reach an ultimate vacuum

of about 5×10^{-3} torr. A U-tube mercury manometer was connected to the thermosyphon for pressure measurements. In addition the vacuum was also measured with high precision, using a Nester/Foust vacuum gauge, recording up to 1×10^{-4} torr.

3.4.4 Coolant flow measurement

The orifice meters, equipped with the cooling jackets, were connected to the U-tube manometers. Coolant flow (lb/sec) corresponding to the pressure difference (inches of mercury) was determined from the calibration curve (Fig. 3.4). The orifice meters were calibrated on a hydraulic bench.

3.5 Choice of a working fluid

The choice of a working fluid depends on several physical and thermodynamic properties. Boiling and freezing temperatures are very significant. Fig. 3.15 illustrates the 'p-T_s' diagram for few refrigerants considered for their suitability as a working fluid for the operation of thermosyphon in a low temperature range ($20^{\circ}F$ to $40^{\circ}F$). Freon-11 was selected as one of the appropriate fluids. Its boiling point being $74.87^{\circ}F$, was convenient in charging into the thermosyphon tube. It has suitable properties and particularly its high latent heat of vaporization is desirable to have a lower mass flow rate for the same heat transfer.

3.6 Procedure

During the final construction stage, the thermosyphon tube was cleaned, vacuum dried, and tested for any leak. After complete set-up, it was connected to a vacuum pump and subjected to a high vacuum of 5×10^{-3} torr. magnitude. The evacuation procedure was repeated at intervals to check for vacuum leak through fittings and adjustments were made till the vacuum gauge indicated a constant reading. The pump was run for forty hours to remove any non-condensable gas.

After a thorough check-up, it was charged with Freon-11, the working fluid. A 250 ml cylindrical graduated funnel, with teflon stopcock (Pyrex brand), was employed for this purpose. Under atmospheric pressure Freon-11 boils at $74.87^{\circ}F$; so the room temperature was kept lower, in order to charge it in liquid state. All the air and Freon-11 vapor bubbles were removed while charging and only a measured quantity of the working fluid was allowed to go inside the thermosyphon tube. This being the first experiment, the charge was 12% of the total volume ($V^{+} = 0.12$), so as to cover 9" of heated section. This provided a submerged heated section at $L^{+} = 0.2$ and partially filled with higher L^{+}.

Heating and cooling systems were switched on. Only one heater, the lowermost, was given power and the coolant was allowed to flow through the full condensing length. It established the operation of the thermosyphon at the heated

and cooled length ratio $L^+ = 0.2$. Power was varied by the transformer (powerstat) and at each level it took 15 to 30 minutes for the stabilization of pressure and temperatures. Extensive preliminary tests for $V^+ = 0.12$ were carried out at different heated length-cooled length ratios, i.e., $L^+ = 0.2$, 0.4, 0.6, 0.8, and 1.0. For each ratio, results were obtained for a range of operating pressures, temperatures and heat fluxes. Care was taken regarding the maximum heat flux to prevent the tube from burn-out. Once, during the later experiments ($V^+ = 0.06$) at $q = 5000$ Btu/hr ft^2 and $L^+ = 0.6$, it was observed from the rapid rise in wall temperature at one place. An immediate power reduction prevented the tube from damage; this has been discussed in the latter chapter. The guard heater operated whenever the pair of thermocouples actuated the relay and it was noticed that the frequency was higher at greater heat flux.

Experiments were carried out both at varying and constant pressures inside the thermosyphon. For constant pressure operation, initially the coolant temperature was kept higher using the auxiliary immersion heaters and was adjusted according to the increase in heat flux. Wall temperatures were recorded by the Data Acquisition System, whereas the vapor core temperatures, by the potentiometer. Atmospheric pressure was also recorded regularly and necessary corrections in the manometer readings were made accordingly. Useful range of operation was investigated. At intervals, experiments were

repeated and they were found to be reproducible. All the test results are not included here.

Further experiments with higher and lesser quantities of working fluid (V^+ = 0.24, 0.03, and 0.06) were carried out within the observed useful range. To reduce the amount of fluid, inside the tube, it was convenient to evacuate completely and recharge. A cold trap of liquid nitrogen was used to collect all the evacuated fluid and prevent it from passing through the vacuum pump. The procedure for handling the cooling system has already been described in Section 3.3.

3.7 Data reduction

As the thermosyphon was operated at low temperature, the temperature in the condensing section ranged between $10^{\circ}F$ to $60^{\circ}F$, whereas in the heating section, it went to the highest value up to $110^{\circ}F$. Heat losses from the insulations were found to be neglible. At a heat-flux of 10,000 Btu/hr ft^2 it went to a maximum of about 2%. q, the rate of heat flux, in terms of Btu/hr ft^2 was calculated from the voltage and amperage measurements.

The different heat transfer coefficients were calculated by the relationships given below:

(a) Tube heat transfer coefficient $h = q/(T_h - T_c)$

(b) Boiling heat transfer coefficient $h_b = q/(T_h - T_s)$

(c) Condensing heat transfer coefficient $h_c = q/(T_s - T_c)$

(d) Condensing heat transfer coefficient based on Nusselt analysis, $h_{NU} = 0.943[\rho^2 h_{fg} k^3 g/\mu(T_s-T_c)L]^{1/4}$

The non-dimensional parameters used were N_u and R_a, defined as

$$N_u = h.D/k \qquad \text{and} \qquad R_a = G_r.P_r$$

where $G_r = \rho^2 g\beta\theta D^3/\mu^2$ and $P_r = \mu C_p/k$.

The experimental errors were estimated by the method suggested by Kline and McClintok (30). The estimated uncertainties in the variables are

D (diameter), ±0.2%

V (voltage), ±2.25%

I (current), ±0.6%

T (temp.), ±0.01%

These possible differences in measurements gave an error of 2.3% in q (heat flux) and h (heat transfer coefficient), and 2.4% in N_u (Nusselt number).

CHAPTER IV

RESULTS AND DISCUSSION

The experimental results of the current investigations have been presented in forms of Tables 4.1 to 4.21, and Figures 4.1 to 4.23. These results provide the basis for analyzing the various characteristics of a two-phase closed thermosyphon operating within a low temperature range, possibly suitable for the preservation of permafrost such as found in the Canadian north. Experiments were carried out for variable operating pressures depending on heat input and condensing temperatures, as well as at constant pressures. Very few results using Freon-11 as the working fluid are available (Mital (4) and Larkin (28)), but even they do not provide a firm basis for comparison, being in a higher range of pressures and temperatures. The following theoretical relationships given by Lee and Mital (29) were used to compare the results.

$$q = \frac{k(T_s - T_c)}{RL^+} \cdot \frac{A}{B} \tag{4.1}$$

Also

$$q = \frac{\rho^2 R^3 h_{fg} g}{2\mu L_h g_c} \cdot A \tag{4.2}$$

where $$A = \frac{1}{8} - \frac{Y_i'^2}{2} + \frac{3}{8} Y_i'^4 - \frac{Y_i'^4}{2} \ln Y_i'$$

$$B = Y_i'^4 \ln Y_i' \left(\frac{\ln Y_i'}{2} - \frac{1}{2}\right) + \frac{Y_i'^4}{8} + Y_i'^2 \left(\frac{\ln Y_i'}{2} - \frac{1}{4}\right) + \frac{1}{8}$$

and $$Y_i' = 1 - \frac{\delta}{R}$$

For a given value of T_s, the heat transfer rate 'q' is calculated from Eqns. (4.1) and (4.2) using different values of Y_i'. The procedure is repeated until the values of 'q' obtained from both the equations match each other within a desired accuracy. This value of 'q' was taken as the theoretical heat flux at the given 'T_s'.

The different terms used in the present study may be defined in the following way. As found by Mital (4) at steady state, for the particular operating pressure inside the thermosyphon tube and the given wall temperature of the condensing section, the heat input had its limiting value, termed the "Maximum heat flux (q_m)." Any further increase in heat input changed the operating pressure. The corresponding heat transfer coefficient was defined as the "Maximum heat transfer coefficient (h_m)." The saturation temperature (T_s) of the working fluid in the tube was taken as the operating temperature, whereas (T_h-T_c) was the overall temperature difference. T_h and T_c being the average temperatures of the heated and cooled sections respectively. The tube heat transfer coefficient 'h' was then defined as

$$h = q/(T_h - T_c)$$

In the present study, for the case of variable operating pressure, heat flux and the corresponding heat transfer coefficients had their maximum limiting magnitudes 'q_m' and 'h_m'.

4.1 Effect of heat flux

The temperatures recorded along the tube length have been plotted as examples in Figs. 4.1(a) and 4.1(b), for different values of the heat fluxes at $V^+ = 0.06$ and $L^+ = 0.6$ and 1.0 respectively. Vapor core temperatures in the adiabatic and condensing sections give a clear picture of condensing temperature drop, while the saturation temperature lies in between the average heated and cooled length temperatures.

The variations of theoretical and experimental maximum heat flux 'q_m' with the operating temperature 'T_s' have been shown in Figs. 4.2(a) and 4.2(b). The theory predicts higher heat transfer rate in low mean operating pressure range, whereas it gives lower values at higher pressure operations. This trend of underestimating was also observed by Lee and Mital (29). The assumption that the shear stress on liquid-vapor interface is negligible does not seem to be true throughout the operating range. As reported by Rohsenow (31) the "interfacial resistance" might partially account for a low heat transfer coefficient. It is also clear from Fig. 4.3 which gives the typical variation of

condensing coefficient 'h_c' with 'T_s' as compared to 'h_{NU}', the Nusselt heat transfer coefficient. Larkin's (28) result, while using water as the working fluid shows a similar trend. As shown in Figs. 4.4(a) and 4.4(b) the overall temperature difference (T_h-T_c) increases with an increase in 'q_m'. This may be due to the fact that the cooling condition of the condensing section was maintained almost constant irrespective of the magnitude of heat input.

The overall temperature difference '(T_h-T_c)' and the operating temperature 'T_s' are separately dependent on the heat flux 'q', but both increase with an increase in 'q' as shown in Fig. 4.5. This confirms that for a particular value of 'T_s' the relationship

$$q = h(T_h-T_c)$$

will give a unique value of 'q', already mentioned as the maximum heat flux 'q_m' at steady state condition.

A two-phase closed thermosyphon is almost unidirectional as far as the heat transfer is concerned. Fig. 4.6 and Fig. 4.7, which are given as examples, show that the heat transfer by conduction happened to be below one percent of the overall heat transfer for the operating temperature above 27^oF in the present investigations. For the possible practical utilization of thermosyphon in permafrost region, the heated end has to be near the structure foundation whereas the cooling end exposed to atmosphere.

Any decrease in atmospheric temperature will cause a heat transfer from the ground to the atmosphere with a comparatively greater reduction in thermal reserve in the lower ground. This may help in building a negative thermal capacity under the structure foundation during the winter period, which may be sufficient to compensate the positive thermal capacity during the summer time. Any heat transfer from the top end to the bottom will be only by conduction, whereas the reverse will take place mainly due to two-phase operation. In the present investigation, it was observed that at $q_m \approx 2000$ Btu/hr ft^2 at $T_s = 30^oF$ with 21^oF of temperature difference, the two-phase heat transfer was 120 times the conduction heat transfer (Fig. 4.8). A similar trend was also reported by Long (24) from his thermopile experiment.

The maximum heat transfer coefficient 'h_m' corresponding to the maximum heat flux 'q_m' for different values of V^+ and L^+ have been plotted as a function of 'T_s' in Figs. 4.9(a) and 4.9(b). It is noted that at higher operating temperatures corresponding increase in 'h_m' was comparatively lower. Mital (4) had also observed a similar trend while using water as the working fluid. Fig. 4.10 shows the variation of heat transfer coefficient with the overall temperature difference, while the typical variation with heat flux for different values of L^+ has been plotted in Fig. 4.11. Within the range of investigation, the heat

transfer coefficient varies almost linearly with the heat flux. Mital had observed 'h_m' becoming constant at 'q_m' $\approx$ 2000 Btu/hr ft^2, but such a trend was not found in the present case even up to a value of $q_m \approx$ 3000 Btu/hr ft^2.

The typical variations of boiling and condensing heat transfer coefficients 'h_b' and 'h_c' with the operating temperature 'T_s' have been shown in Figs. 4.12 and 4.13. 'h_b' increased with a rise in 'T_s', which was also reported by Larkin (28) using water as the working fluid.

4.2 Effect of the quantity of working fluid (V^+)

The variations of 'h_m' with 'T_s' for different values of 'V^+' are given in Figs. 4.14(a) and 4.14(b). 'h_m' as a function of 'V^+' for different operating temperatures are shown in Figs. 4.15(a) and 4.15(b). The behaviour of maximum heat flux with 'T_s' at different 'V^+' are given in Figs. 4.16(a) and 4.16(b).

Within the range of 'V^+' studied, it may be noted that beyond certain minimum quantity of the working fluid, 'h_m' becomes independent of 'V^+'. This confirms the trend reported by Lee and Mital (29), and Cohen and Bayley (20). In Fig. 4.14(a), comparison has been made with that of Larkin's (28) result and it seems that in a higher pressure range, there seems to be a good agreement.

Cohen and Bayley (20) had postulated that the condensate returns in the form of a film over the heated

surface, which cools down the portion not submerged in liquid. The heat transfer takes place by conduction through the film and by evaporation from the surface of the returning condensate. The boiling and condensation form a closed cycle. For the most effective operation, there should be a uniform and continuous flow of fluid in both the phases and should cover the whole surface of the tube, with the quantity of fluid being sufficient to pick up all the heat input in the evaporator section. If the heat flux is in excess, the returning condensate may be completely evaporated before reaching the bottom end of the heated section. This situation creates rapid rise in the temperature of the lower portion of the heated section and an immediate reduction in heat input is essential to prevent the tube from burn-out. In the present experimental study, once it occurred at a heat input of 5000 Btu/hr ft^2 for $L^+ = 1.0$ and $V^+ = 0.06$. Fig. 4.17 shows an unusual increase in temperature from 105^oF to 247^oF in the bottom region of the tube. Noticing a rapid and continuous increase in temperature, the power was shut down to prevent burn-out. Similar observation was also reported by Lee and Mital (29) and Larkin (28).

4.3 Effect of the heated length-cooled length ratio (L^+)

Wall temperatures increase with an increase in the heated length-cooled length ratio 'L^+' as shown in Fig. 4.18, whereas the maximum heat transfer coefficient 'h_m' has the

reverse effect (Fig. 4.19). This is evident from the relationship

$$q_m = q_c/L^+$$

based on energy balance, given by Lee and Mital (29), where q_c is the condensation heat flux at particular operating condition. At higher 'L^+' heat transfer coefficient decreases due to an effective increase in the heated section compared to that of cooled section. Similar observation was also reported by Bayley and Lock (7) during their experiments on a single-phase closed thermosyphon.

4.4 Effect of mean operating pressure 'p' (Corresponding to mean operating temperature 'T_s')

The wall temperatures for different mean operating pressures were shown in Figs. 4.1(a) and 4.1(b). They increase with a rise in pressure, because of increase in mean operating temperature. Mean operating pressure has significant effect on the maximum heat transfer coefficient 'h_m' as seen from Figs. 4.14(a) and 4.14(b). Due to an increase in pressure 'p' the vapor density increases. For a particular heat transfer rate the mass flow rate is constant and this results in a low vapor velocity, in turn reducing the interfacial shear stress. Again with an increase in pressure, the corresponding temperature increases giving a decreasing effect to surface tension. These factors help in a fast condensate return and high heat transfer coefficient.

Experiments at two different constant pressures were run, but the results, showing the effect of pressure, were not very conclusive due to small pressure difference. However, the typical variations of 'h' with 'q' and '$T_h - T_c$' have been shown in Figs. 4.20 and 4.21, respectively.

4.5 Comparison of the present results with those of other investigators

For comparison of the results of present investigations, only few experimental findings of Mital's (4) and Larkin's (28) using Freon-11 were available. In some cases, the results of water as the working fluid have also been included to compare the trend of variations. The typical variation of Nusselt number 'Nu_d' with Rayleigh number 'Ra_m' has been shown in Fig. 4.22. Rayleigh number was modified as $Ra \times \frac{D}{L_h}$ to include the effect of tube geometry and provide a basis for the correlation of the results of the previous investigators. The present results are in good agreement with that of Lee and Mital (29). The results of Bayley and Lock (7) and Pucci and Gerretsen (11) of single-phase closed thermosyphon have also been included for comparison, which lead to a conclusion that the heat transfer capability of a two-phase closed thermosyphon is far better than that of a single-phase closed thermosyphon. The reproducibility of the present results has been demonstrated by Fig. 4.23.

CHAPTER V

CONCLUDING REMARKS

The results of the present investigation lead to the following conclusions.

1. A two-phase system has the capability of transferring thermal energy several hundred times greater than a solid conductor of same geometry, is confirmed.
2. The quantity of working fluid beyond certain minimum amount has no significant effect on the heat transfer coefficient.
3. Within the range of investigation, an increase in 'L^+' has a decreasing effect on heat transfer coefficient.
4. The heat transfer coefficient increases significantly with an increase in operating pressure.

The results are very encouraging and for further study it is suggested to have an experimental work on models placed in atmospheric and soil conditions similar to the permafrost region, maintained in the laboratory.

REFERENCES

1. E. Schmidt, "General Discussion on Heat Transfer," Institution of Mechanical Engineers, London, Section IV, p.361 (1951).
2. T. H. Davies and W. D. Morris, "Thermosyphons," Engineers Digest, Vol. 26, No. 11, p.87-91 (1965).
3. T. H. Davies and W. D. Morris, "Thermosyphons (Part II)," Engineer's Digest, Vol. 26, No. 12, p.80-83 (1965).
4. U. Mital, "A Two Phase Closed Thermosyphon," M.A.Sc. Thesis, University of Ottawa (1970).
5. B. W. Martin and H. Cohen, "Heat Transfer by Free Convection in an Open Thermosyphon Tube," British Journal of Applied Physics, Vol. 5, p.91, (1954).
6. M. J. Lighthill, "Theoretical Considerations on Free Convection in Tubes," Quarterly Journal of Mechanics and Applied Mathematics, Vol. 6, Part 4, p.398 (1953).
7. F. J. Bayley and G. S. H. Lock, "Heat Transfer Characteristics of the Closed Thermosyphon," A.S.M.E. paper 64-HT-6 (1964).
8. D. Japikse and E. R. F. Winter, "Single-Phase Transport Processes In The Open Thermosyphon," Int. J. Heat Mass Transfer, Vol. 14, p.427-441 (1971).
9. D. Japikse, P. A. Jallouk and E. R. F. Winter, "Single-Phase Transport Processes In The Closed Thermosyphon," Int. J. Heat Mass Transfer, Vol. 14, p.869-887 (1971).

10. D. H. Everaarts, "Free-Convection Heat Transfer with Mercury and Water in a Closed Thermosyphon," Technische Hogeschool Delft Report No. 10.M.006, Delft, Netherlands, July (1967).

11. P. F. Pucci and J. C. R. Gerretsen, "Heat Transfer Characteristics of a Liquid-Metal Filled Closed Thermosyphon," An A.S.M.E. publication, Paper No. 72-GT-36, (1972).

12. G. M. Grover, T. P. Cotter and G. E. Erickson, "Structures of Very High Conductance," Journal of App. Physics, Vol. 35, p.1950-91 (1964).

13. J. E. Deverall and J. E. Kemme, "Satellite Heat Pipe," Los Alamos Scientific Laboratory, University of California (1965).

14. J. E. Deverall, E. W. Salmi and R. J. Knapp, "Orbital Heat Pipe Experiment," Los Alamos Scientific Laboratory, University of California (1967).

15. K. T. Feldman, Jr., and G. H. Whiting, "The Heat Pipe," Mechanical Engineering, Vol. 89, p.30-33 (1967).

16. K. T. Feldman, Jr., and G. H. Whiting, "Applications of the Heat Pipe," Mechanical Engineering, p.48-53 (1968).

17. G. Y. Eastman, "The Heat Pipe," Scientific American, p.38-46 (1968).

18. H. Hwang-Bo, W. E. Hilding, "Optimization of a Heat Pipe with a Wick and Annulus Liquid Flow," A.S.M.E., Paper No. 71-HT-V (1972).

19. B. F. Armaly and J. Dudheker, "Experimental Study of a Nitrogen Heat Pipe," A.S.M.E., Paper No. 71-WA/HT-28 (1972).

20. H. Cohen and F. J. Bayley, "Heat Transfer Problems of Liquid Cooled Gas Turbine Blades," Proceedings Institution Mechanical Engineers, Vol. 169, p.1063-80 (1955).

21. E. Schmidt, "Heat Transfer by Natural Convection," Presented at the International Heat Transfer Conference held at the University of Colorado (U.S.A.), August 28 - September 1 (1961).

22. L. Bewilogua and R. Knoner, "The Thermosyphon as a Nitrogen Cryostat for Operation in the Horizontal Reaction Channel," Cryogenics, p.46-47, September (1961).

23. L. Bewilogua, R. Knoner and G. Kappler, "Application of the Thermosyphon for Pre-cooling Apparatus," Cryogenics, p.34-35, February (1966).

24. E. L. Long, "The Long Thermopile," Proc. Permafrost International Conference, p.487-491 (1963).

25. J. C. Y. Koh, E. M. Sparrow and J. P. Hartnett, "The Two Phase Boundary Layer in Laminar Film Condensation," Int. J. Heat Mass Transfer, Vol. 2, p.69-82 (1961).

26. B. S. Larkin, "Heat Transfer in a Two-Phase Thermosyphon Tube," Canada N.R.C. No. 3, p.45-53 (1967).

27. Y. Lee, "Preservation of Permafrost by Means of Two-Phase Closed Thermosyphon," Annual Reports, DRB 9511-96, University of Ottawa, October 25 (1969).

28. B. S. Larkin, "An Experimental Study of the Two-Phase Thermosyphon Tube," The Engineering Journal, Transactions of C.S.M.E., Aug./Sept. (1971).

29. Y. Lee and U. Mital, "A Two-Phase Closed Thermosyphon," International Symposium on Two-Phase Systems, Paper 7-9, Aug. 29 - Sept. 2 (1971).

30. S. J. Kline and F. A. McClintock, "Describing Uncertainties in Single-Sample Experiments," Mechanical Engineering, p.3-8, January (1953).

31. W. M. Rohsenow, "Film Condensation of Liquid Metals," Transactions of the C.S.M.E., Vol. 1, No. 1, March (1972).

TABLE 4.1

QUANTITY OF THE WORKING FLUID $(V^+)=0.03$

HEATED LENGTH=COOLED LENGTH RATIO $(L^+)=0.20$

OPERATING PRESSURE (PSIA) P= 3.80 TO 6.40

No.	q_m	h_m	T_h	T_c	T_v	T_s	h_b	h_c	h_{NU}	Nu_d	$Ra \times D/L_h$
1	195.4	20.1	22.4	12.7	16.2	16.0	30.8	11.0	239.5	38.8	5679877.2
2	977.8	79.2	25.6	13.2	16.7	17.0	114.1	56.2	232.4	152.7	7228224.7
3	2496.2	136.0	34.7	16.4	21.0	21.0	181.7	109.1	220.8	262.1	10751544.9
4	4580.2	197.5	43.5	20.3	26.1	26.0	262.0	156.7	209.1	380.7	13581720.9
5	6559.3	238.6	50.6	23.1	32.0	31.5	343.7	147.3	189.6	459.9	16100470.2
6	9025.4	319.9	57.6	29.4	38.0	37.5	448.7	211.2	191.1	616.6	16524166.8

TABLE 4.2

QUANTITY OF THE WORKING FLUID (V^+)=0.03

HEATED LENGTH=COOLED LENGTH RATIO (L^+)=0.60

OPERATING PRESSURE (PSIA) P= 4.50 TO 9.00

No.	q_m	h_m	T_h	T_c	T_v	T_s	h_b	h_c	h_{NU}	Nu_d	Ra x D/L_h
1	145.4	11.2	25.7	12.8	16.3	21.0	30.8	24.8	191.5	21.7	2523630.6
2	587.9	39.9	29.9	15.2	19.5	24.0	99.4	80.9	187.7	76.9	2876060.2
3	1233.1	71.1	36.3	19.0	25.3	28.5	157.9	117.2	183.8	137.1	3384691.4
4	2172.6	103.3	45.4	24.3	32.8	35.5	220.0	153.4	176.4	199.1	4107123.3
5	3345.1	130.6	55.9	30.3	40.2	43.0	260.0	201.2	170.3	251.7	5001051.5
6	4715.4	141.3	69.7	36.4	50.3	52.0	265.7	203.5	161.4	272.3	6517507.8

TABLE 4,3

QUANTITY OF THE WORKING FLUID (V^+)=0,03

HEATED LENGTH=COOLED LENGTH RATIO (L^+)=1,00

OPERATING PRESSURE (PSIA) P= 4,10 TO 8,00

No.	q_m	h_m	T_h	T_c	T_v	T_s	h_b	h_c	h_{NU}	Nu_d	Ra x D/L_h
1	52,0	6,1	22,3	13,8	16,8	18,5	13,6	17,3	219,5	11,7	1003074,0
2	194,6	17,2	26,1	14,8	18,4	20,0	31,9	54,8	214,4	33,2	1322375,9
3	438,3	32,0	30,8	17,1	25,3	27,0	115,9	53,4	182,1	61,7	1604970,5
4	827,5	46,3	38,9	21,1	27,1	27,5	72,3	137,0	203,0	89,3	2092970,0
5	1274,7	82,2	40,5	25,0	33,2	32,5	159,9	154,9	194,7	158,4	1816948,9
6	1834,5	93,8	50,4	30,8	40,4	40,0	176,6	191,4	184,8	180,8	2291411,0
7	2492,3	99,7	60,3	35,3	46,6	46,0	174,8	219,8	177,6	192,1	2929038,6

TABLE 4.4

QUANTITY OF THE WORKING FLUID (V^+)=0.03

HEATED LENGTH-COOLED LENGTH RATIO (L^+)=0.20

OPERATING PRESSURE (PSIA) P= 5.50 (CONST)

No.	q_m	h_m	T_h	T_c	T_v	T_s	h_b	h_c	h_{NU}	Nu_d	Ra x D/L_h
1	135.3	10.0	35.0	21.5	28.4	28.5	20.9	3.9	198.4	19.3	7913558.8
2	755.1	42.9	38.8	21.2	25.5	28.5	73.1	35.7	196.7	82.7	10313204.4
3	1566.5	79.1	39.8	20.0	24.7	28.5	138.8	65.7	189.0	152.4	11603819.3
4	2816.9	107.2	45.3	19.0	25.1	29.0	173.3	91.4	181.5	206.6	15392682.1
5	3449.7	125.9	46.9	19.5	25.7	29.5	198.1	111.5	181.6	242.6	16055562.2

TABLE 4.5

QUANTITY OF THE WORKING FLUID (V^+)=0.03

HEATED LENGTH=COOLED LENGTH RATIO (L^+)=0.60

OPERATING PRESSURE (PSIA) P= 5.50 (CONST)

No.	q_m	h_m	T_h	T_c	T_v	T_s	h_b	h_c	h_{NU}	Nu_d	Ra x D/L_h
1	70.6	6.1	34.5	22.8	26.6	30.0	15.8	11.2	197.2	11.7	2273708.2
2	206.1	14.9	34.9	21.0	25.2	30.0	42.5	29.0	186.3	28.6	2709445.3
3	347.2	23.1	35.3	20.2	25.1	30.0	66.1	42.7	182.6	44.5	2935449.3
4	695.4	41.4	37.5	20.7	25.0	30.0	92.2	98.0	185.1	79.7	3282672.3
5	948.0	49.0	37.2	17.9	25.6	29.5	122.4	74.3	175.0	94.5	3774707.0

TABLE 4.6

QUANTITY OF THE WORKING FLUID (V^+)=0,03

HEATED LENGTH=COOLED LENGTH RATIO (L^+)=1,00

OPERATING PRESSURE (PSIA) P= 6,00 (CONST)

No.	q_m	h_m	T_h	T_c	T_v	T_s	h_b	h_c	h_{NU}	Nu_d	Ra x D/L_h
1	59,1	4,9	34,6	22,5	26,4	32,0	22,6	15,1	183,7	9,4	1422735,4
2	140,1	10,2	35,1	21,4	25,5	31,5	38,8	34,5	181,1	19,7	1605881,6
3	240,0	16,7	36,6	22,3	26,5	32,5	58,2	56,3	180,5	32,3	1680142,4
4	352,8	22,4	35,6	19,9	25,7	31,5	85,6	60,4	174,8	43,2	1845000,1
5	513,9	30,4	37,0	20,1	25,8	32,0	102,0	90,3	173,9	58,6	1978942,9
6	663,4	35,8	37,8	19,2	26,4	32,0	114,4	92,4	170,8	68,9	2173218,5

TABLE 4.7

QUANTITY OF THE WORKING FLUID (V^+)=0.06

HEATED LENGTH-COOLED LENGTH RATIO (L^+)=0.20

OPERATING PRESSURE (PSIA) P= 5.20 TO 7.00

No.	q_m	h_m	T_h	T_c	T_v	T_s	h_b	h_c	h_{NU}	Nu_d	Ra x D/L_h
1	167.6	7.5	37.0	14.7	17.8	28.5	19.7	10.7	167.6	14.5	13062350.9
2	699.4	28.4	39.6	14.9	18.7	29.0	66.1	36.9	166.8	54.7	14426185.3
3	1545.0	55.8	43.9	16.2	20.5	30.0	111.2	72.0	167.5	107.5	16220550.1
4	2757.8	92.4	48.4	18.6	23.7	32.5	173.3	107.7	167.0	178.0	17486758.5
5	4571.2	151.0	52.0	21.7	28.6	36.0	286.3	133.0	165.8	291.1	17726918.3
6	6452.4	207.9	56.2	25.2	34.6	39.5	386.0	137.8	165.5	400.6	18183807.7

TABLE 4.8

QUANTITY OF THE WORKING FLUID (V^+)=0.06

HEATED LENGTH=COOLED LENGTH RATIO (L^+)=0.60

OPERATING PRESSURE (PSIA) P= 5.20 TO 16.00

No.	q_m	h_m	T_h	T_c	T_v	T_s	h_b	h_c	h_{NU}	Nu_d	Ra x D/L_h
1	147.0	7.7	32.7	13.6	17.9	27.5	28.3	20.4	167.3	14.8	3728985.5
2	580.8	29.0	36.6	16.6	21.7	30.0	87.6	67.6	168.7	55.8	3915939.2
3	1272.8	58.2	42.2	20.3	27.3	34.5	164.9	110.2	166.2	112.1	4273412.9
4	2201.8	89.2	50.9	26.2	36.2	39.5	193.3	132.7	168.7	172.0	4818491.0
5	3295.2	119.7	59.6	32.1	45.1	45.0	225.6	152.1	169.7	230.8	5372843.7
6	4781.0	149.8	71.2	39.3	54.3	54.5	286.1	191.2	162.4	288.7	6231463.8
7	6472.6	169.5	84.2	46.0	65.2	65.0	336.8	202.4	153.3	326.7	7455367.7
8	8272.6	174.3	100.8	53.4	78.8	78.0	362.6	195.2	143.0	335.9	9267305.1

TABLE 4.9

QUANTITY OF THE WORKING FLUID (V^+)=0.06

HEATED LENGTH=COOLED LENGTH RATIO (L^+)=1.00

OPERATING PRESSURE (PSIA) P= 5.60 TO 16.30

No.	q_m	h_m	T_h	T_c	T_v	T_s	h_b	h_c	h_{NU}	Nu_d	Ra x D/L_h
1	198.3	11.3	34.7	17.2	24.0	31.0	53.1	29.3	167.4	21.8	2056392.8
2	803.8	40.0	42.3	22.2	28.7	35.5	118.5	123.7	168.8	77.1	2353891.6
3	1765.4	72.8	56.0	31.8	42.8	45.5	167.8	160.8	167.1	140.3	2840784.7
4	2666.4	93.0	66.7	38.0	53.0	53.5	202.0	178.3	161.8	179.3	3357160.9
5	3759.0	108.7	81.4	46.9	66.0	66.5	251.6	196.5	151.9	209.6	4049784.4
6	4995.4	112.9	99.1	54.9	80.0	80.0	261.5	198.7	142.2	217.6	5183416.8

TABLE 4.10

QUANTITY OF THE WORKING FLUID (V^+)=0,06

HEATED LENGTH=COOLED LENGTH RATIO (L^+)=0,20

OPERATING PRESSURE (PSIA) P= 6,00 (CONST)

No.	q_m	h_m	T_h	T_c	T_v	T_s	h_b	h_c	h_{NU}	Nu_d	Ra x D/L_h
1	165,0	8,9	41,4	22,8	27,1	34,5	24,0	7,7	174,3	17,1	10897007,5
2	779,3	34,2	46,6	23,8	25,3	35,0	67,4	101,6	176,0	65,9	13353276,2
3	4083,4	163,2	46,3	21,3	24,2	32,0	285,6	278,1	178,3	314,5	14657558,8
4	2857,5	101,7	49,9	21,7	25,8	34,5	186,2	142,4	170,7	196,0	16461686,2
5	3544,2	114,0	52,6	21,5	26,4	34,5	196,4	142,5	169,7	219,7	18209190,5

TABLE 4.11

QUANTITY OF THE WORKING FLUID (V^+)=0,06

HEATED LENGTH=COOLED LENGTH RATIO (L^+)=0,60

OPERATING PRESSURE (PSIA) P= 6,00 (CONST)

No.	q_m	h_m	T_h	T_c	T_v	T_s	h_b	h_c	h_{NU}	Nu_d	Ra x D/L_h
1	82,6	5,0	40,5	23,8	26,6	34,0	12,7	18,0	180,6	9,5	3256150,5
2	204,6	12,0	40,2	23,2	25,5	33,5	30,7	52,5	179,9	23,2	3320095,5
3	383,8	20,8	41,1	22,6	25,5	34,0	54,1	80,1	175,6	40,0	3606627,7
4	797,2	37,7	42,7	21,6	25,1	33,5	86,6	134,9	173,5	72,6	4130390,8
5	1088,3	48,3	43,5	20,9	25,3	33,5	109,1	148,0	171,3	93,0	4401953,7

TABLE 4.12

QUANTITY OF THE WORKING FLUID (V^+)=0.06

HEATED LENGTH=COOLED LENGTH RATIO (L^+)=1.00

OPERATING PRESSURE (PSIA) P= 6.00 (CONST)

No.	q_m	h_m	T_h	T_c	T_v	T_s	h_b	h_c	h_{NU}	Nu_d	Ra x D/L_h
1	58.6	4.0	38.5	23.8	26.0	33.5	11.6	26.8	182.7	7.7	1727588.6
2	123.1	7.9	38.9	23.3	25.3	33.5	22.9	61.7	180.5	15.2	1824954.3
3	207.2	12.2	39.5	22.5	25.4	33.5	34.7	71.4	177.3	23.6	1982522.5
4	401.4	21.5	39.5	20.9	24.9	33.0	61.6	100.1	172.9	41.5	2184868.6
5	642.3	32.2	40.8	20.9	25.4	33.5	87.4	141.5	171.1	62.0	2340028.7

TABLE 4.13

QUANTITY OF THE WORKING FLUID (V^+)=0.12

HEATED LENGTH=COOLED LENGTH RATIO (L^+)=0.20

OPERATING PRESSURE (PSIA) P= 4.90 TO 7.20

No.	q_m	h_m	T_h	T_c	T_v	T_s	h_b	h_c	h_{NU}	Nu_d	Ra x D/L_h
1	2279.7	113.3	33.8	13.6	18.3	25.0	260.0	97.5	176.1	218.3	11789308.6
2	3738.7	161.2	39.4	16.2	21.1	27.5	314.6	151.1	176.1	310.7	13583673.4
3	5507.1	208.0	46.2	19.7	29.2	31.5	375.1	116.3	174.2	401.0	15504951.9
4	7739.8	248.0	54.0	22.8	34.4	37.0	454.4	134.2	166.1	478.0	18279481.2
5	9819.2	283.2	60.7	26.0	39.5	42.0	526.5	145.4	160.9	545.7	20312053.3

TABLE 4.14

QUANTITY OF THE WORKING FLUID (V^+)=0.12

HEATED LENGTH-COOLED LENGTH RATIO (L^+)=0.60

OPERATING PRESSURE (PSIA) P= 4.00 TO 9.50

No.	q_m	h_m	T_h	T_c	T_v	T_s	h_b	h_c	h_{NU}	Nu_d	Ra x D/L_h
1	124.5	11.9	22.2	11.7	16.9	17.0	24.0	14.4	213.7	22.9	2042334.7
2	335.6	30.0	23.8	12.6	18.4	18.0	57.6	34.9	212.8	57.8	2186007.5
3	801.9	63.0	27.9	15.2	21.9	21.0	116.5	71.8	208.1	121.4	2485556.5
4	1402.9	91.8	34.2	18.9	26.9	26.0	171.4	105.7	197.9	176.8	2985401.3
5	2251.6	115.3	43.4	23.9	33.9	34.0	238.9	135.1	180.9	222.3	3811642.2
6	3119.6	131.0	52.6	28.8	40.9	41.0	269.9	154.5	172.1	252.5	4648621.9
7	3961.9	141.3	61.1	33.0	47.3	47.0	281.7	166.9	166.3	272.4	5473561.1
8	4809.7	148.5	70.0	37.6	54.2	54.5	310.8	173.4	158.2	286.1	6325184.7

TABLE 4.15

QUANTITY OF THE WORKING FLUID (V^+)=0.12

HEATED LENGTH=COOLED LENGTH RATIO (L^+)=1.00

OPERATING PRESSURE (PSIA) P= 4.00 TO 8.50

No.	q_m	h_m	T_h	T_c	T_v	T_s	h_b	h_c	h_{NU}	Nu_d	Ra x D/L_h
1	93.6	10.7	19.9	11.1	18.5	17.5	39.1	12.7	203.9	20.6	1026374.1
2	199.7	22.0	21.8	12.8	19.9	18.5	60.0	27.9	209.1	42.4	1063081.4
3	406.7	39.0	25.6	15.1	22.8	21.0	88.8	53.0	208.0	75.1	1222797.5
4	596.6	51.1	28.4	16.8	25.0	23.0	110.1	72.8	204.6	98.6	1366698.1
5	824.1	63.3	32.0	18.9	27.7	26.0	138.5	94.2	198.2	122.0	1524917.2
6	1195.1	78.2	37.8	22.5	32.0	31.0	175.2	126.2	189.2	150.7	1790785.2
7	1495.4	87.0	42.6	25.4	35.7	34.5	184.8	144.9	185.7	167.7	2013242.2
8	1834.5	91.3	50.0	29.9	41.3	41.0	204.2	160.5	176.3	175.9	2354347.2
9	2303.5	95.2	58.4	34.2	48.2	48.0	221.0	165.0	166.8	183.5	2834471.6

TABLE 4.16

QUANTITY OF THE WORKING FLUID $(V^+)=0,24$

HEATED LENGTH-COOLED LENGTH RATIO $(L^+)=0,20$

OPERATING PRESSURE (PSIA) P= 4,40 TO 11,80

No.	q_m	h_m	T_h	T_c	T_v	T_s	h_b	h_c	h_{NU}	Nu_d	Ra x D/L_h
1	1003,6	39,8	37,8	12,6	18,9	20,0	56,3	31,6	196,2	76,6	14786425,0
2	4552,1	158,2	47,8	19,0	25,8	27,0	218,7	134,9	192,4	304,9	16854142,4
3	9951,1	279,4	63,5	27,9	40,0	40,0	423,8	164,0	172,5	538,4	20864616,1
4	13756,6	331,0	75,6	34,0	48,7	48,5	507,6	188,1	164,8	637,9	24344004,6
5	22732,6	472,2	93,7	45,5	64,1	64,0	765,8	245,1	154,4	910,0	28200229,3

TABLE 4.17

QUANTITY OF THE WORKING FLUID (V^+)=0.24

HEATED LENGTH=COOLED LENGTH RATIO (L^+)=0.60

OPERATING PRESSURE (PSIA) P= 4.20 TO 13.40

No.	q_m	h_m	T_h	T_c	T_v	T_s	h_b	h_c	h_{NU}	Nu_d	Ra x D/L_h
1	132.3	8.6	28.6	13.1	19.2	19.0	13.8	13.0	208.1	16.5	3017943.3
2	556.2	32.1	33.0	15.7	22.1	22.0	50.5	52.1	204.2	61.9	3382413.4
3	1275.8	65.1	38.8	19.2	26.4	26.0	99.9	106.2	200.0	125.5	3825635.2
4	2211.5	93.2	48.6	24.9	34.0	33.5	146.2	145.9	188.4	179.7	4631700.1
5	3393.3	122.2	57.8	30.0	43.0	42.5	222.5	157.0	171.1	235.6	5420843.1
6	4875.9	140.9	70.7	36.1	53.2	52.5	268.0	170.6	159.4	271.5	6757993.0
7	6449.4	157.8	83.3	42.4	62.3	61.5	296.0	194.9	153.2	304.1	7980758.0
8	8450.1	183.3	96.0	50.0	70.8	70.0	324.4	243.0	151.0	353.3	9000460.9

TABLE 4,18

QUANTITY OF THE WORKING FLUID (V^+)=0,24

HEATED LENGTH=COOLED LENGTH RATIO (L^+)=1,00

OPERATING PRESSURE (PSIA) P= 4,10 TO 12,80

No.	q_m	h_m	T_h	T_c	T_v	T_s	h_b	h_c	h_{NU}	Nu_d	Ra x D/L_h
1	471,1	32,9	32,0	17,6	24,0	23,0	52,6	74,0	212,5	63,4	1676823,2
2	845,7	54,9	36,4	21,0	28,2	27,0	89,8	117,2	206,6	105,8	1804387,7
3	1280,6	74,4	41,3	24,1	33,5	31,5	130,1	137,1	195,9	143,4	2015975,7
4	1790,8	90,1	50,8	30,9	40,4	39,0	152,4	187,8	190,8	173,6	2328899,4
5	2421,2	99,7	58,9	34,6	47,7	46,0	187,4	185,1	175,2	192,2	2843908,7
6	3197,7	105,1	71,5	41,0	57,8	57,0	221,0	191,1	160,4	202,5	3564908,9
7	4069,3	110,0	83,9	47,0	68,6	68,0	255,2	188,0	149,2	212,0	4334266,4

TABLE 4.19

QUANTITY OF THE WORKING FLUID (V^+)=0,24

HEATED LENGTH=COOLED LENGTH RATIO (L^+)=0,20

OPERATING PRESSURE (PSIA) P= 5,00 (CONST)

No.	q_m	h_m	T_h	T_c	T_v	T_s	h_b	h_c	h_{NU}	Nu_d	Ra x D/L_h
1	132,1	4,6	49,5	20,7	26,4	26,0	5,6	4,7	213,4	8,9	16817044,6
2	700,8	36,7	40,1	21,0	26,8	26,5	51,6	24,3	210,9	70,8	11181099,0
3	1511,7	73,6	42,5	21,9	24,7	26,5	94,8	108,8	220,8	141,8	12033373,5
4	2681,2	110,4	45,4	21,1	26,8	26,5	142,2	94,4	211,7	212,7	14228004,6
5	4504,9	164,2	49,2	21,7	27,0	27,5	208,1	171,7	208,3	316,4	16071182,4

TABLE 4.20

QUANTITY OF THE WORKING FLUID (V+)=0.24

HEATED LENGTH=COOLED LENGTH RATIO (L^+)=0.60

OPERATING PRESSURE (PSIA) P= 5.00 (CONST)

No.	q_m	h_m	T_h	T_c	T_v	T_s	h_b	h_c	h_{NU}	Nu_d	Ra x D/L_h
1	120.9	3.6	55.1	21.5	25.9	25.5	4.1	16.5	228.7	6.9	6554605.7
2	430.6	29.2	37.9	23.2	28.2	27.5	41.2	51.3	224.5	56.3	2877036.5
3	787.9	49.0	38.2	22.1	26.4	26.5	67.5	110.5	223.2	94.5	3136396.1
4	1050.5	61.0	39.0	21.8	26.4	26.5	83.9	137.2	219.4	117.5	3364189.9
5	1384.2	74.1	41.3	22.6	28.7	28.0	103.9	136.9	212.4	142.9	3645352.6

TABLE 4.21

QUANTITY OF THE WORKING FLUID (V^+)=0.24

HEATED LENGTH=COOLED LENGTH RATIO (L^+)=1.00

OPERATING PRESSURE (PSIA) P= 5.00 (CONST)

No.	q_m	h_m	T_h	T_c	T_v	T_s	h_b	h_c	h_{NU}	Nu_d	$Ra \times D/L_h$
1	41.6	3.9	32.8	22.3	26.9	26.0	6.1	9.1	232.4	7.6	1239328.8
2	126.6	11.2	32.9	21.6	26.9	26.0	18.4	24.2	223.5	21.7	1318340.7
3	243.9	20.2	33.4	21.3	27.3	26.5	35.6	40.3	213.7	38.9	1417268.3
4	417.8	31.1	33.4	20.0	27.3	26.0	56.4	57.0	206.4	60.0	1573014.2
5	615.3	43.3	35.0	20.8	27.3	26.5	72.4	94.1	209.0	83.4	1665889.1
6	849.0	53.6	36.8	21.0	28.2	27.5	91.0	117.3	202.4	103.4	1854242.0

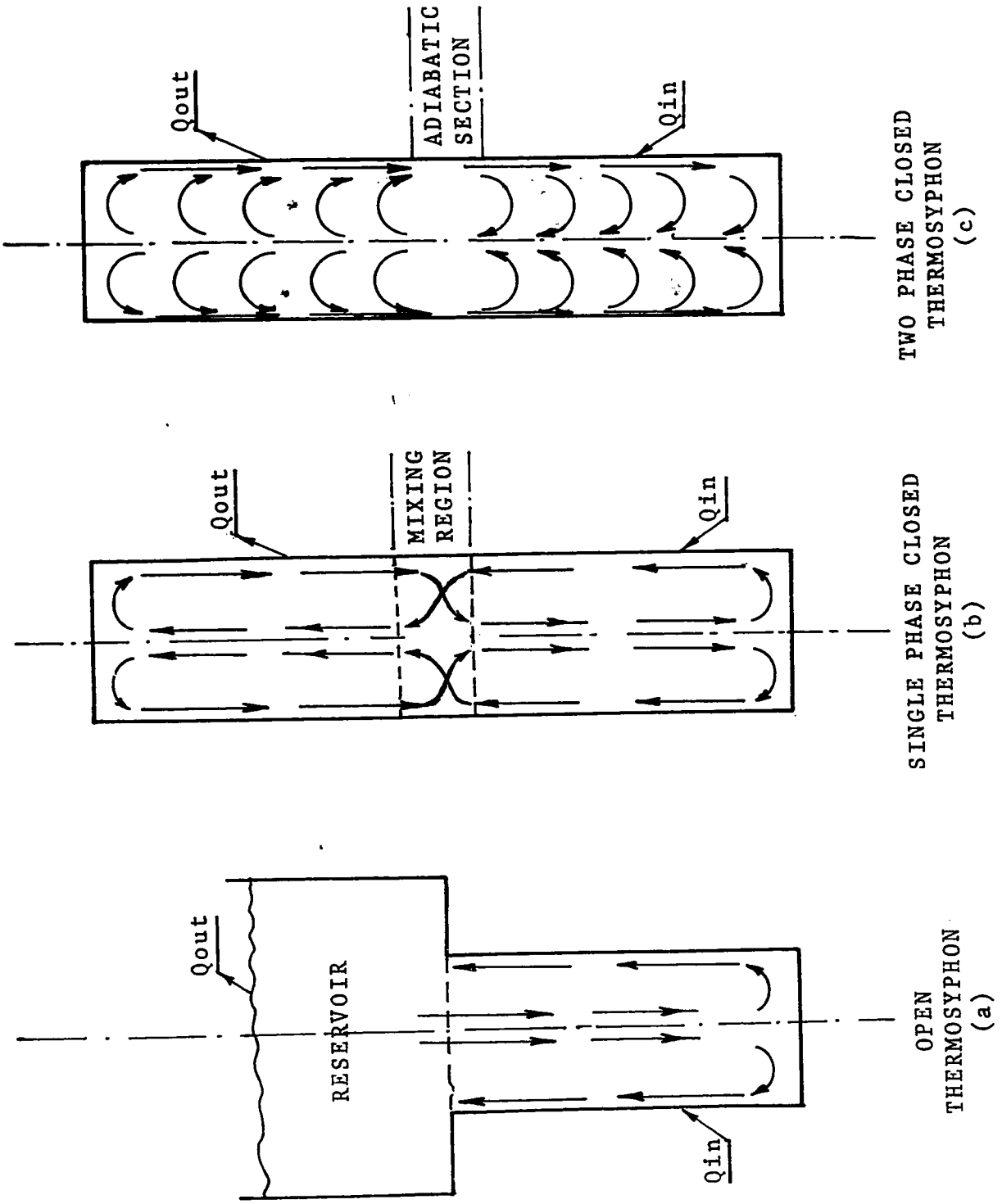
Qout
ADIABATIC SECTION
Qin
TWO PHASE CLOSED THERMOSYPHON (c)
Qout
MIXING REGION
Qin
SINGLE PHASE CLOSED THERMOSYPHON (b)
Qout
RESERVOIR
Qin
OPEN THERMOSYPHON (a)

Fig. 1.1

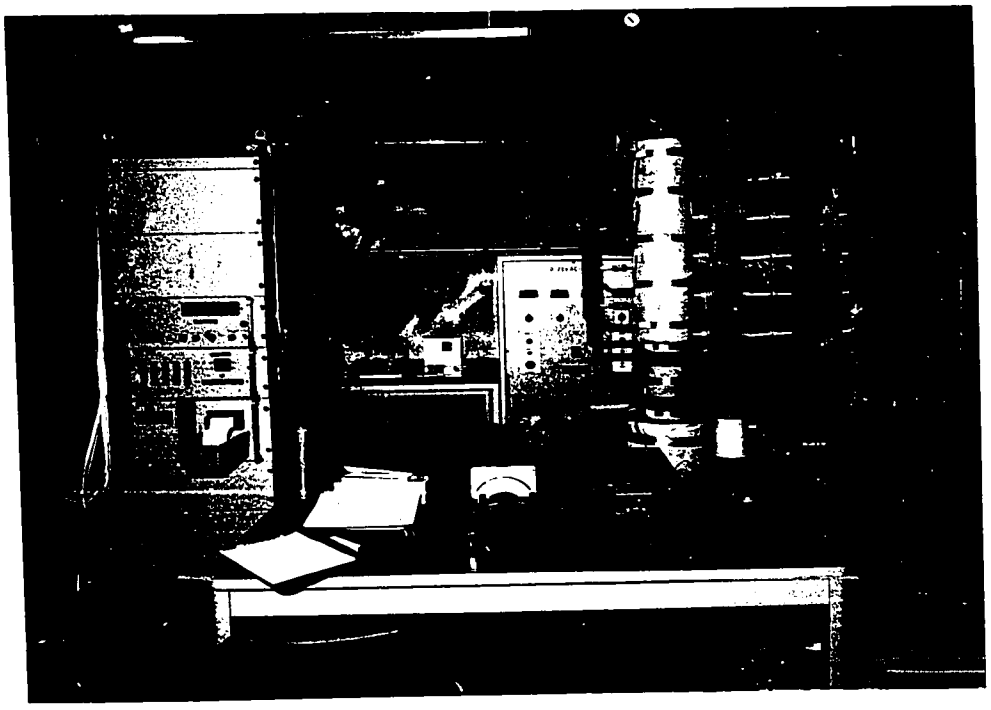

Fig. 3.1 Experimental set-up

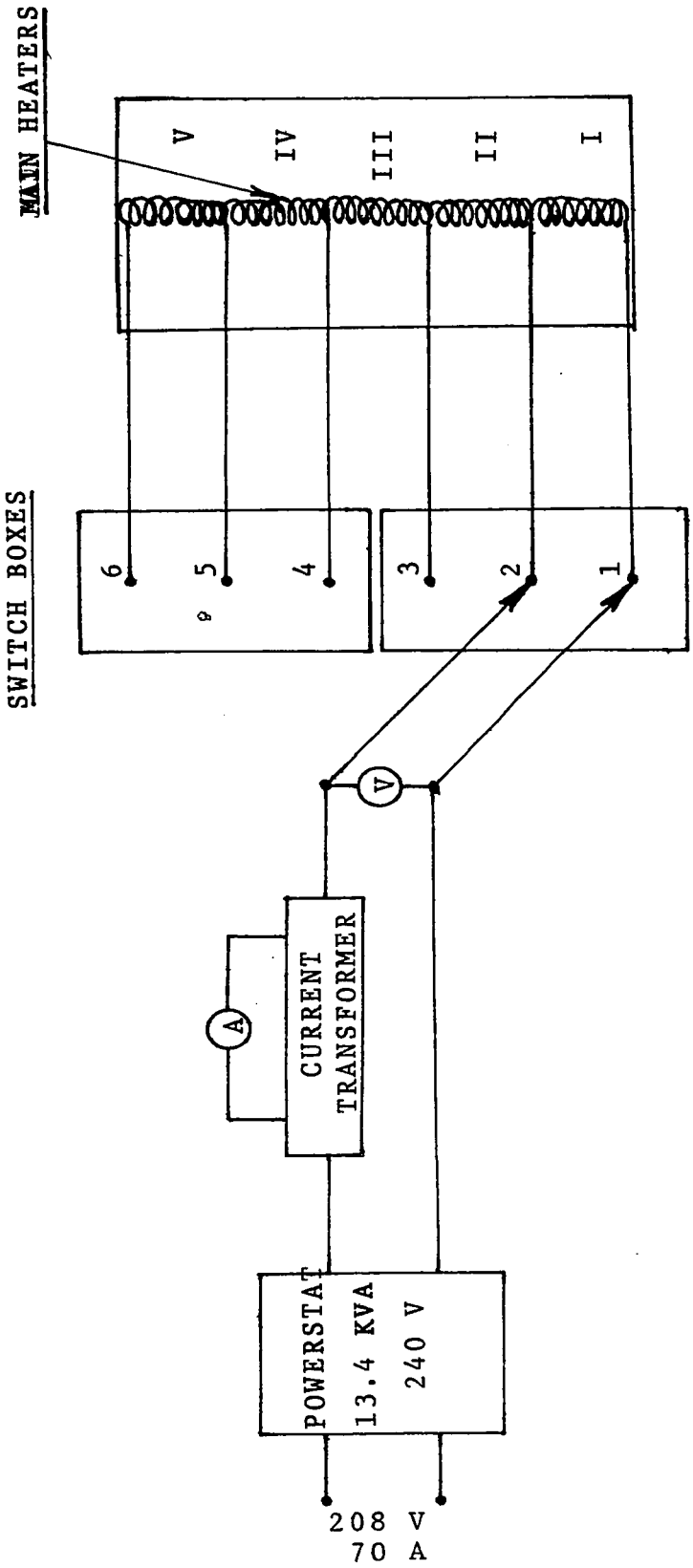

Fig. 3.2 Circuit Diagram for Heating Unit

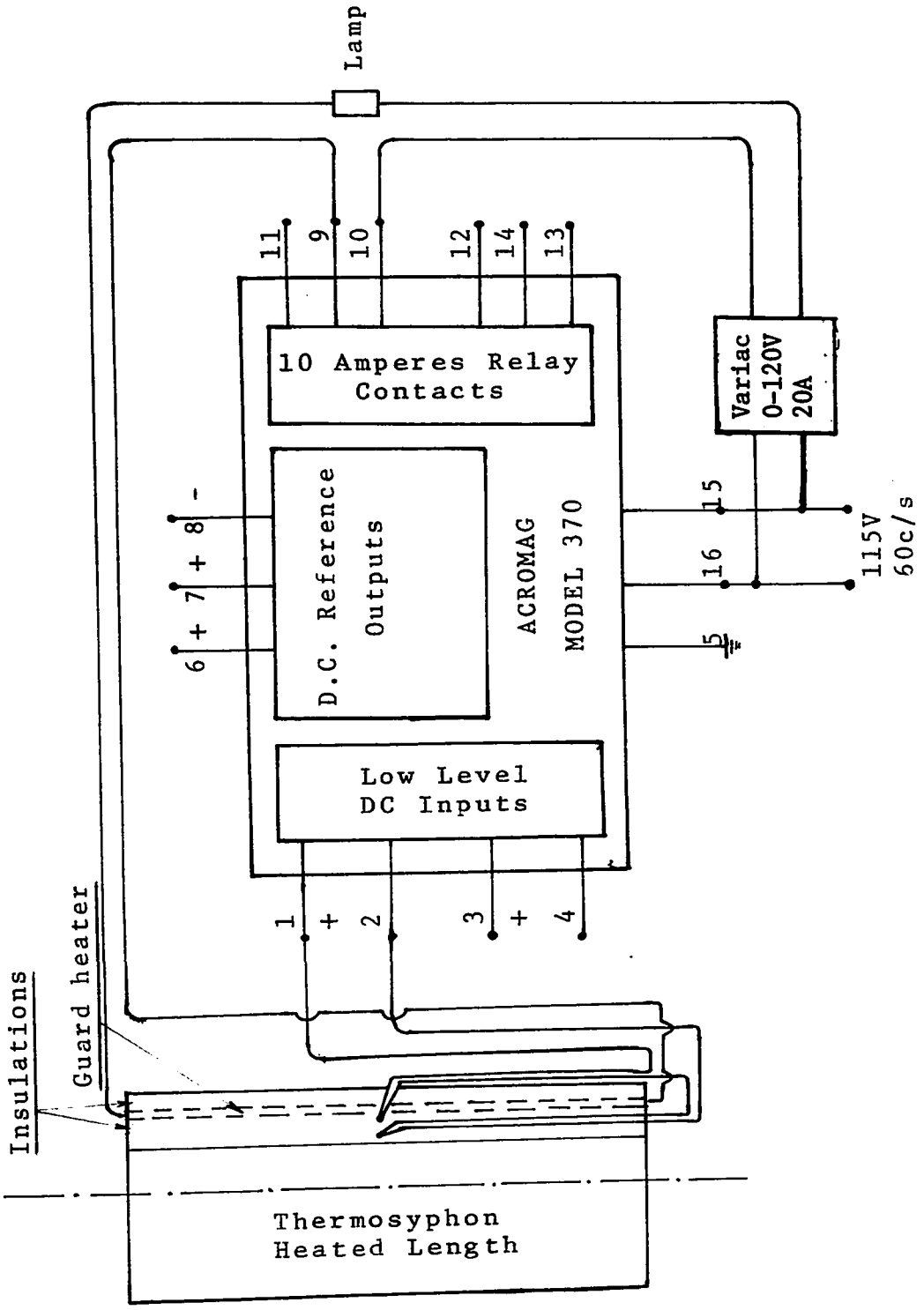

Fig. 3.3 Relay circuit for guard heater

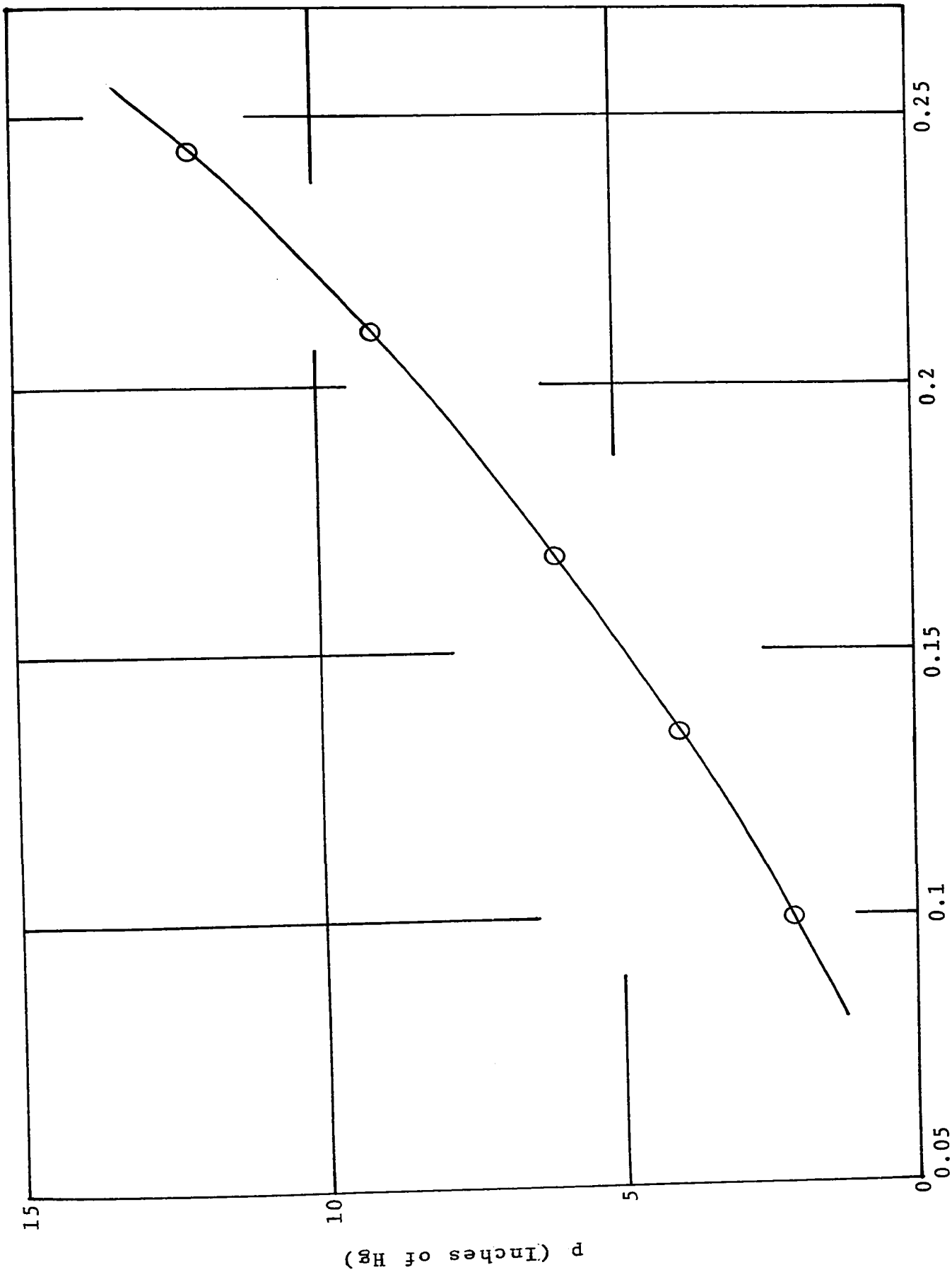

Fig. 3.4 Orifice calibration curve for coolant flow

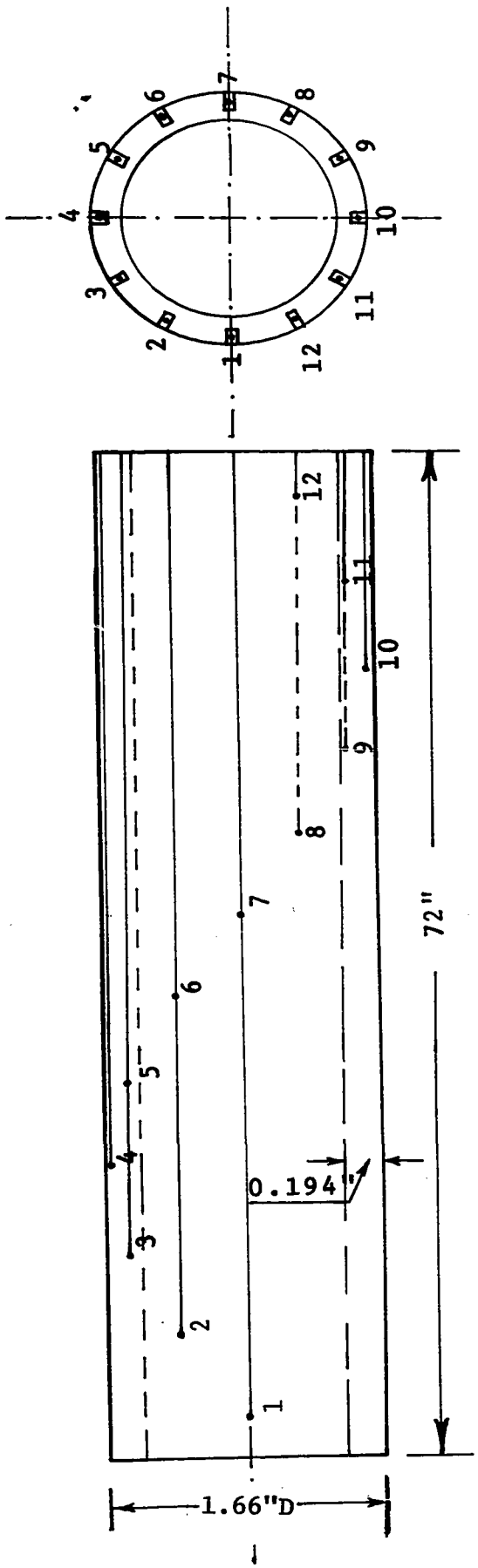

Fig. 3.5 Thermocouples (1-12) placement in the wall of the thermosyphon tube

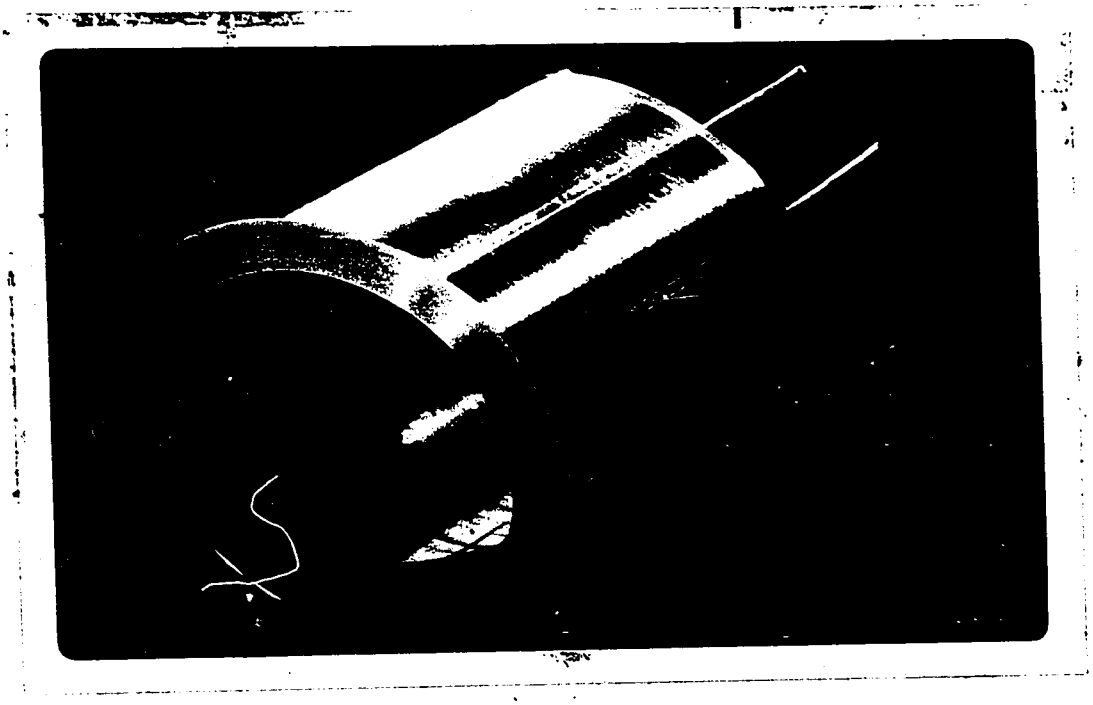

Fig. 3.6 A finished copper tube sample after embedding thermocouples

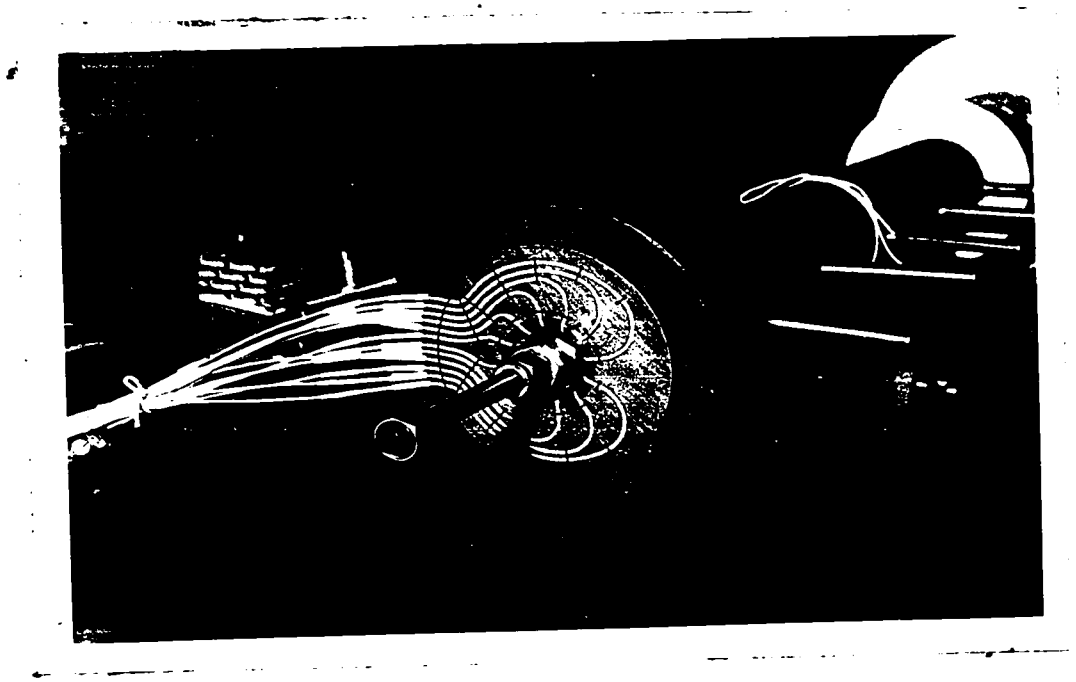

Fig. 3.7 Thermocouples in teflon tubing supported on a brass disc

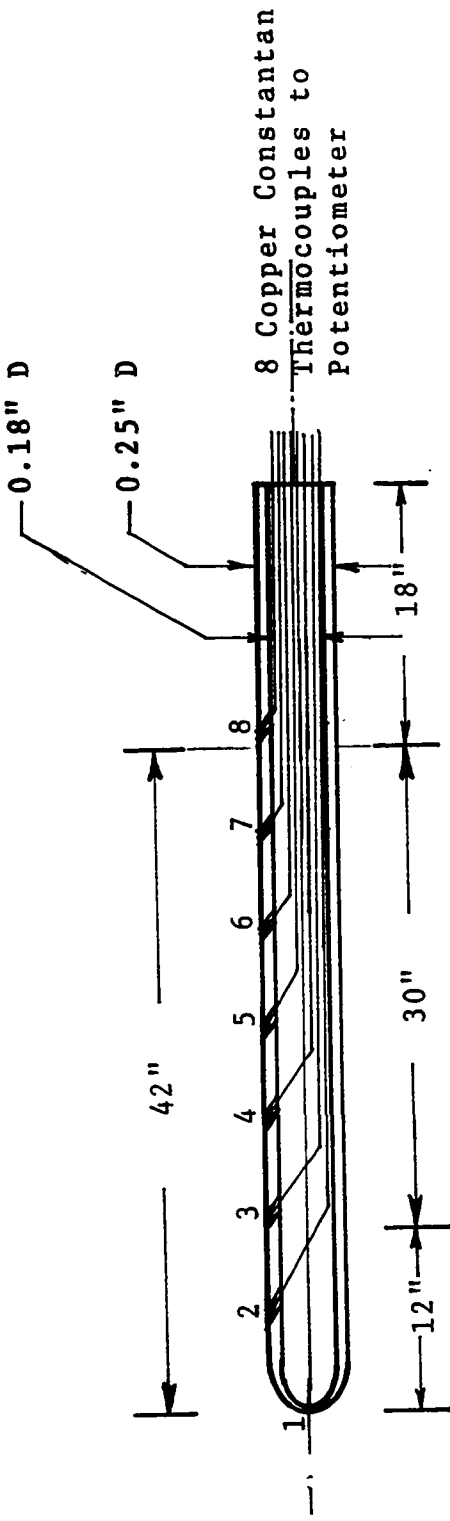

Fig. 3.8 Locations of the thermocouples inside the stainless steel probe

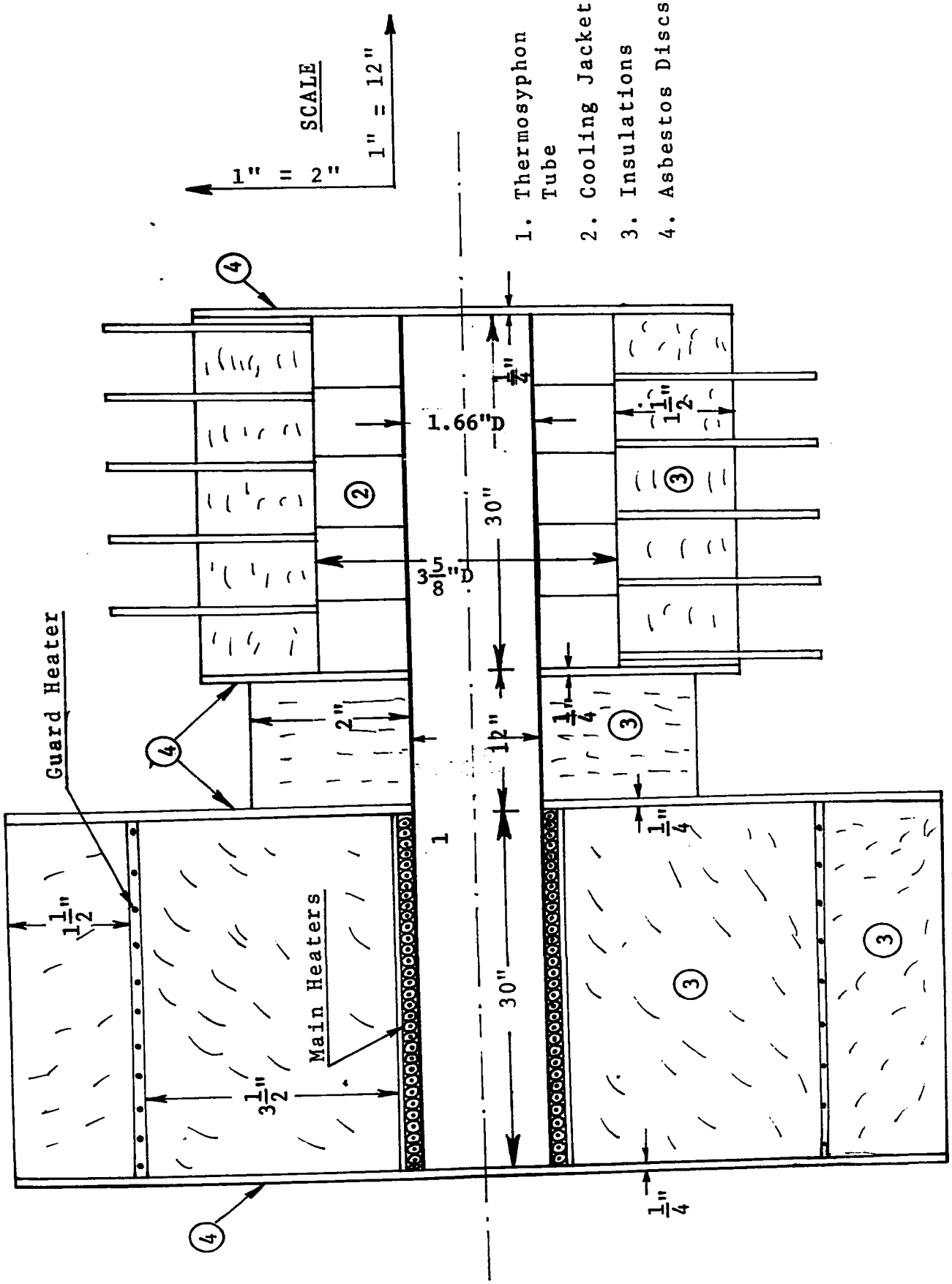

Fig. 3.9 Details of the test section

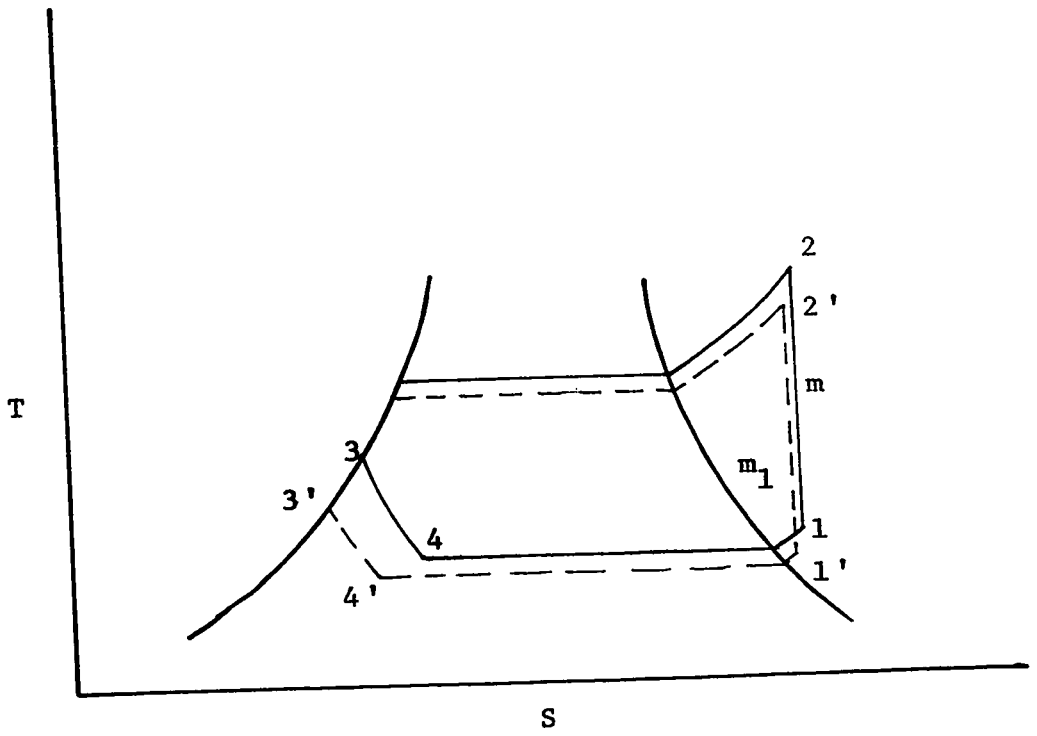

——— At Full Load

---- At Low Load

Fig. 3.10(a) Refrigeration cycle

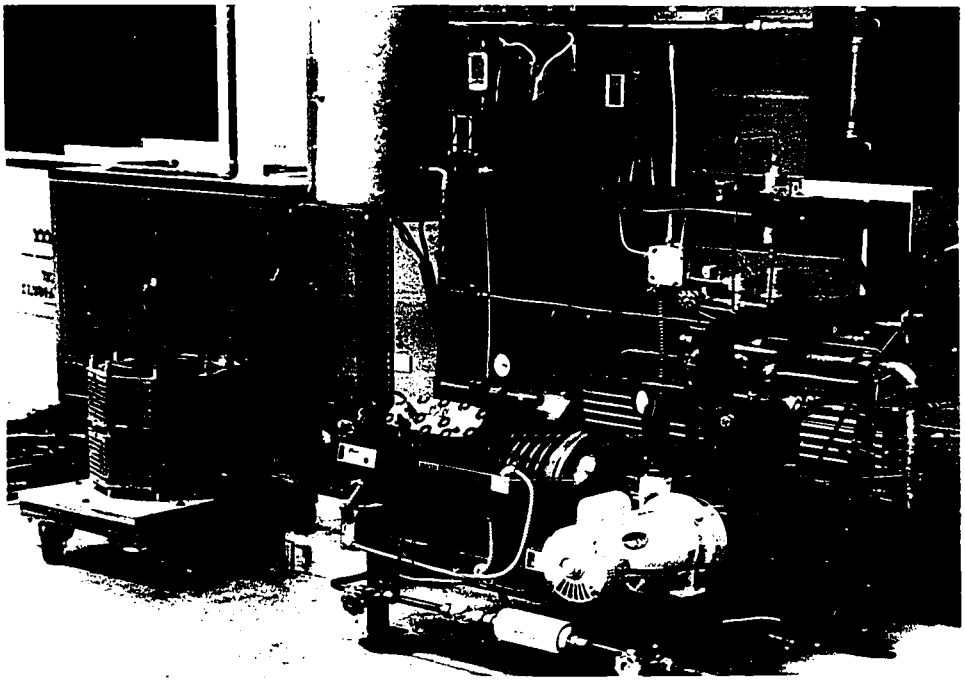

Fig. 3.10(b) Modified cooling unit

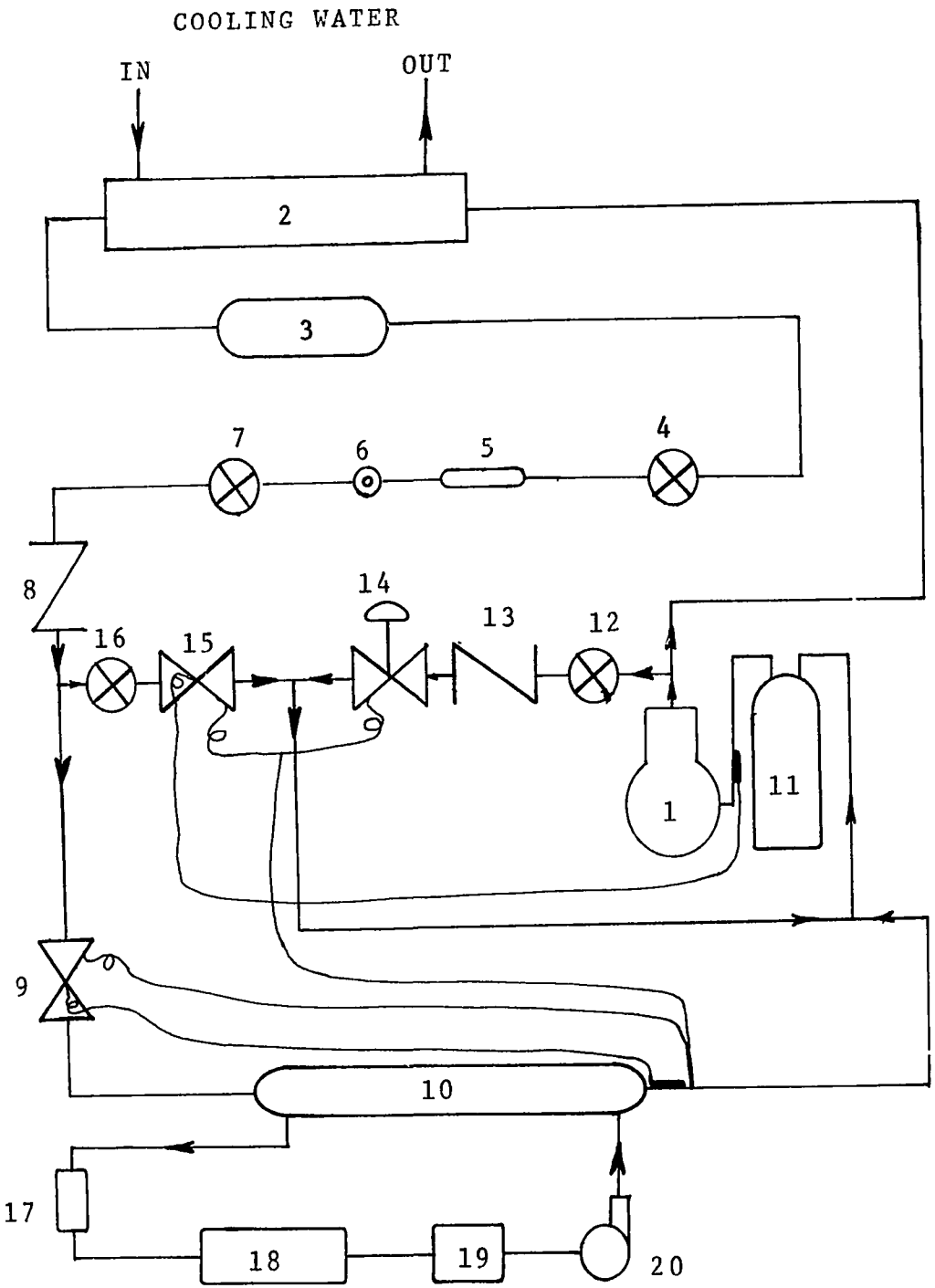

1. Compressor 50 PEL, 5 LP, 230 V, 1Ph, 60 c/s
2. Condenser
3. Receiver
4. Valve
5. Drier, Sporlan, Type C-305
6. Sight Glass, Sporlan
7. Valve
8. Solenoid Valve, Sporlan, Type 12P
9. Thermostatic Expansion Valve
10. Evaporator, Model CH348AITS
11. Suction Accumulator
12. Valve
13. Solenoid Valve, Sporlan Type A1052
14. Discharge by pass valve, Sporlan, ADRPE3
15. Thermostatic Expansion Valve ALCO, LCL2B
16. Valve
17. Test Section
18. Coolant tank with four heaters
19. Tank with 1.5 KW additional heaters
20. Pump

Fig. 3.11 Details of Cooling System

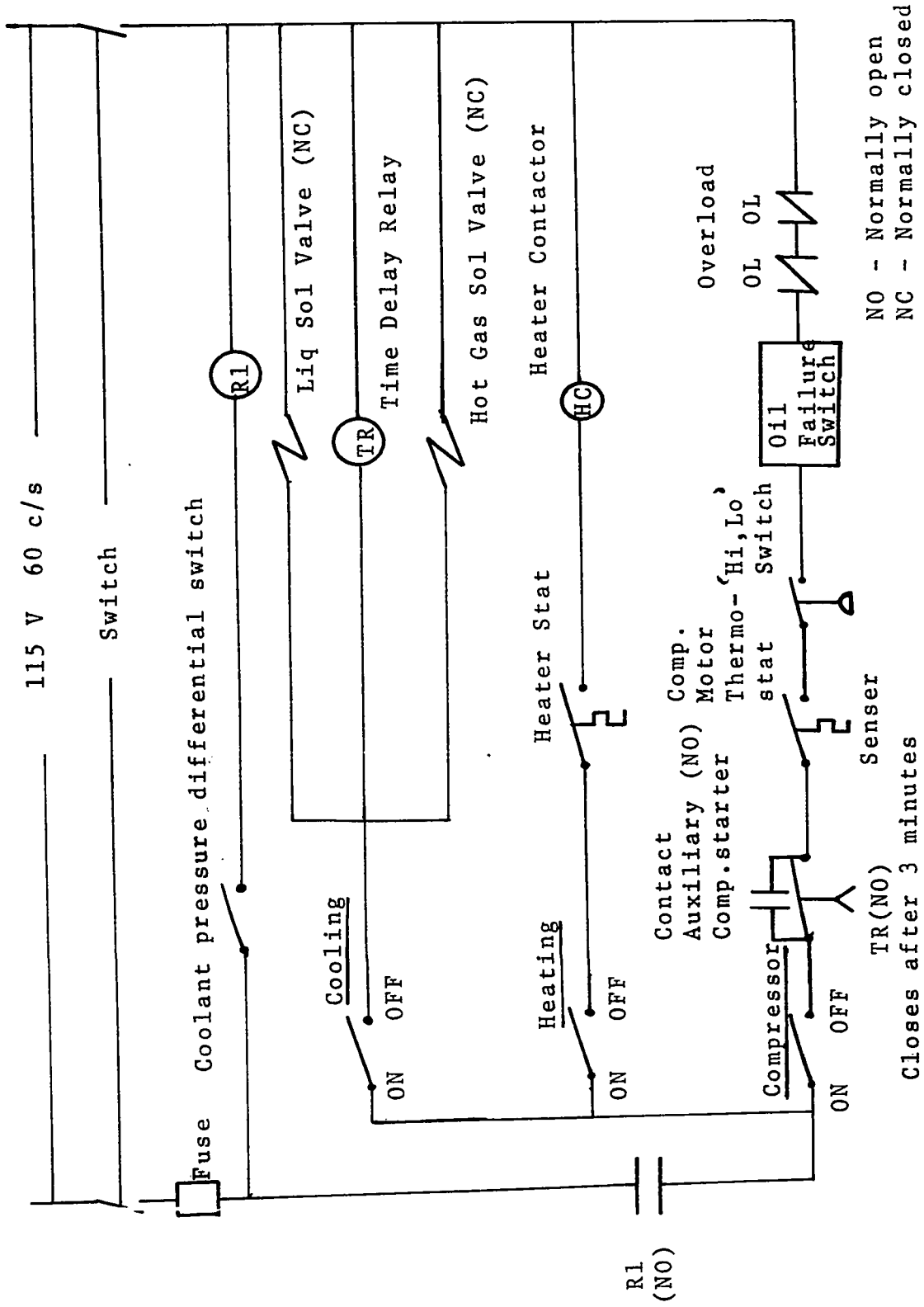

Fig. 3.12 Cooling system control

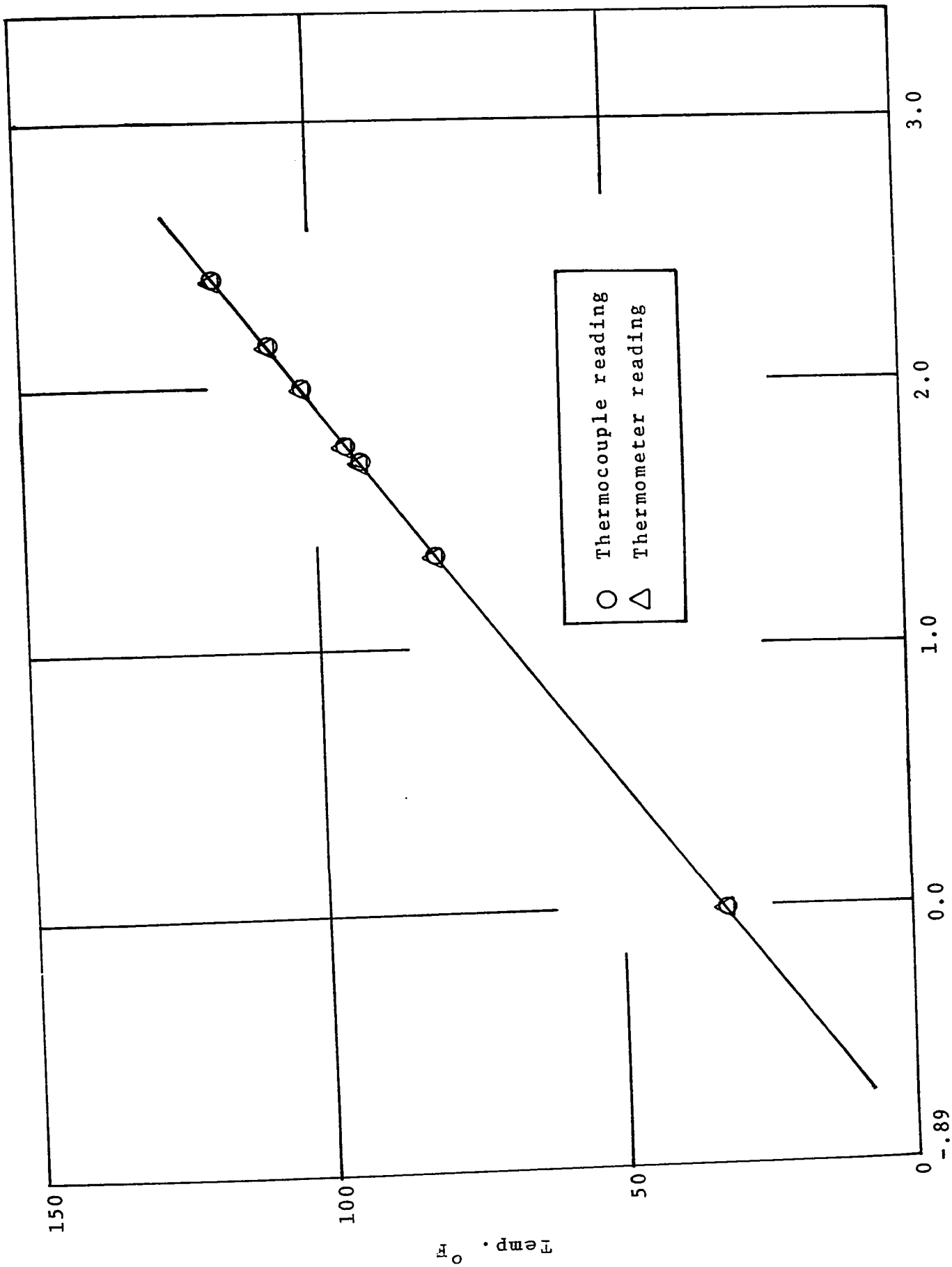

Fig. 3.13 Calibration curve for Iron-Constantan thermocouples

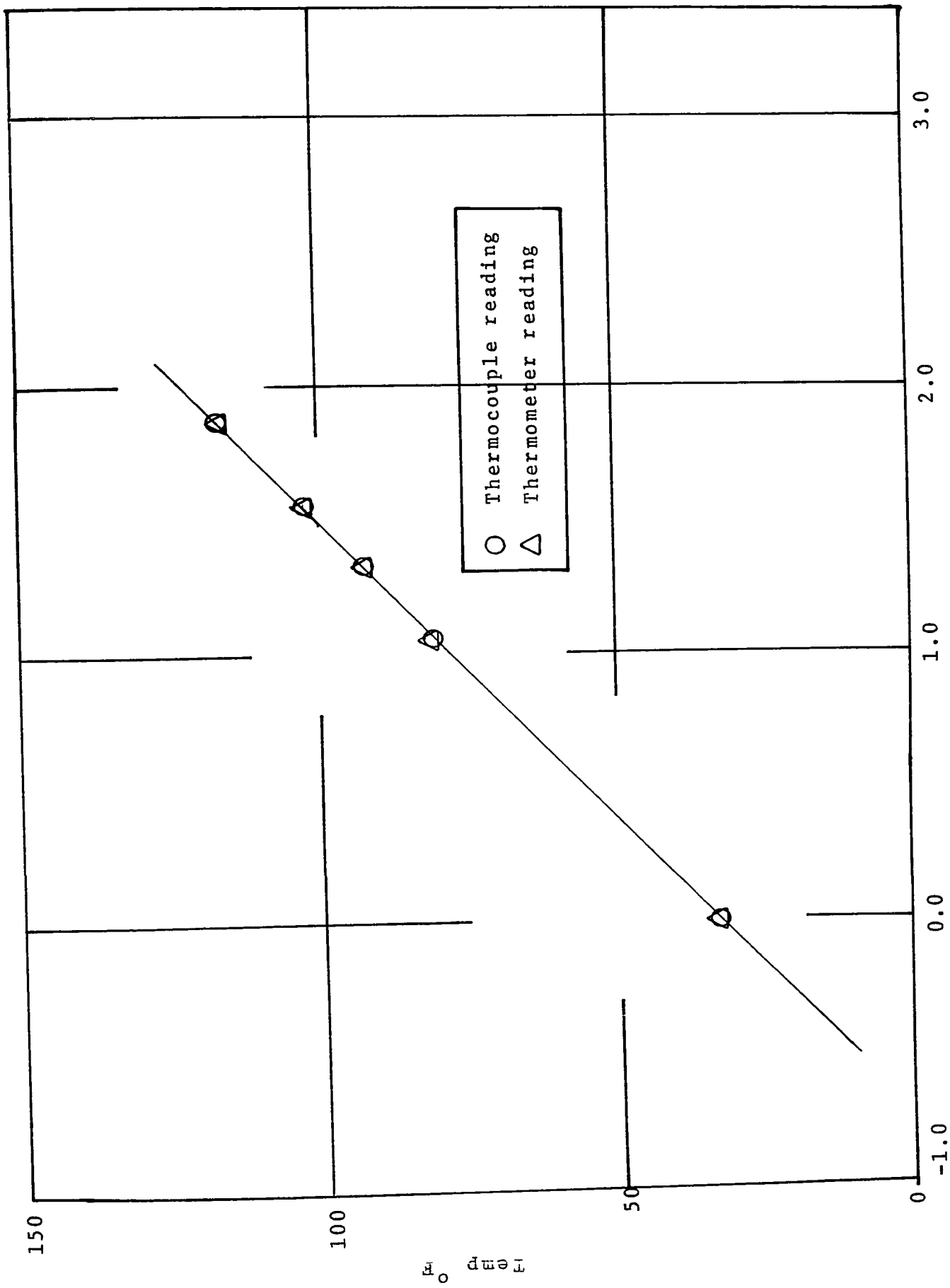

Fig. 3.14 Calibration curve for Copper-Constanton thermocouples

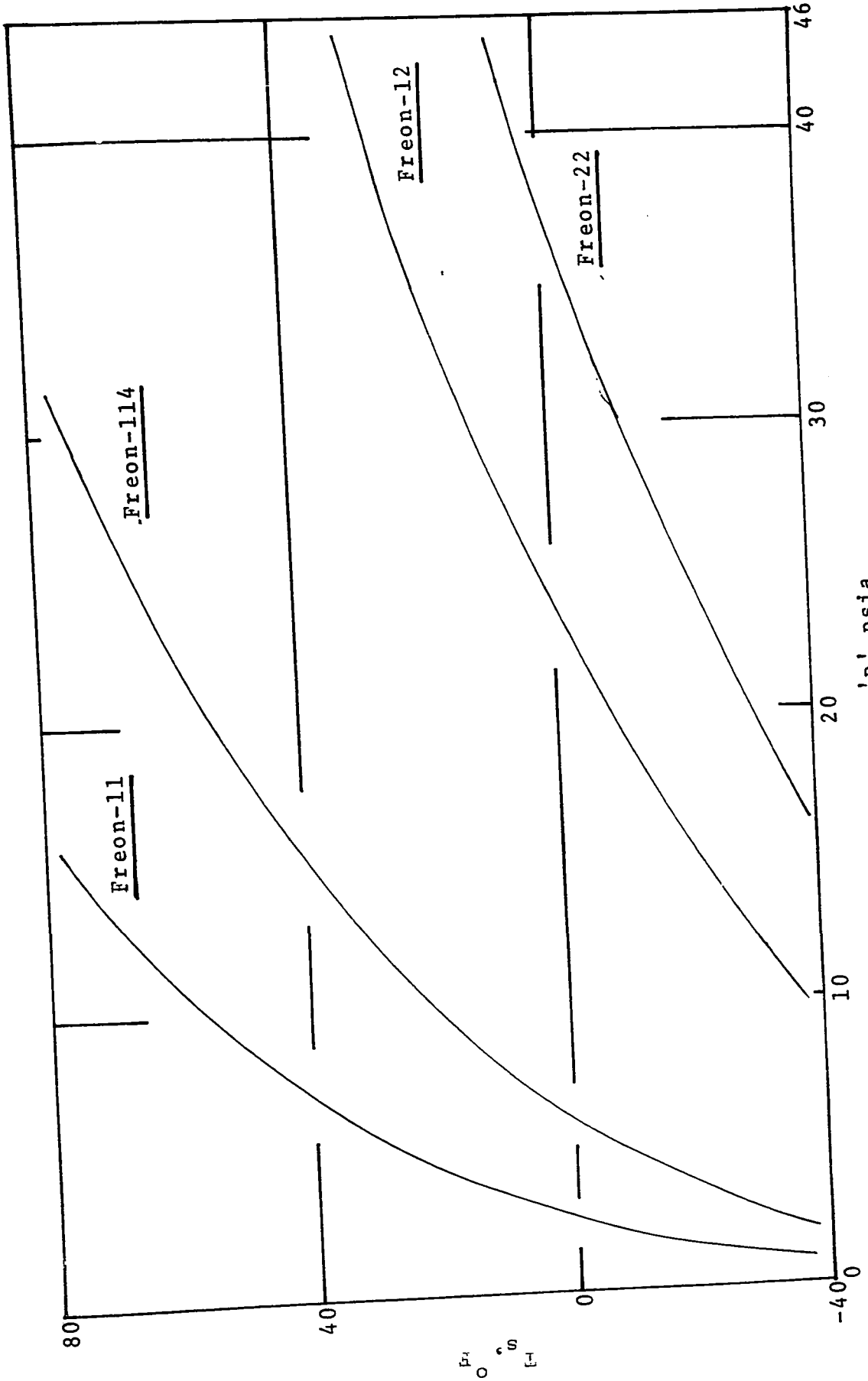

Fig. 3.15 Pressure-Saturation temperature relationship for different refrigerants

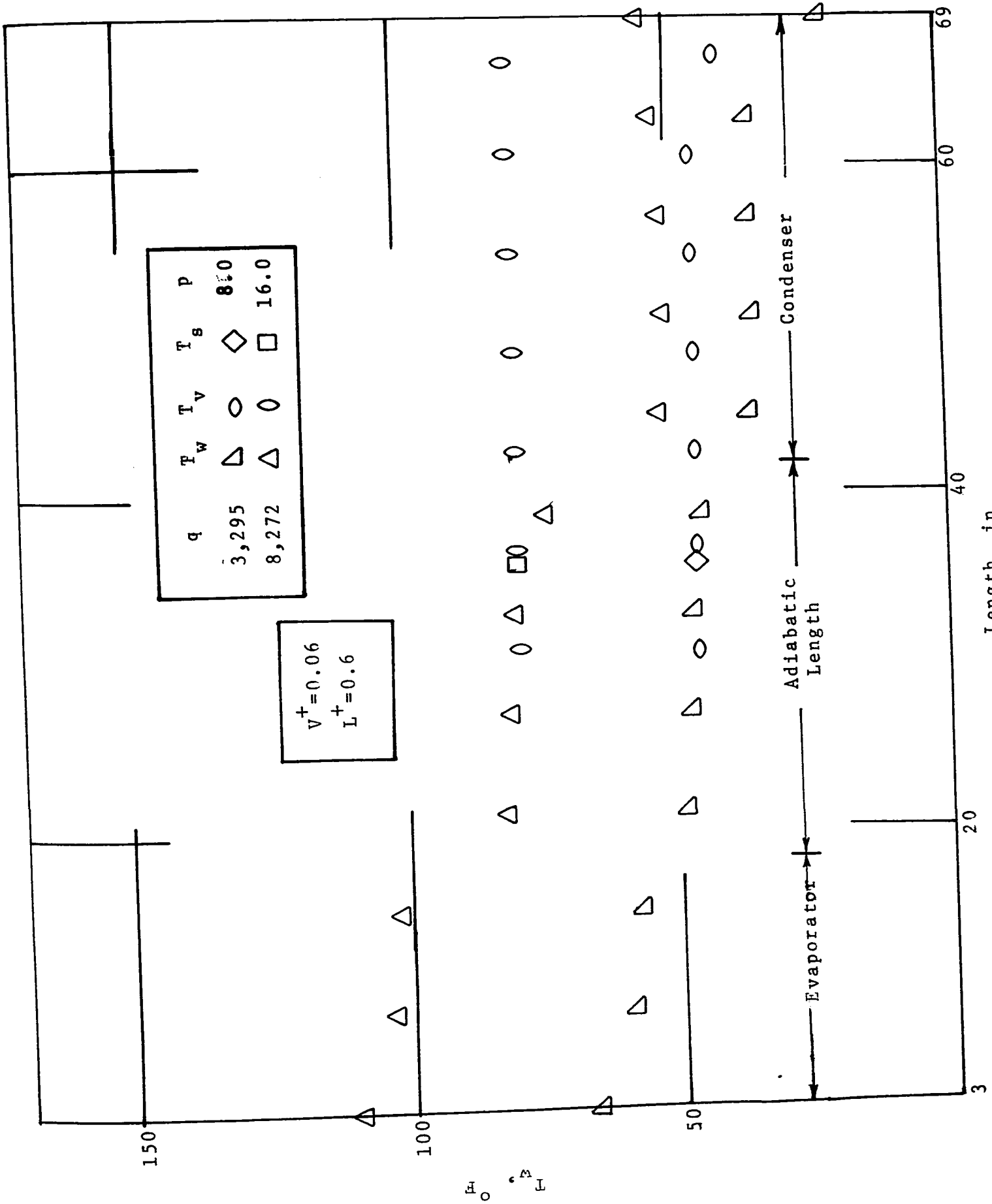

Fig. 4.1(a) Effect of heat flux on wall temperature distribution

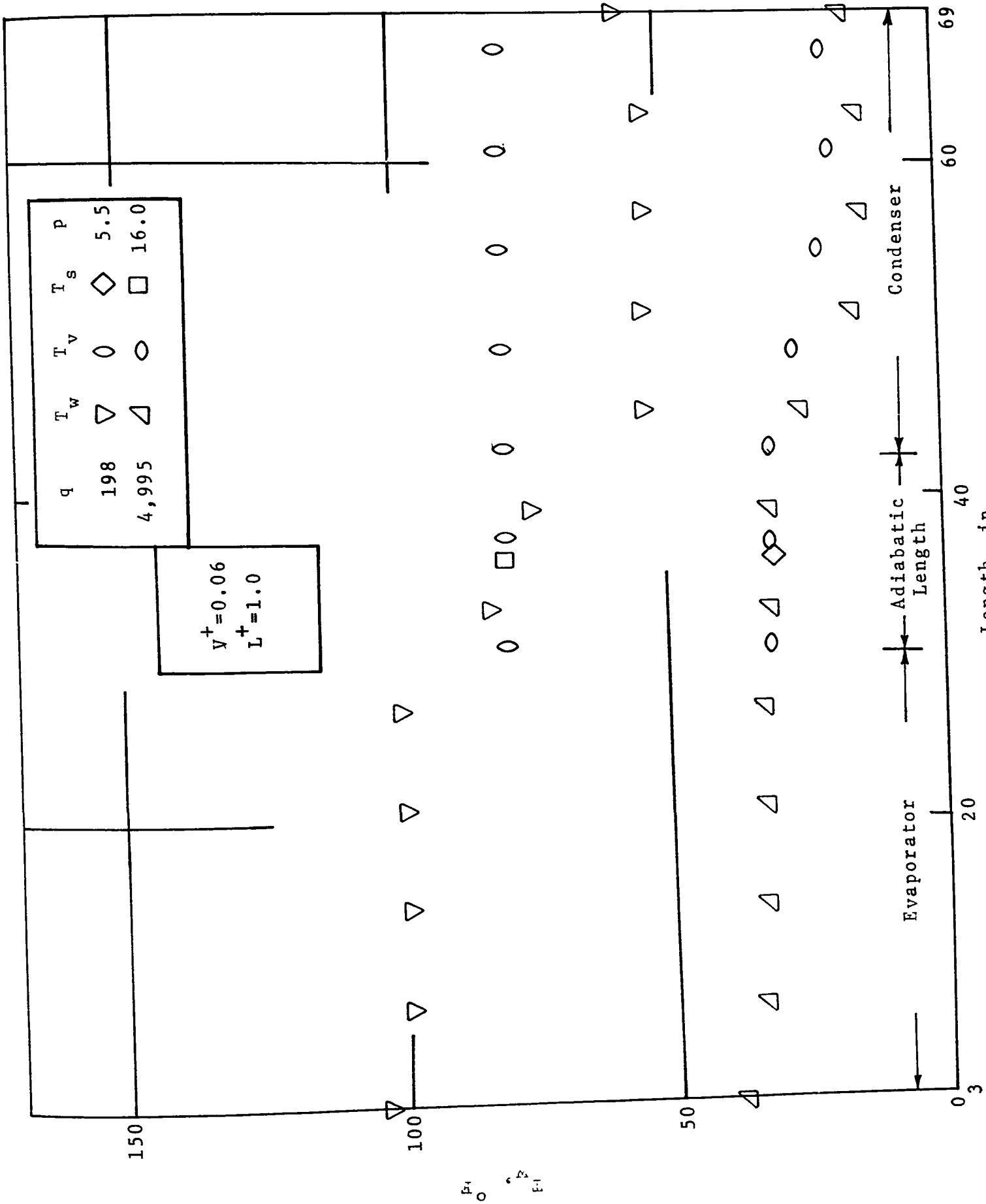

Fig. 4.1(b) Effect of heat flux on wall temperature distribution

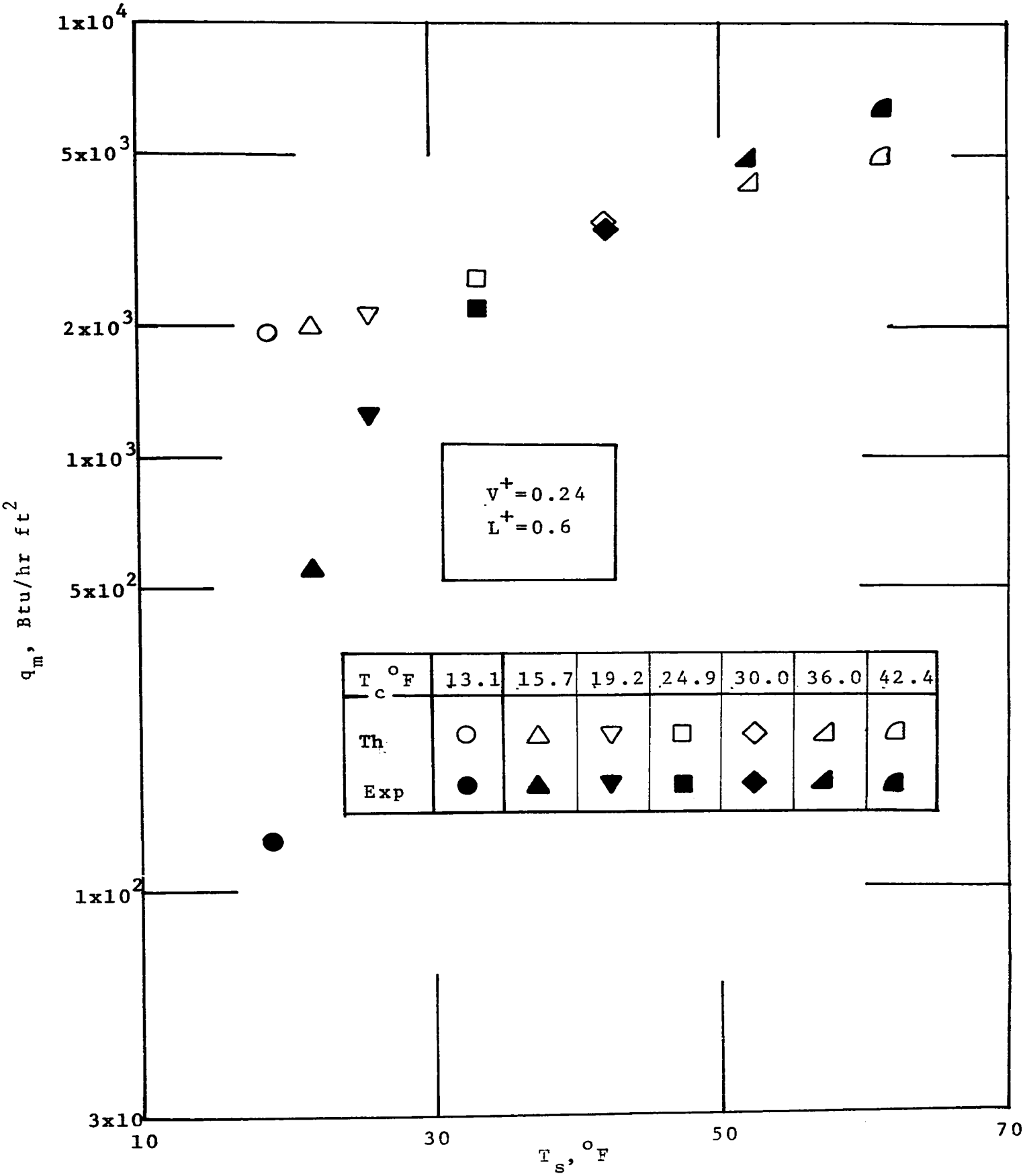

Fig. 4.2(a) Comparison of the experimental results with the theoretical values for maximum heat flux

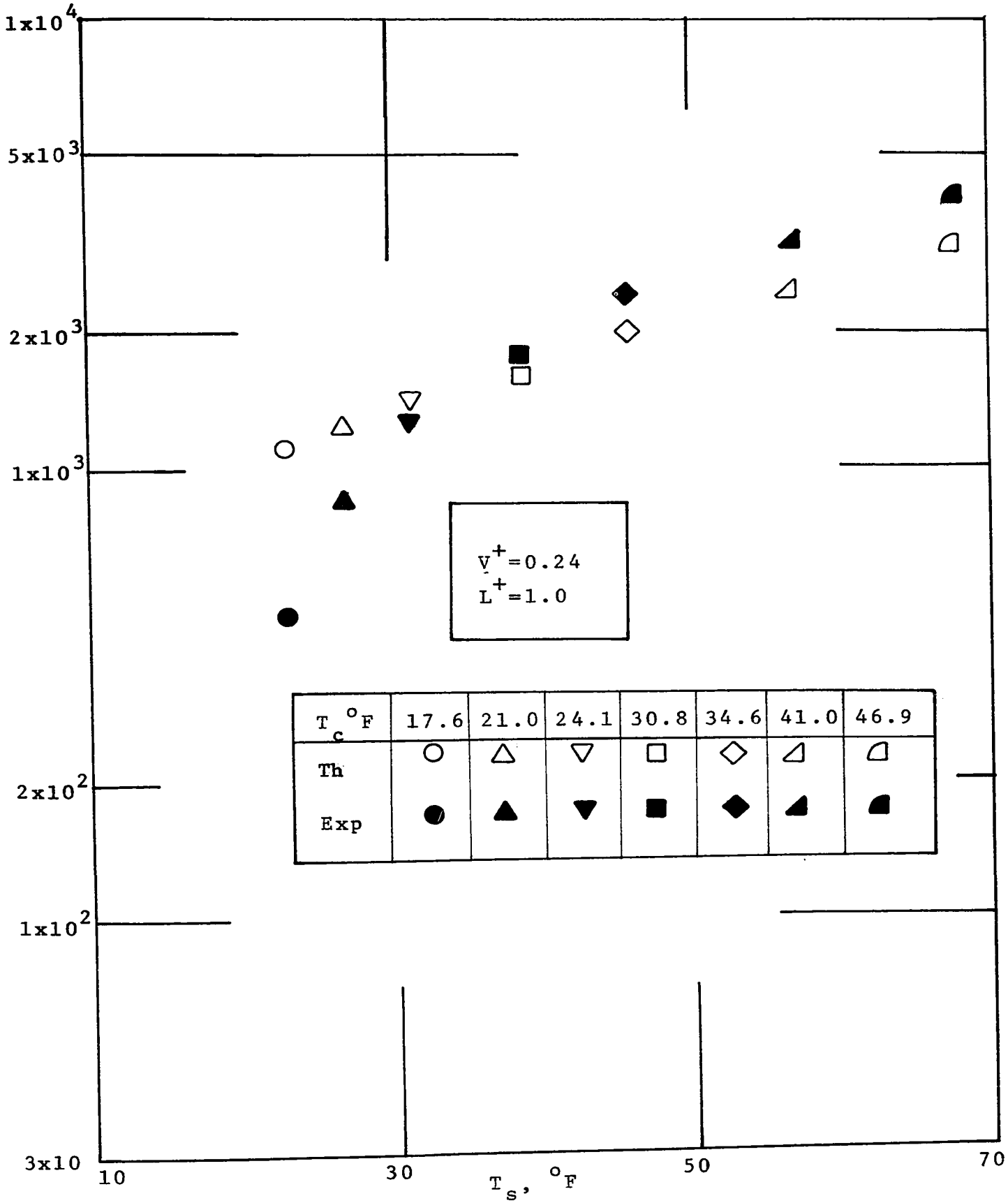

Fig. 4.2(b) Comparison of the experimental results with the theoretical values for maximum heat flux

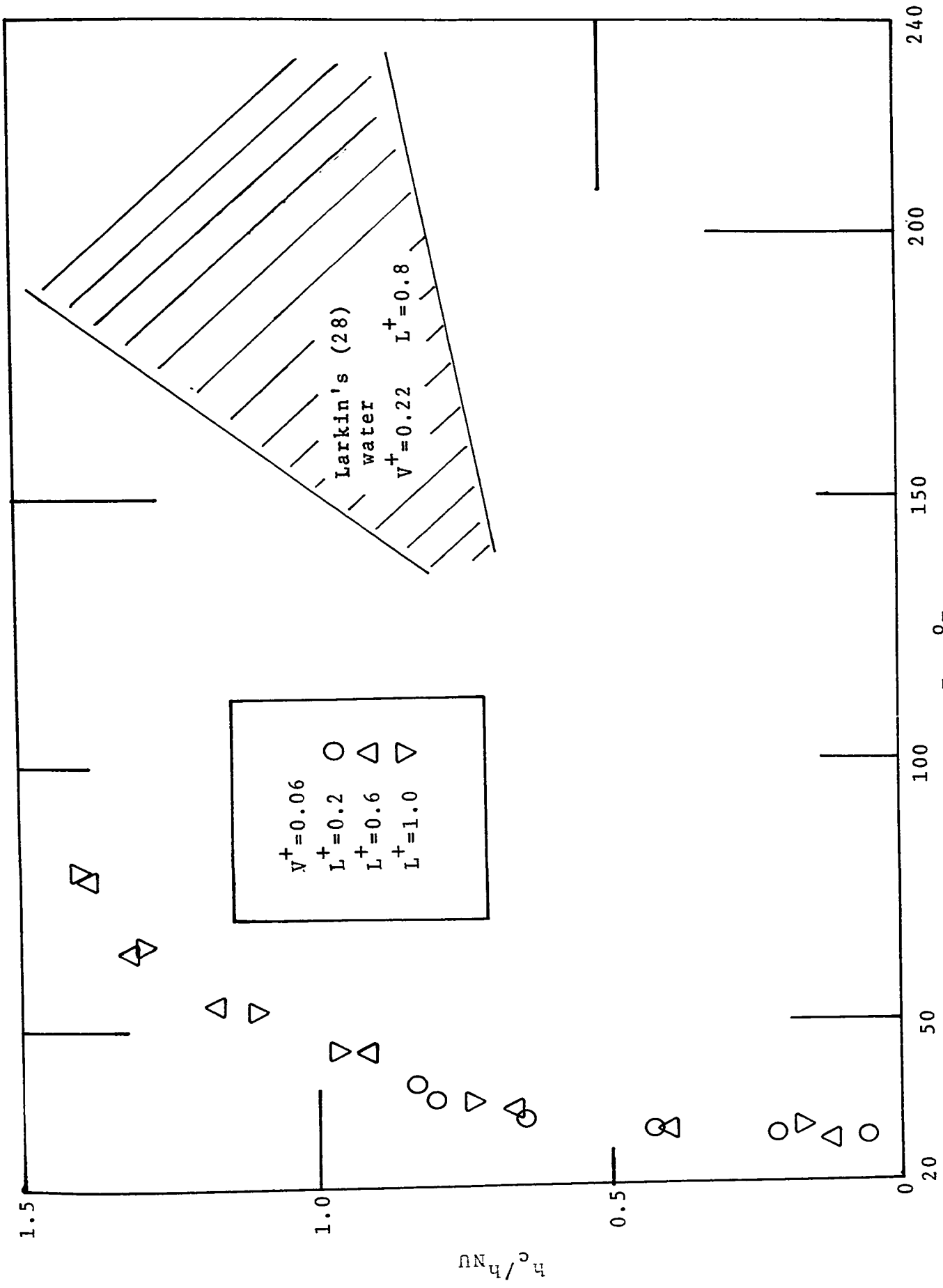

Fig. 4.3 Variation of condensing heat transfer coefficient as compared to Nusselt heat transfer coefficient

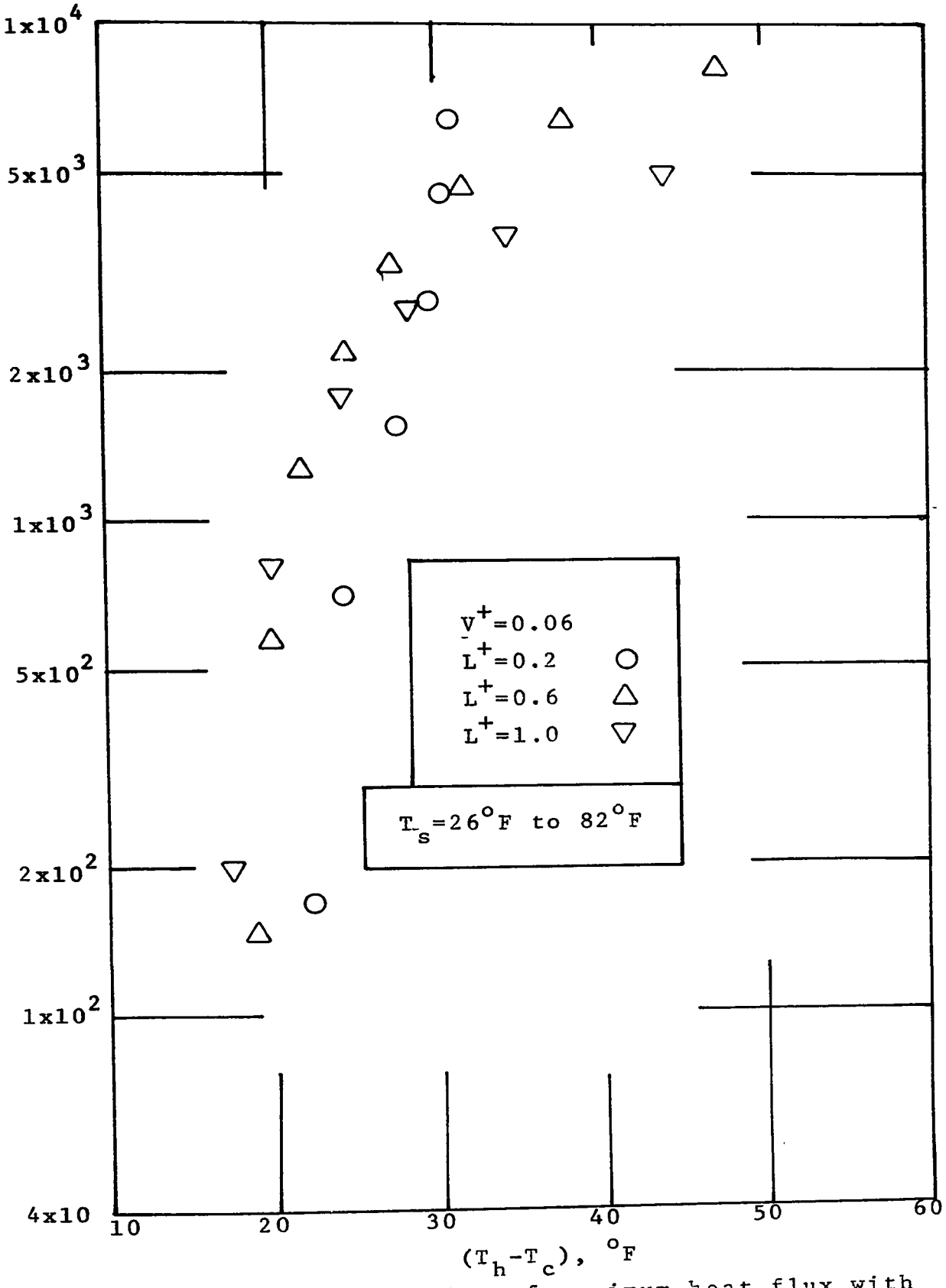

Fig. 4.4(a) Variation of maximum heat flux with (T_h-T_c)

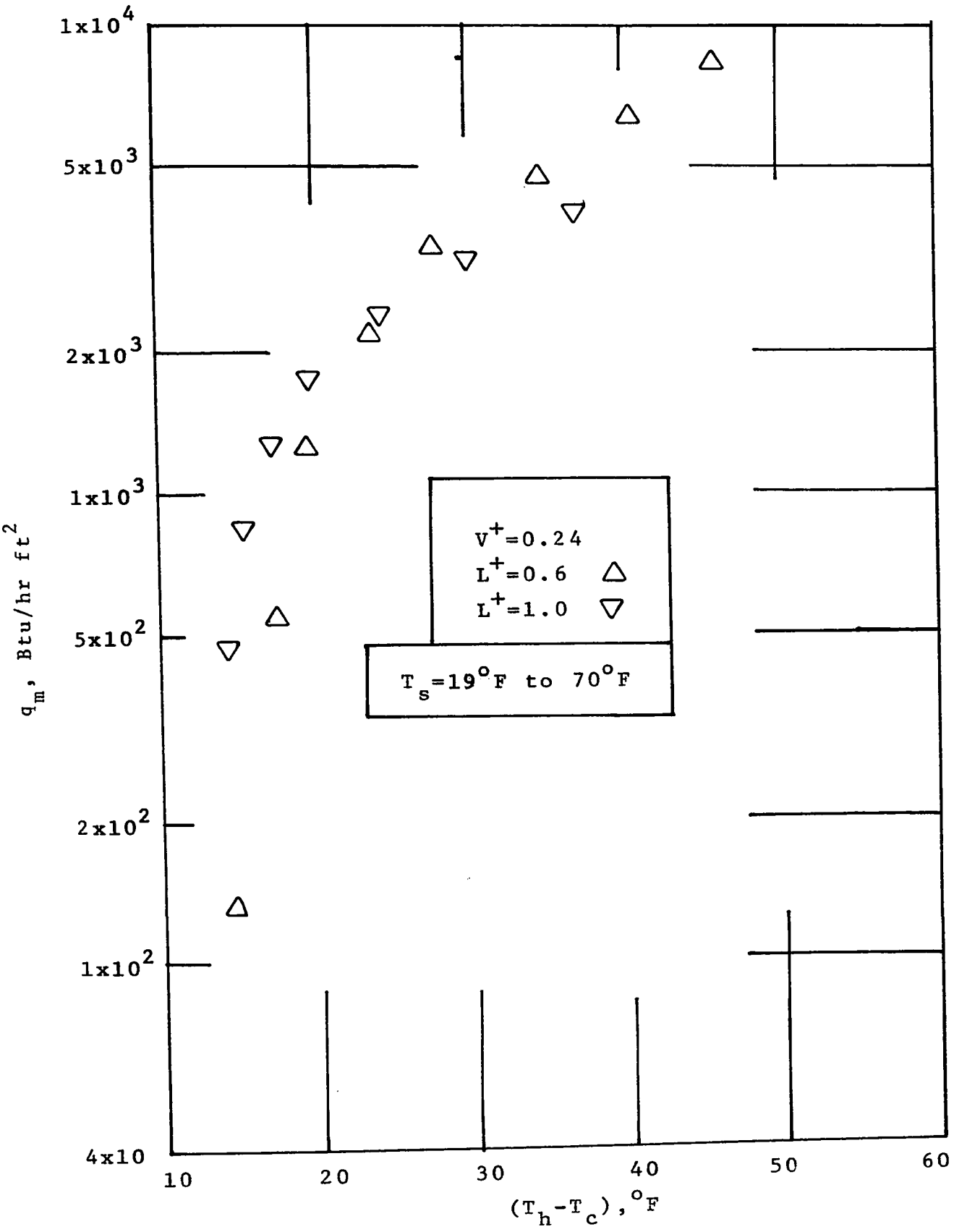

Fig. 4.4(b) Variation of maximum heat flux with (T_h-T_c)

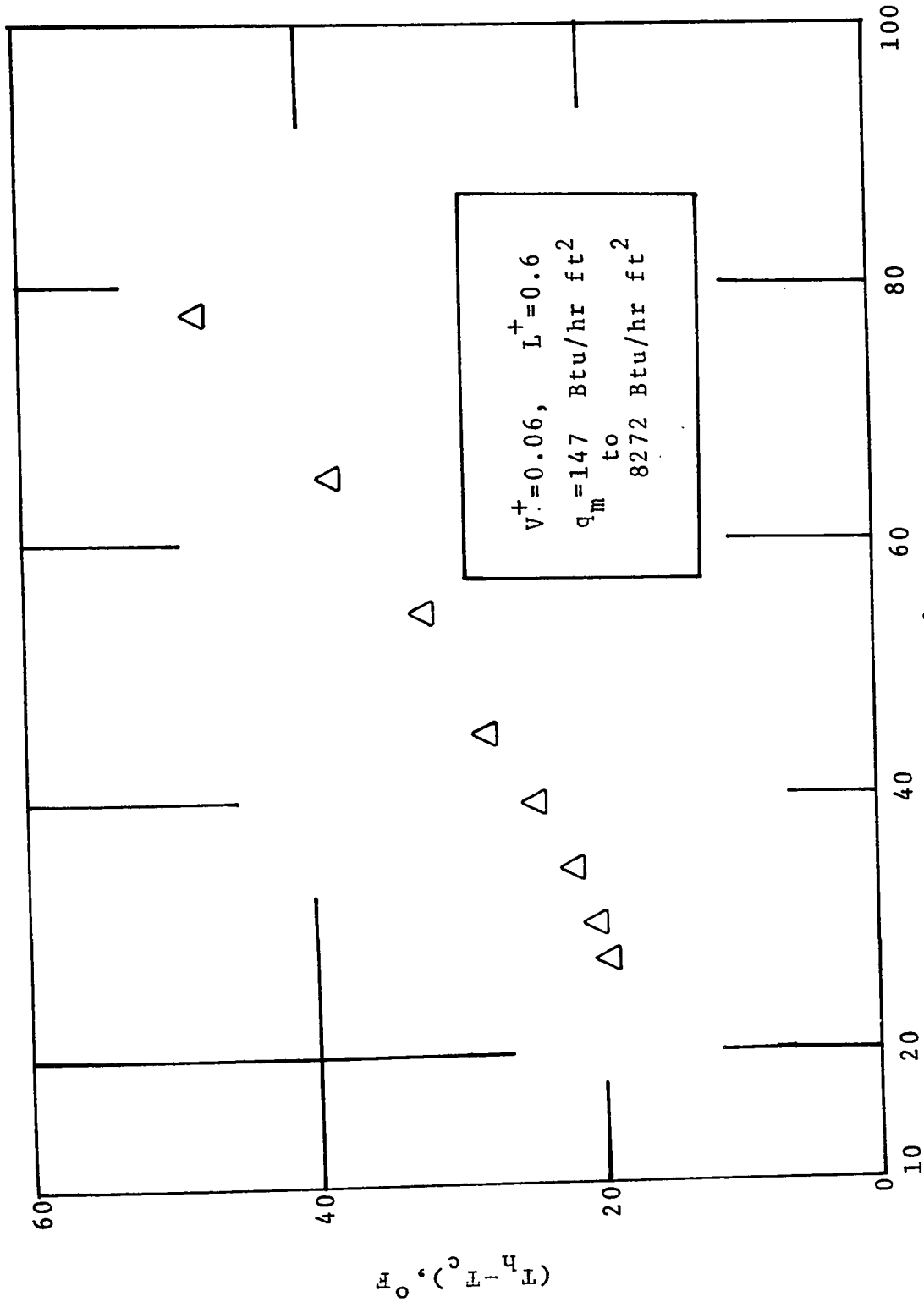

Fig. 4.5 The comparative dependence of (T_h-T_c) and T_s on maximum heat flux

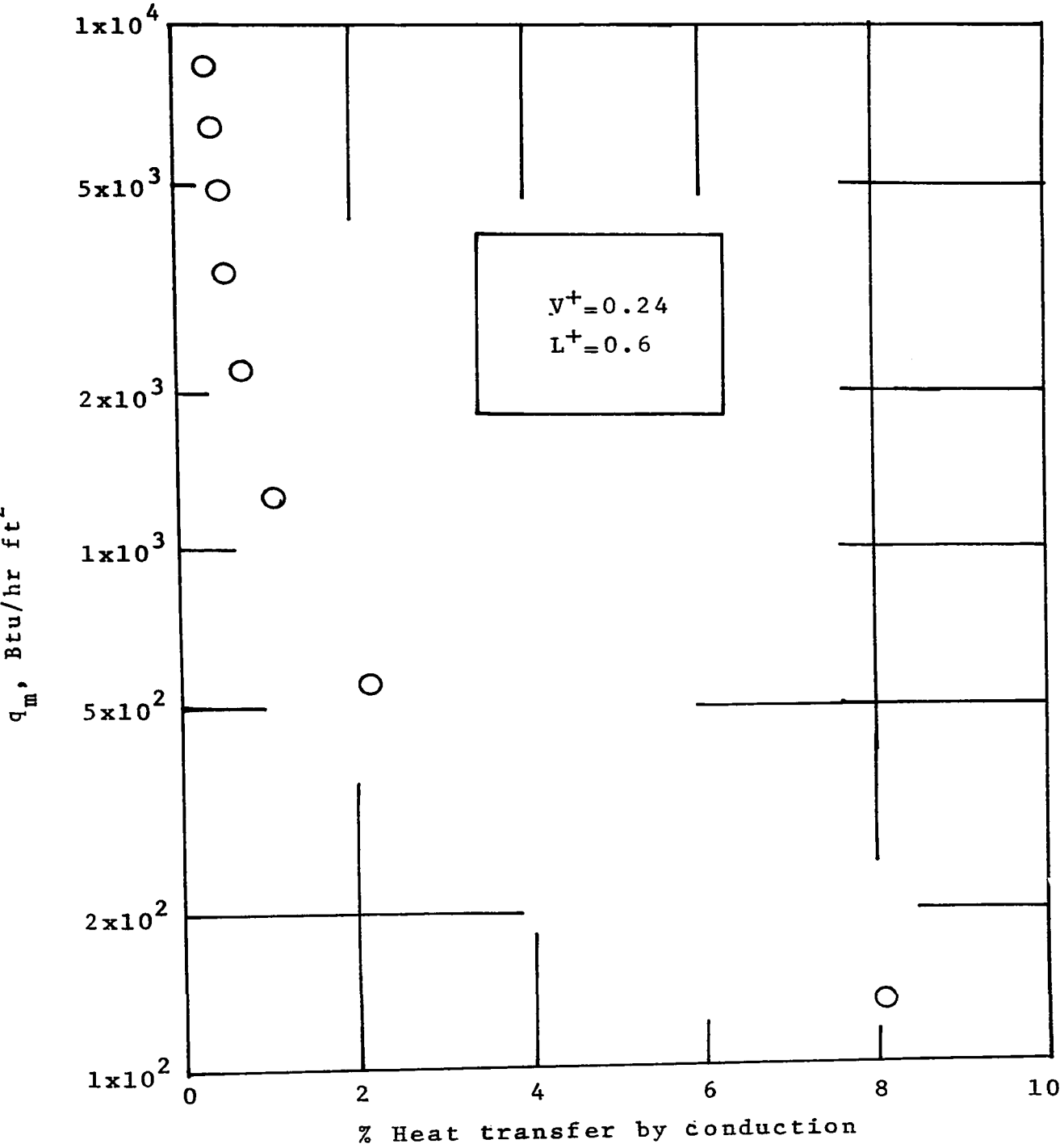

Fig. 4.6 Maximum heat flux vs $\left(\frac{\text{conduction heat trasfer}}{\text{overall heat transfer}} \times 100\right)$

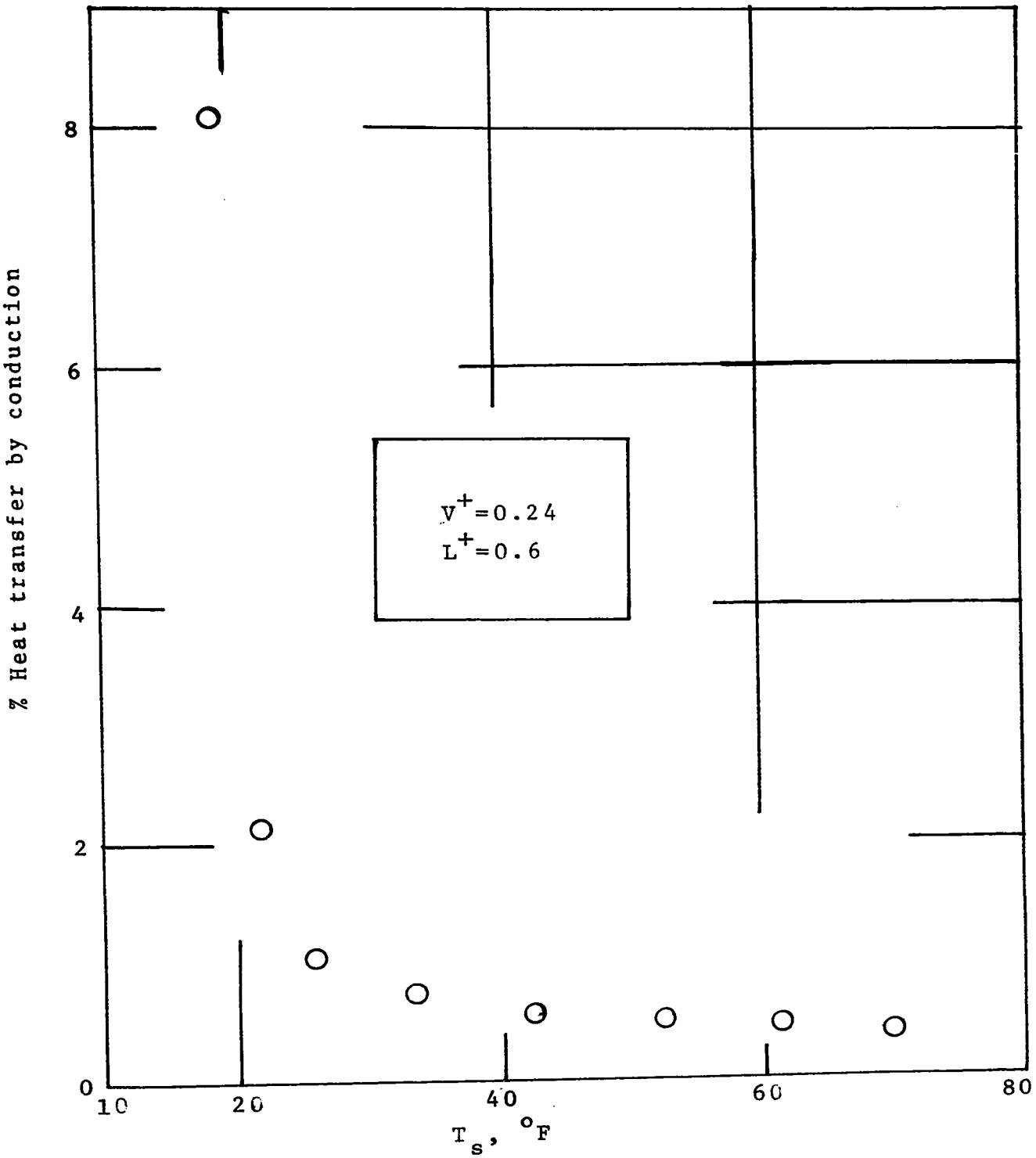

Fig. 4.7 ($\frac{\text{conduction heat transfer}}{\text{overall heat transfer}}$ x 100) vs T_s

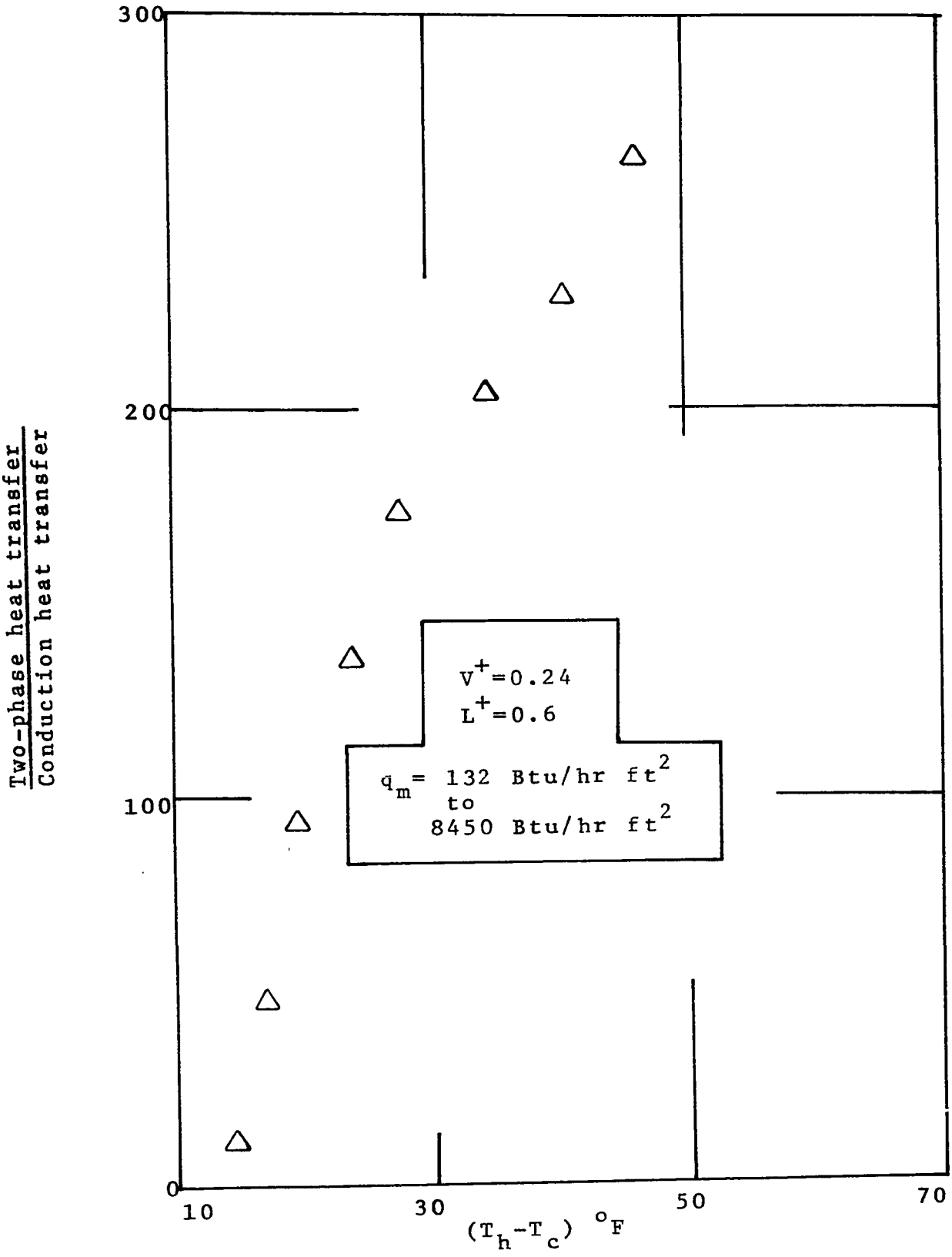

Fig. 4.8 Two-phase heat transfer as compared to conduction heat transfer vs (T_h-T_c)

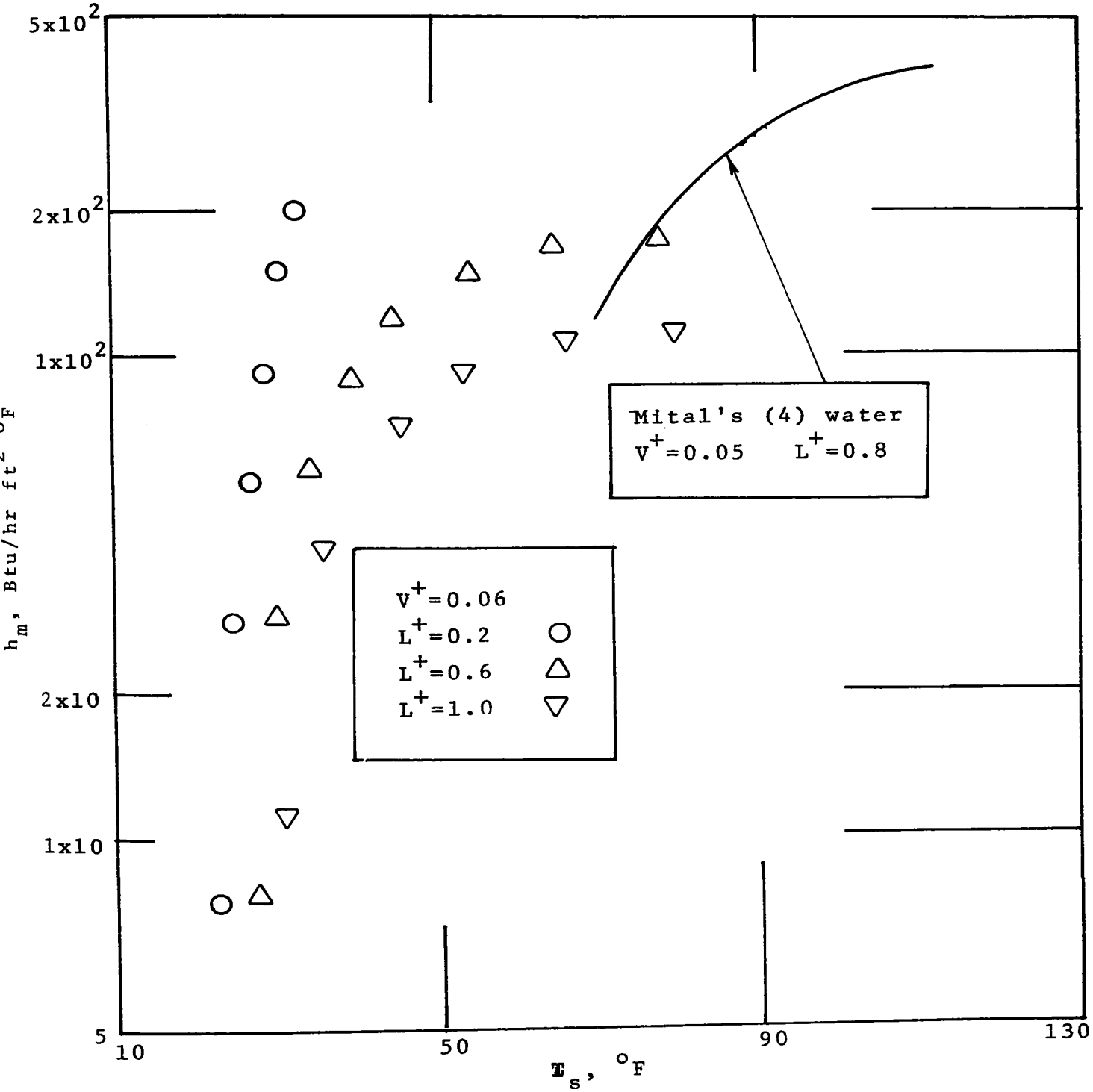

Fig. 4.9(a) Variation of maximum heat transfer coefficient with T_s for different L^+

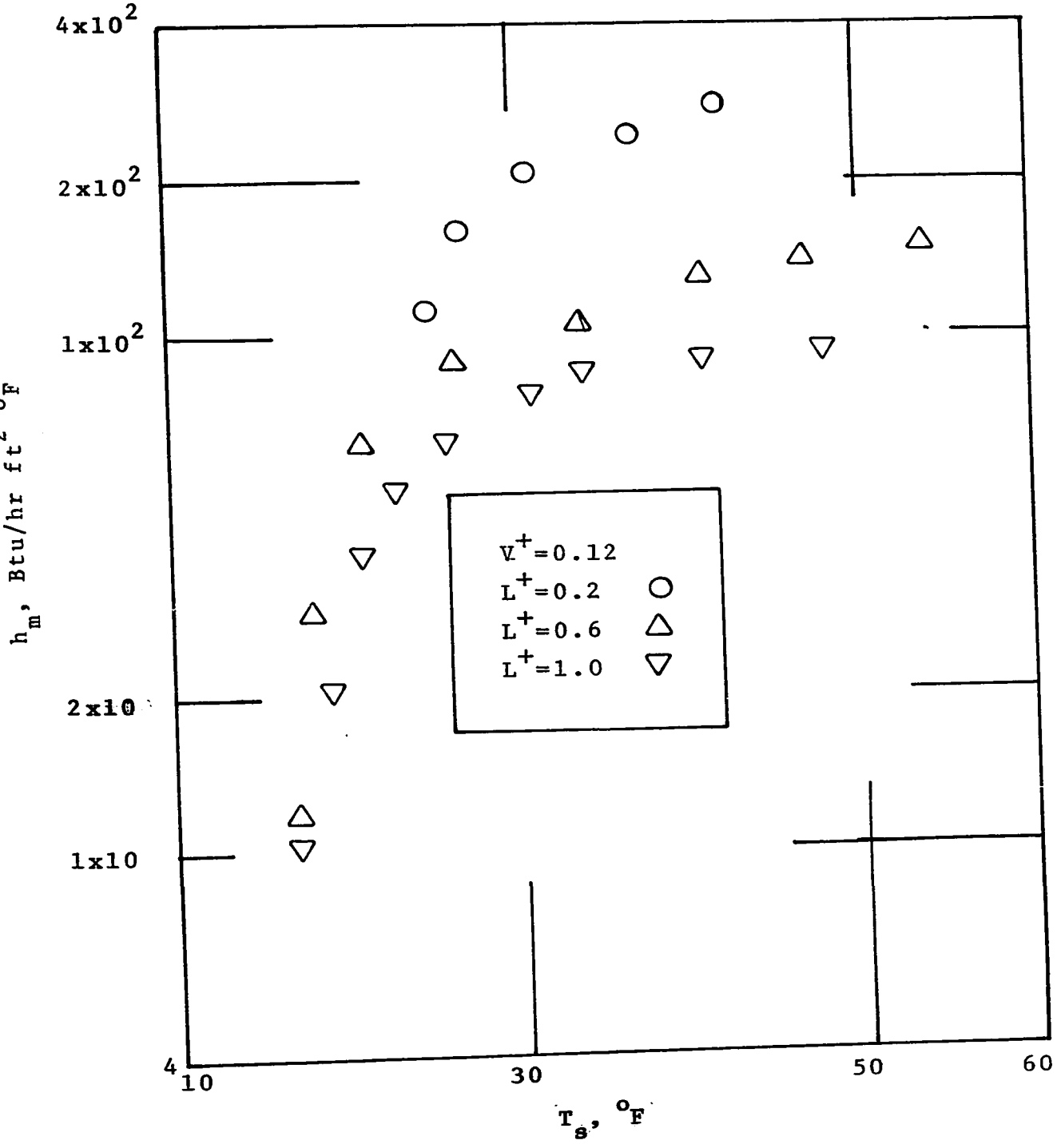

Fig. 4.9(b) Variation of maximum heat transfer coefficient with T_s for different L^+

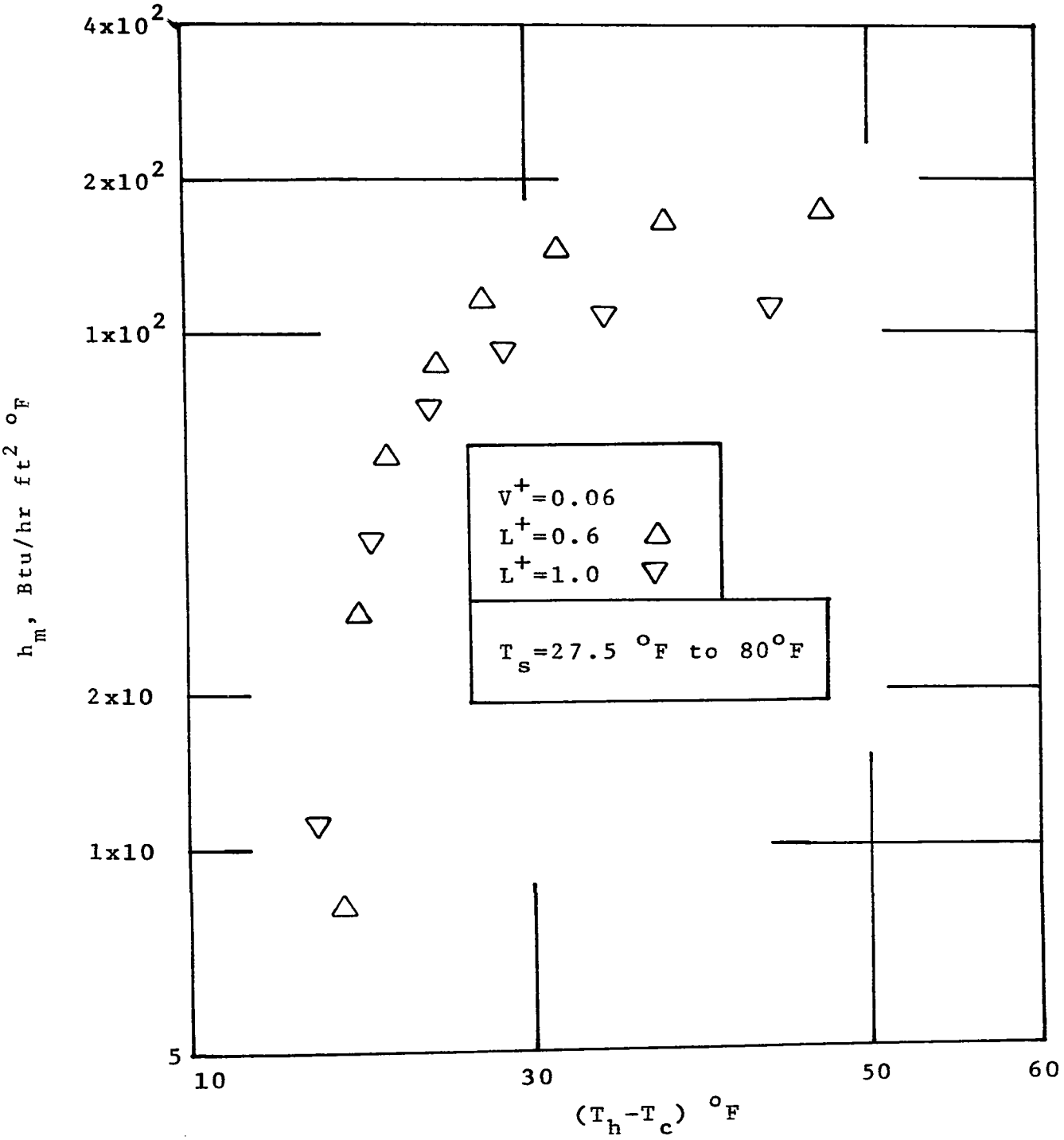

Fig. 4.10 Maximum heat transfer coefficient vs (T_h-T_c)

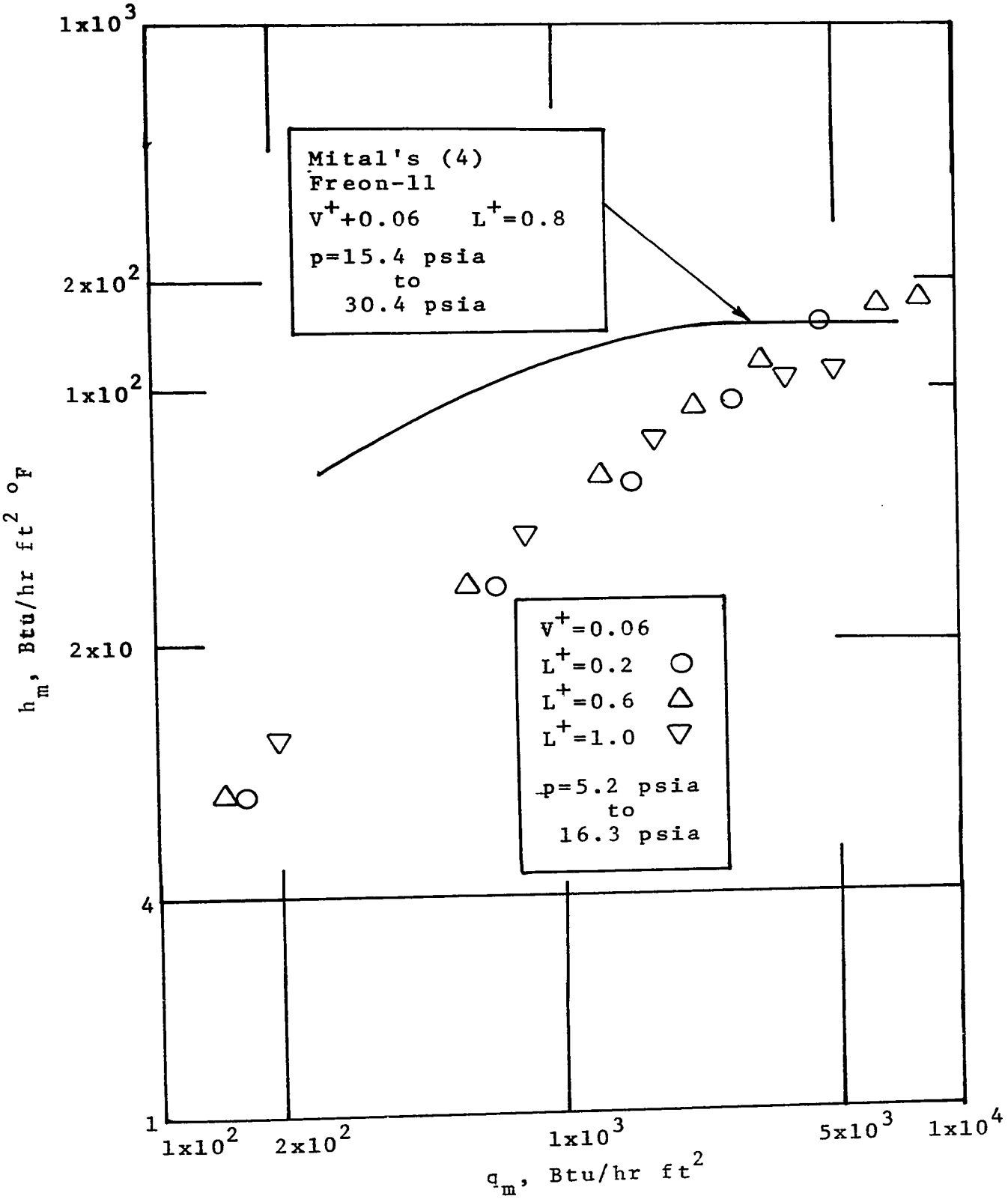

Fig. 4.11 Maximum heat transfer coefficient vs maximum heat flux

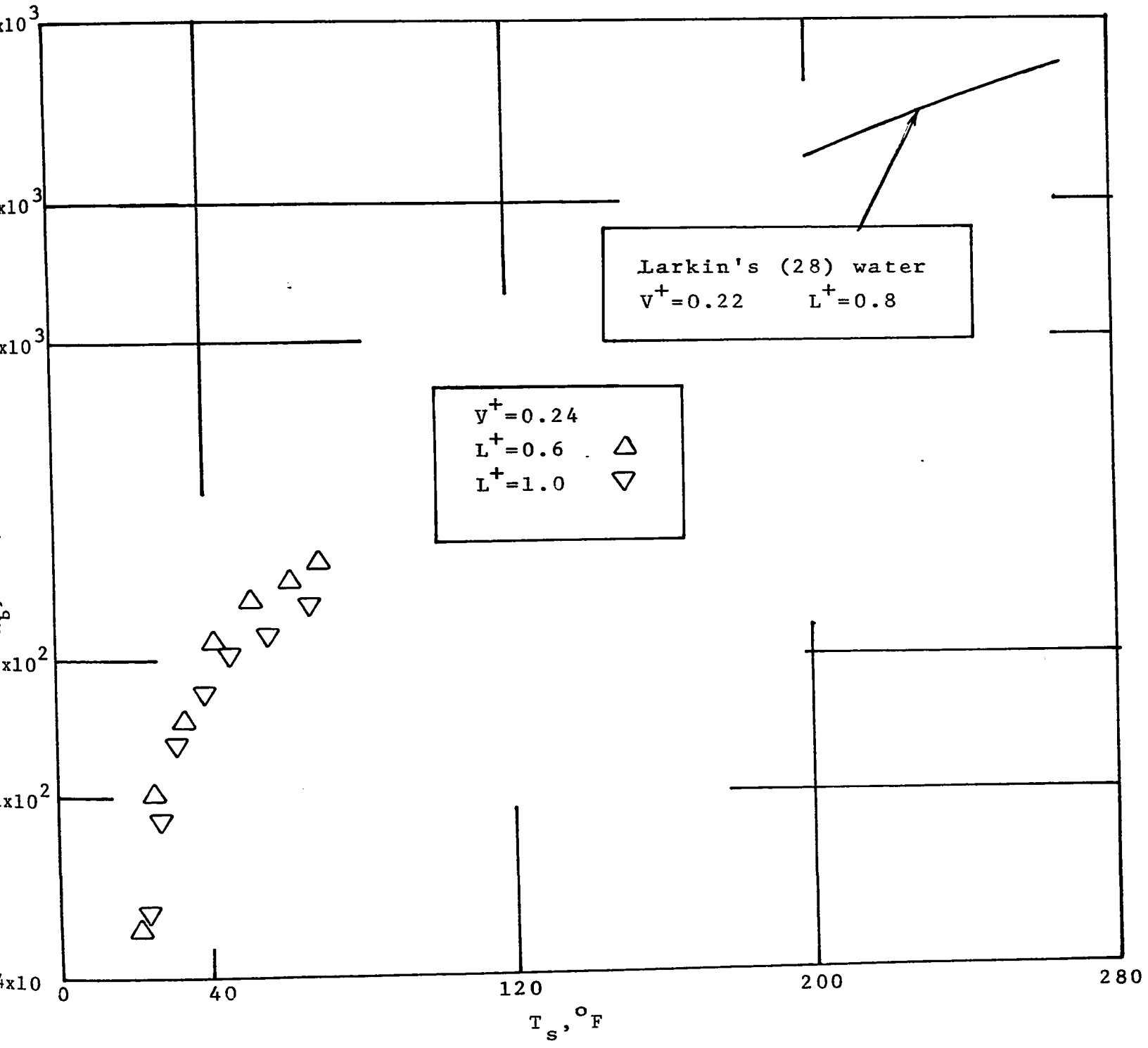

Fig. 4.12 Boiling heat transfer coefficient vs T_s

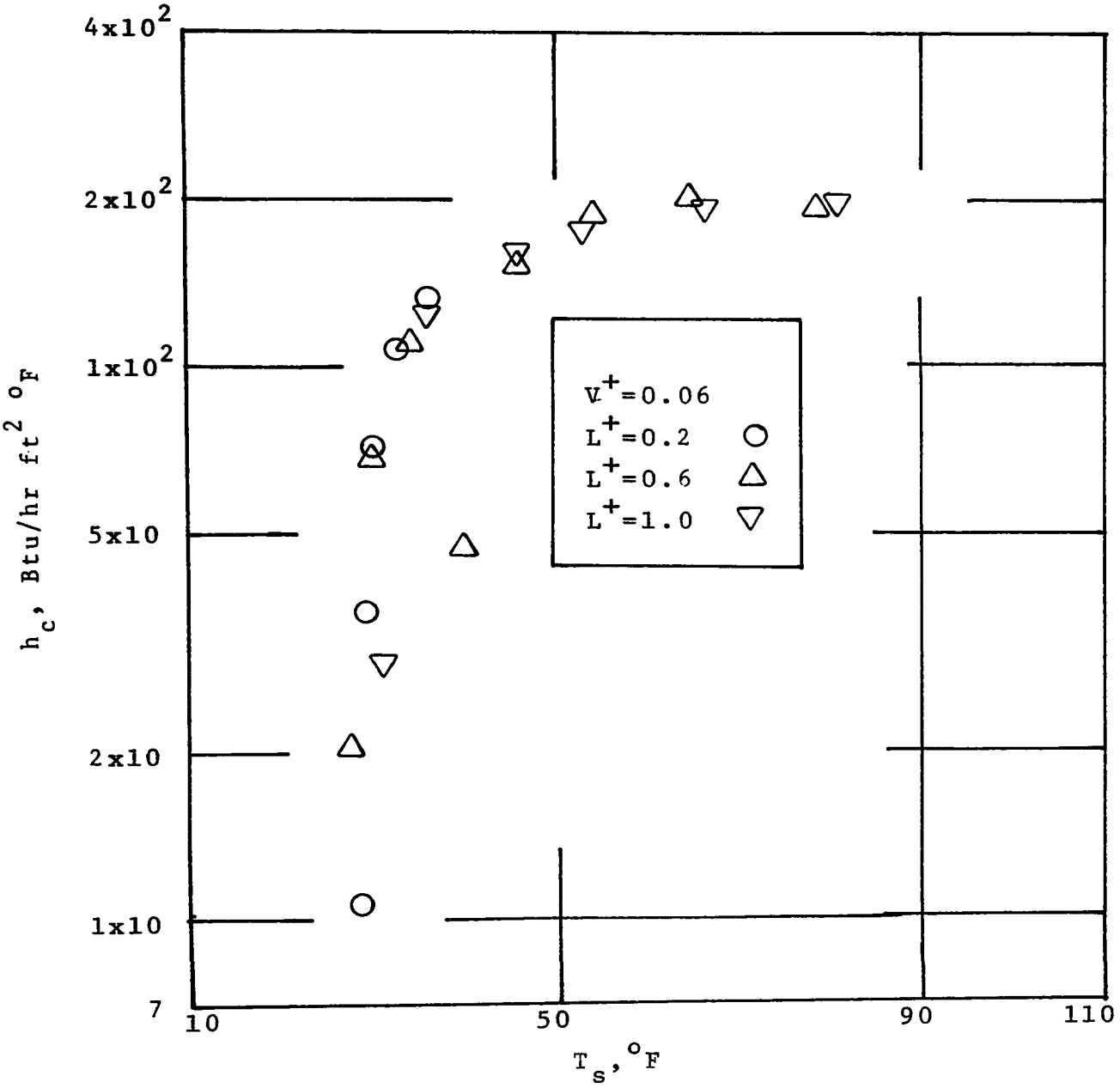

Fig. 4.13 Condensing heat transfer coefficient vs T_s

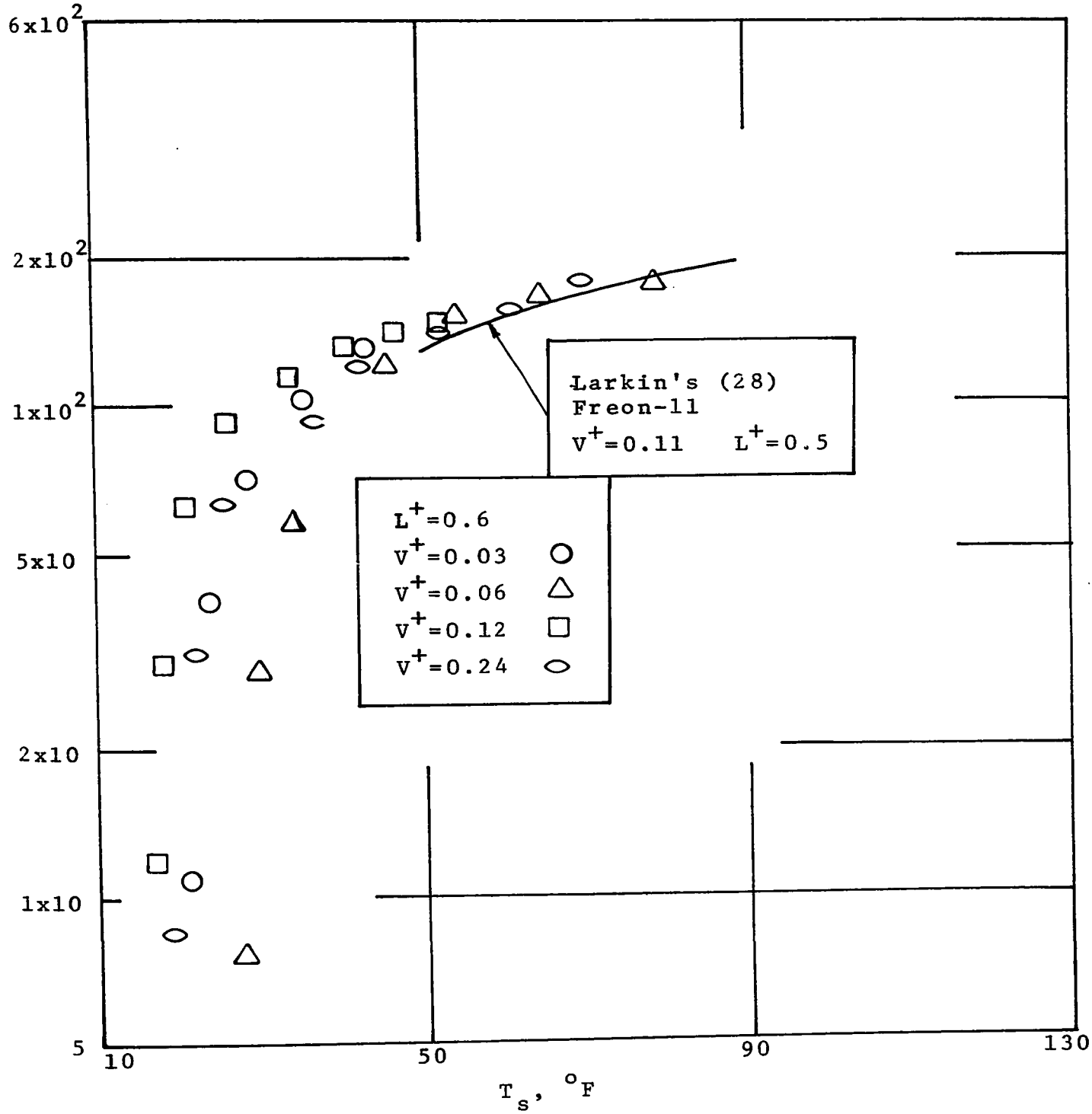

Fig. 4.14(a) Variation of maximum heat transfer coefficient with T_s for different values of V^+

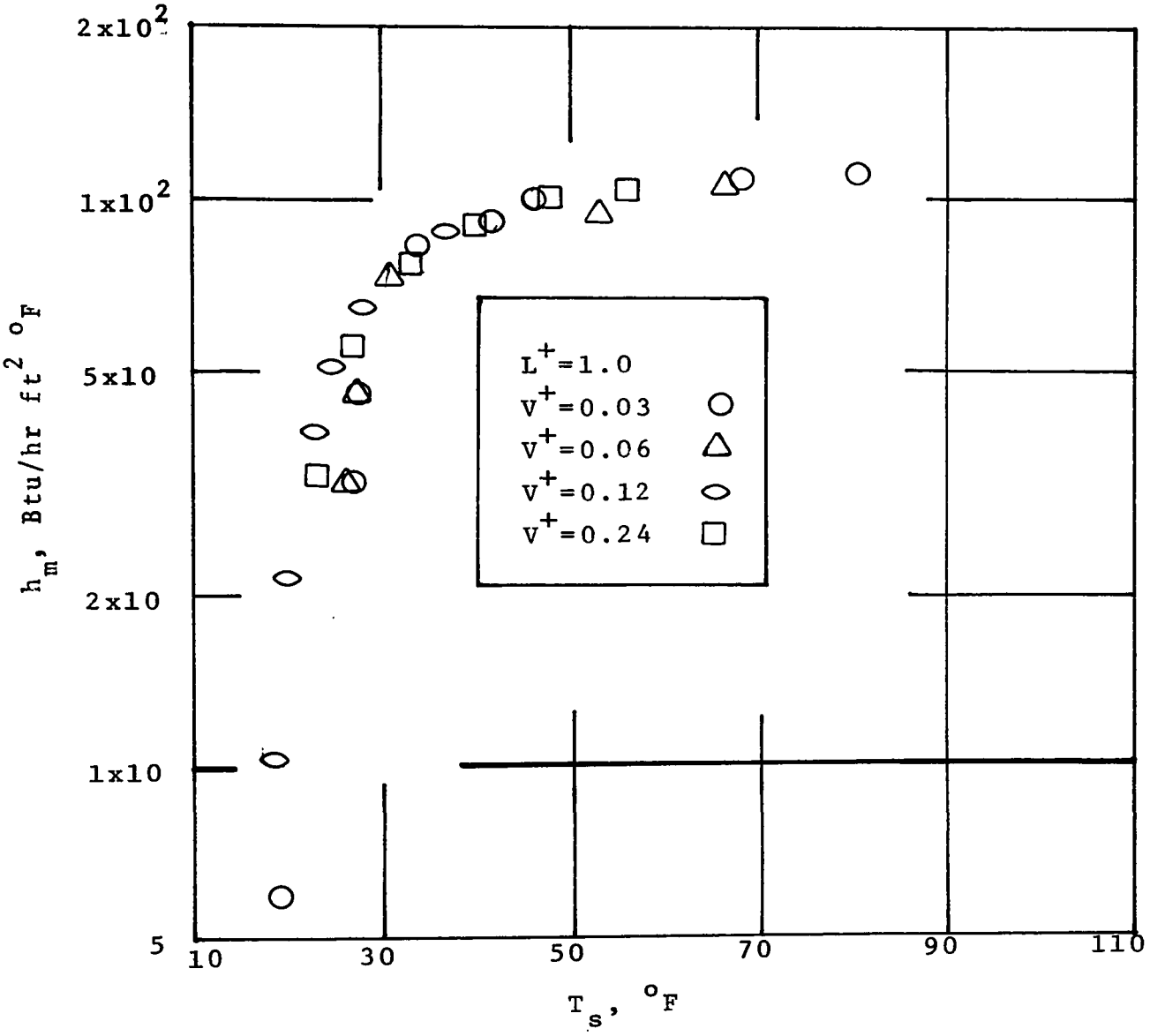

Fig. 4.14(b) Variation of maximum heat transfer coefficient with T_s for different V^+

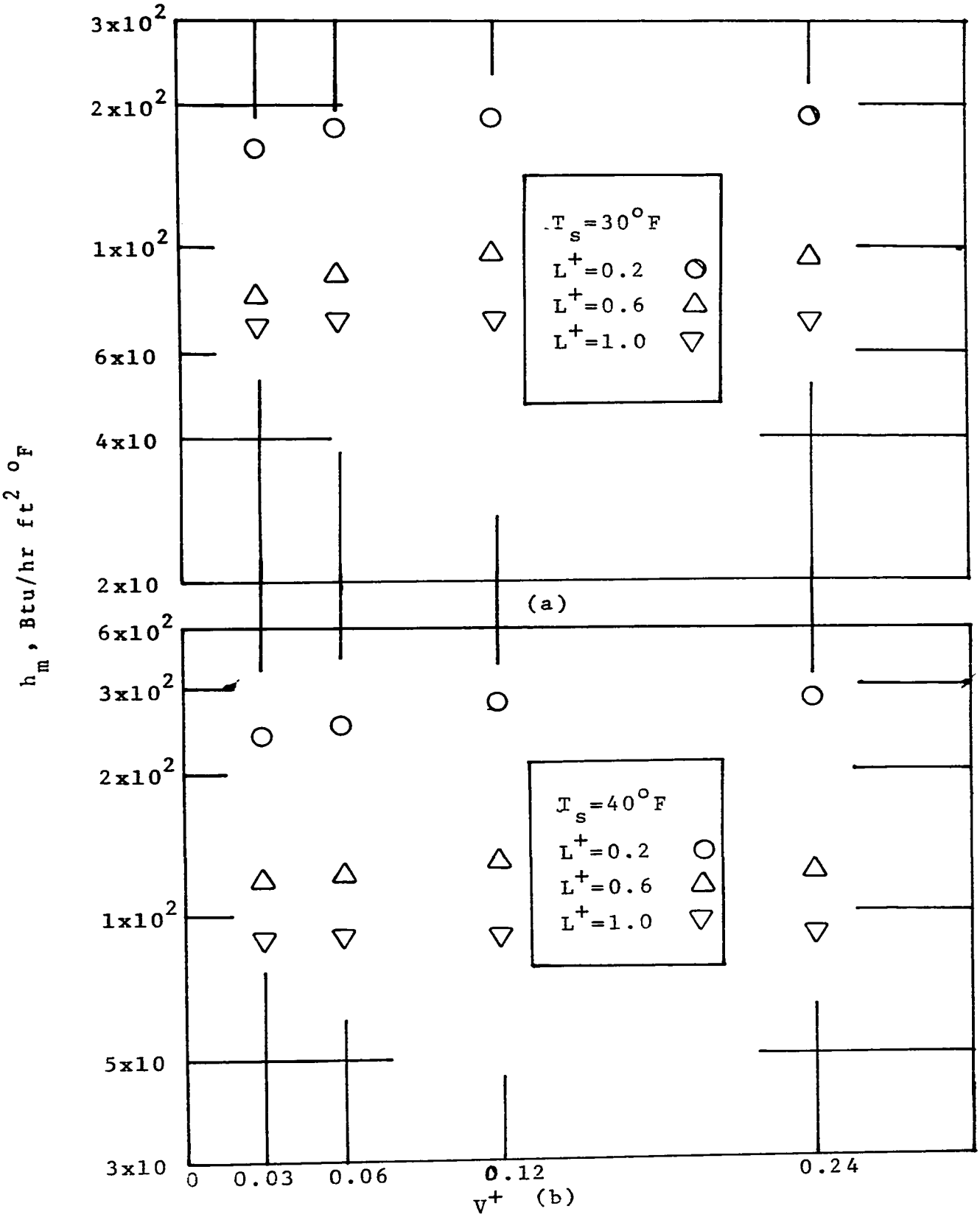

Fig. 4.15(a) and (b) Effect of V^+ on maximum heat transfer coefficient

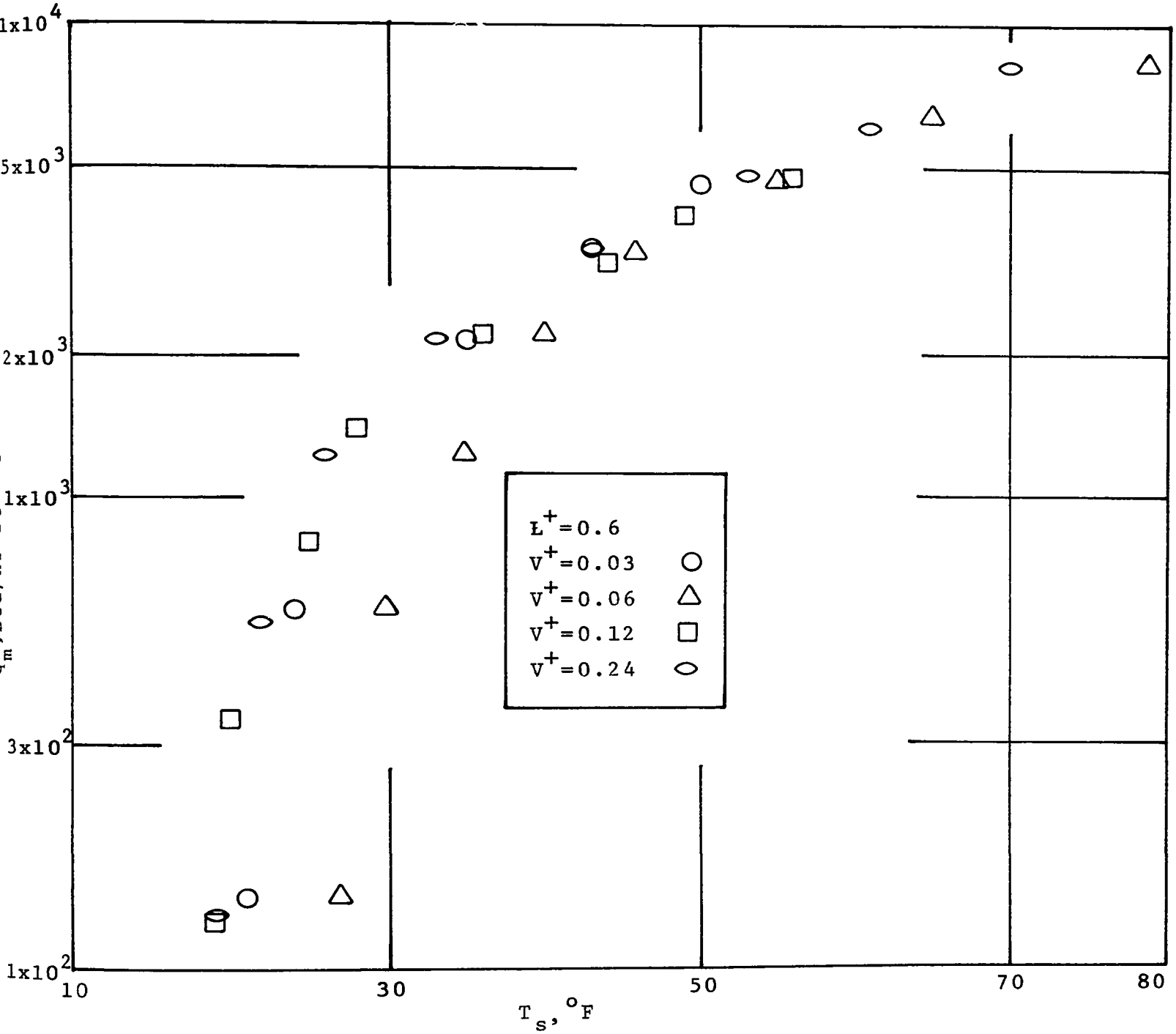

Fig. 4.16(a) Maximum heat flux vs T_s for different V^+

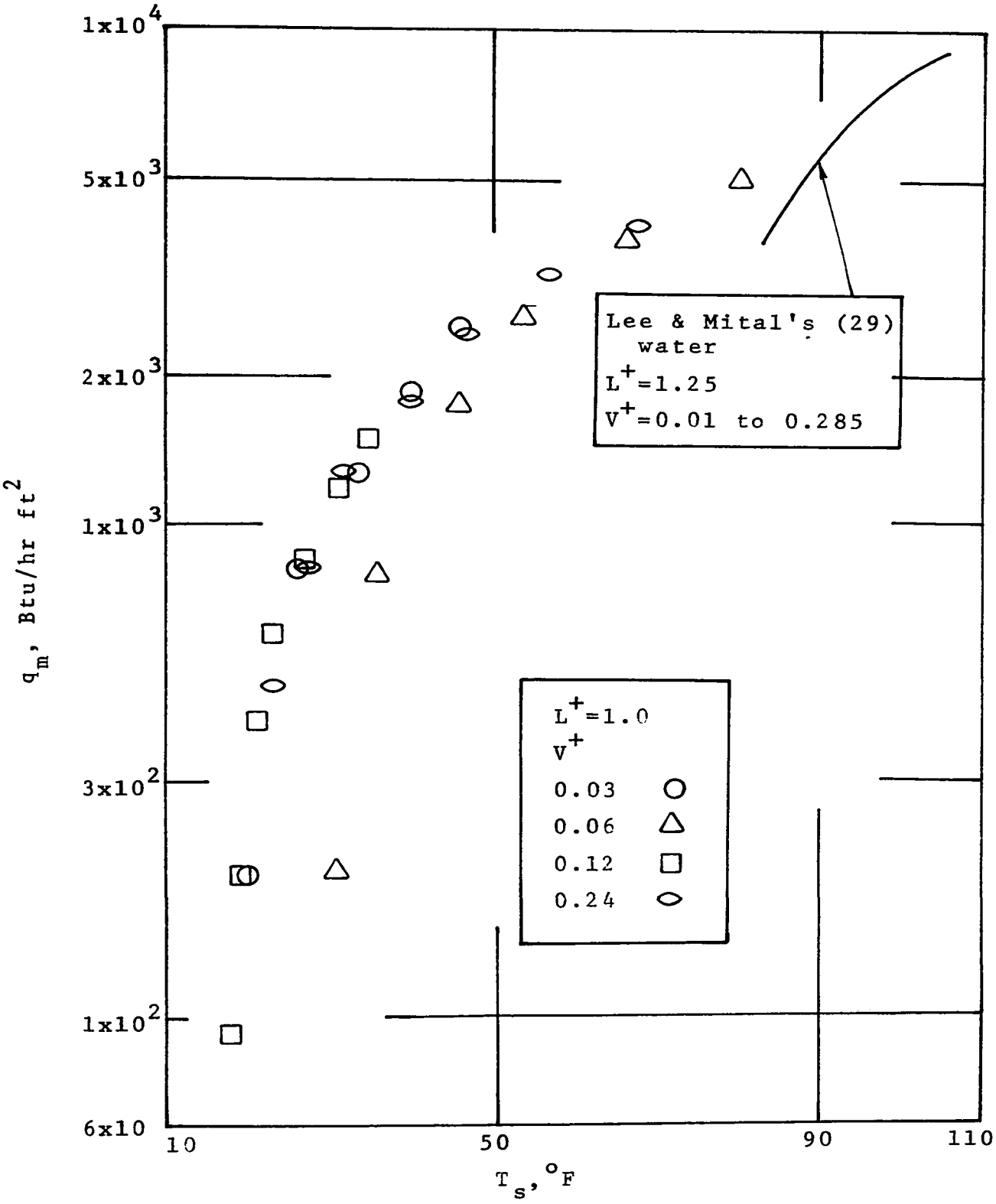

Fig. 4.16(b) Maximum heat flux vs T_s for different V^+

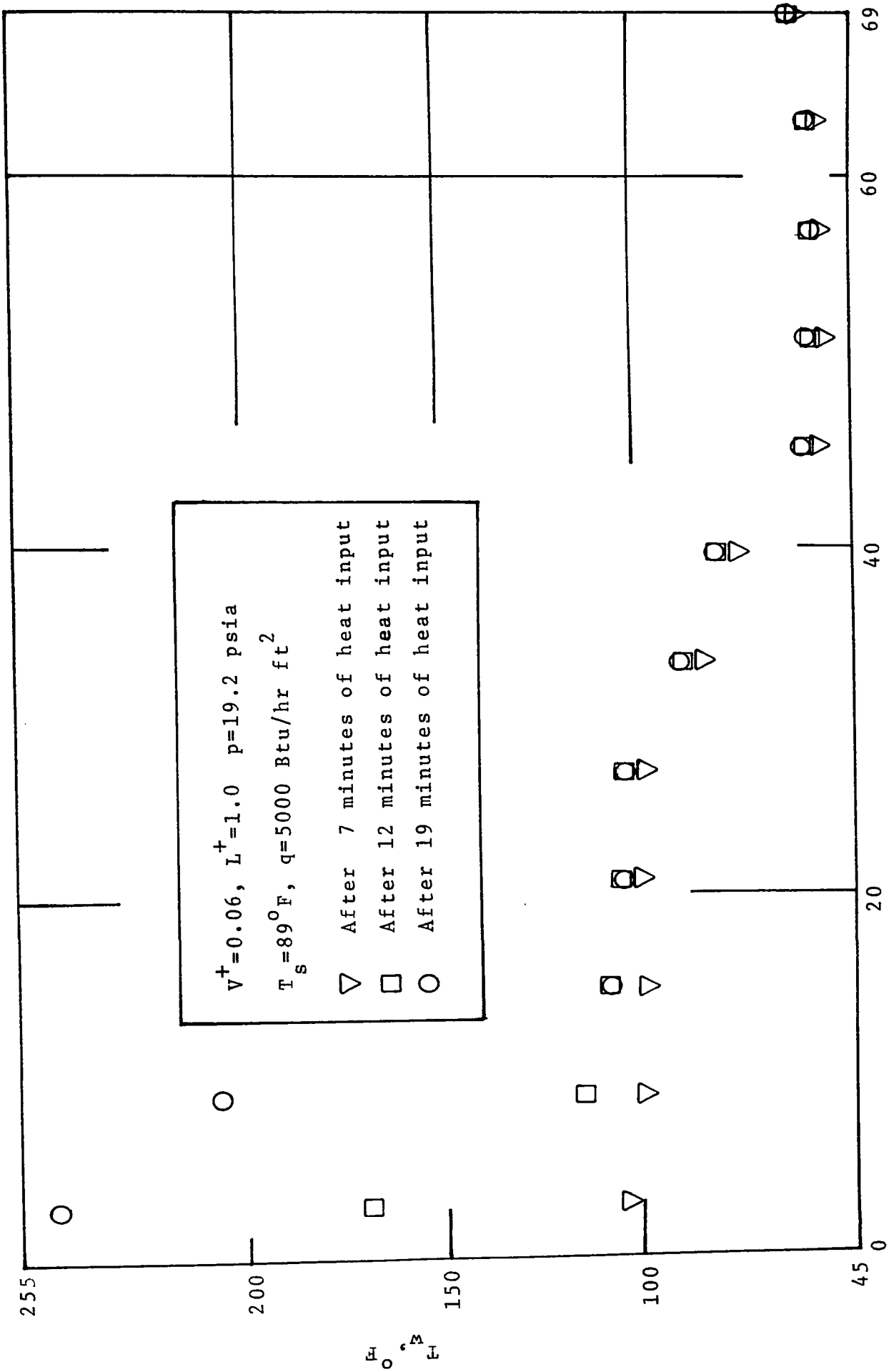

Fig. 4.17 Observation of dry-out phenomena

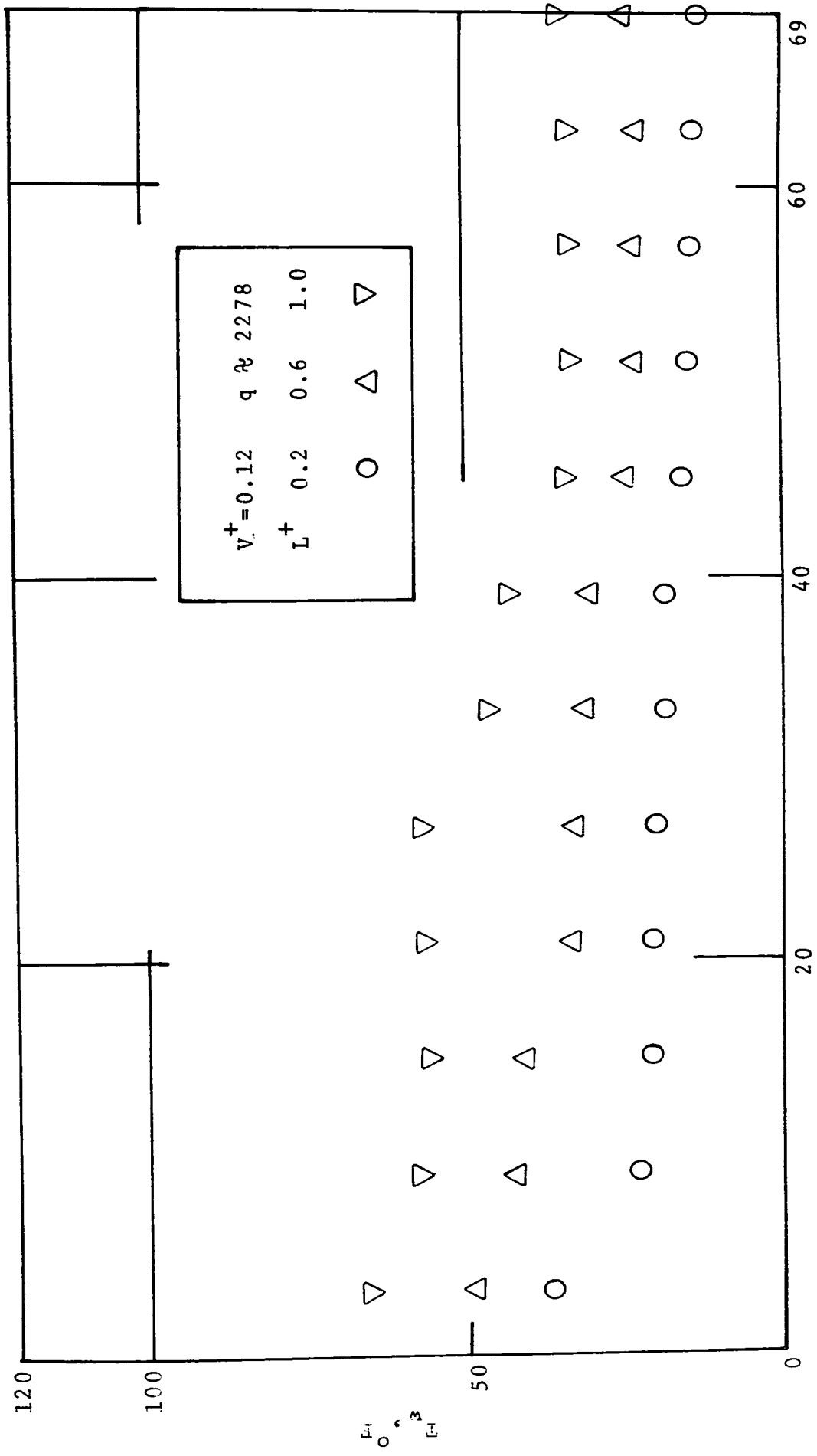

Fig. 4.18 Effect of L^+ on wall temperatures

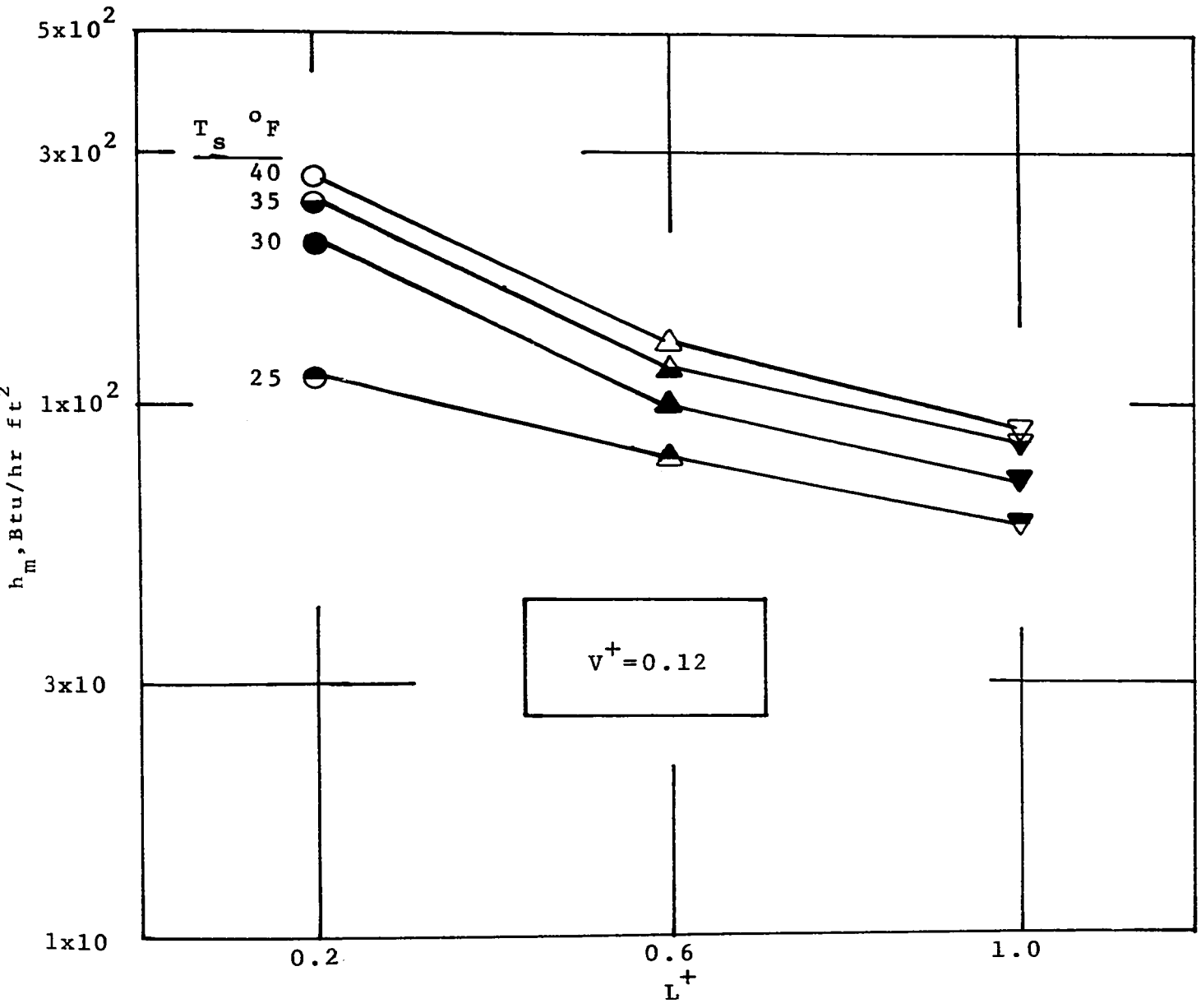

Fig. 4.19 Effect of L^+ on maximum heat transfer coefficient

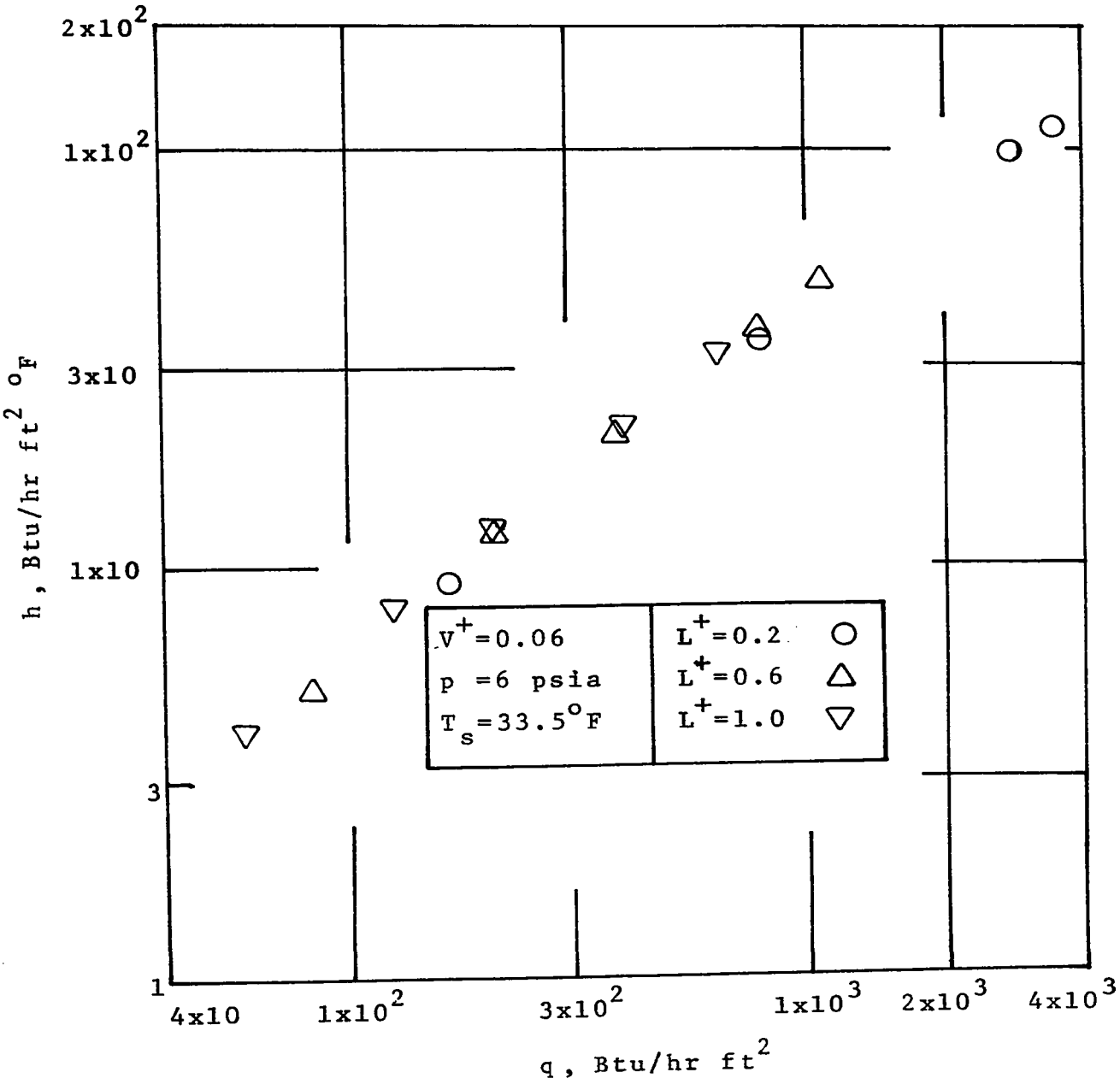

Fig. 4.20 Heat transfer coefficient vs heat flux, at constant pressure operation

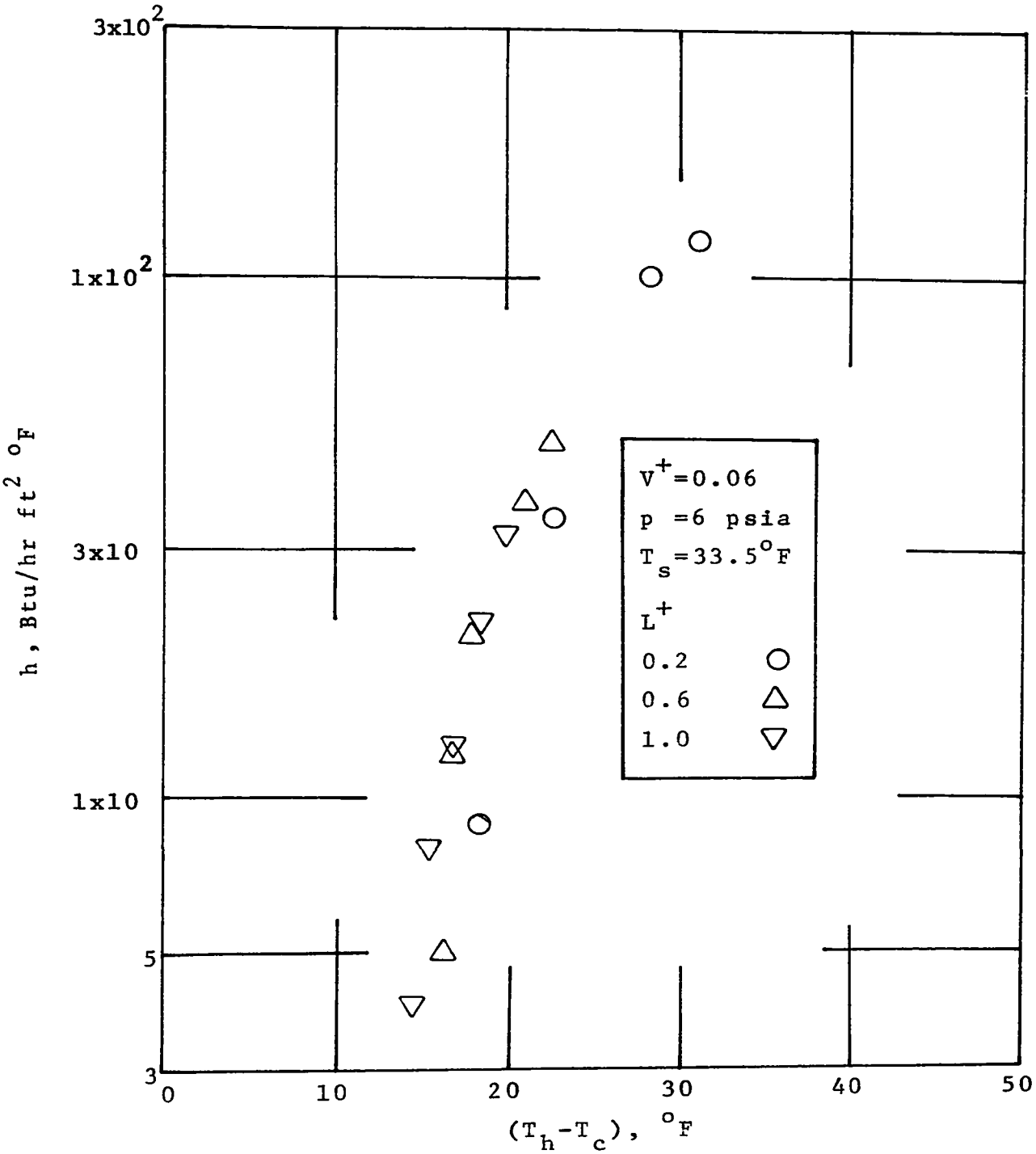

Fig. 4.21 Variation of 'h' with overall temperature differences at constant pressure operation

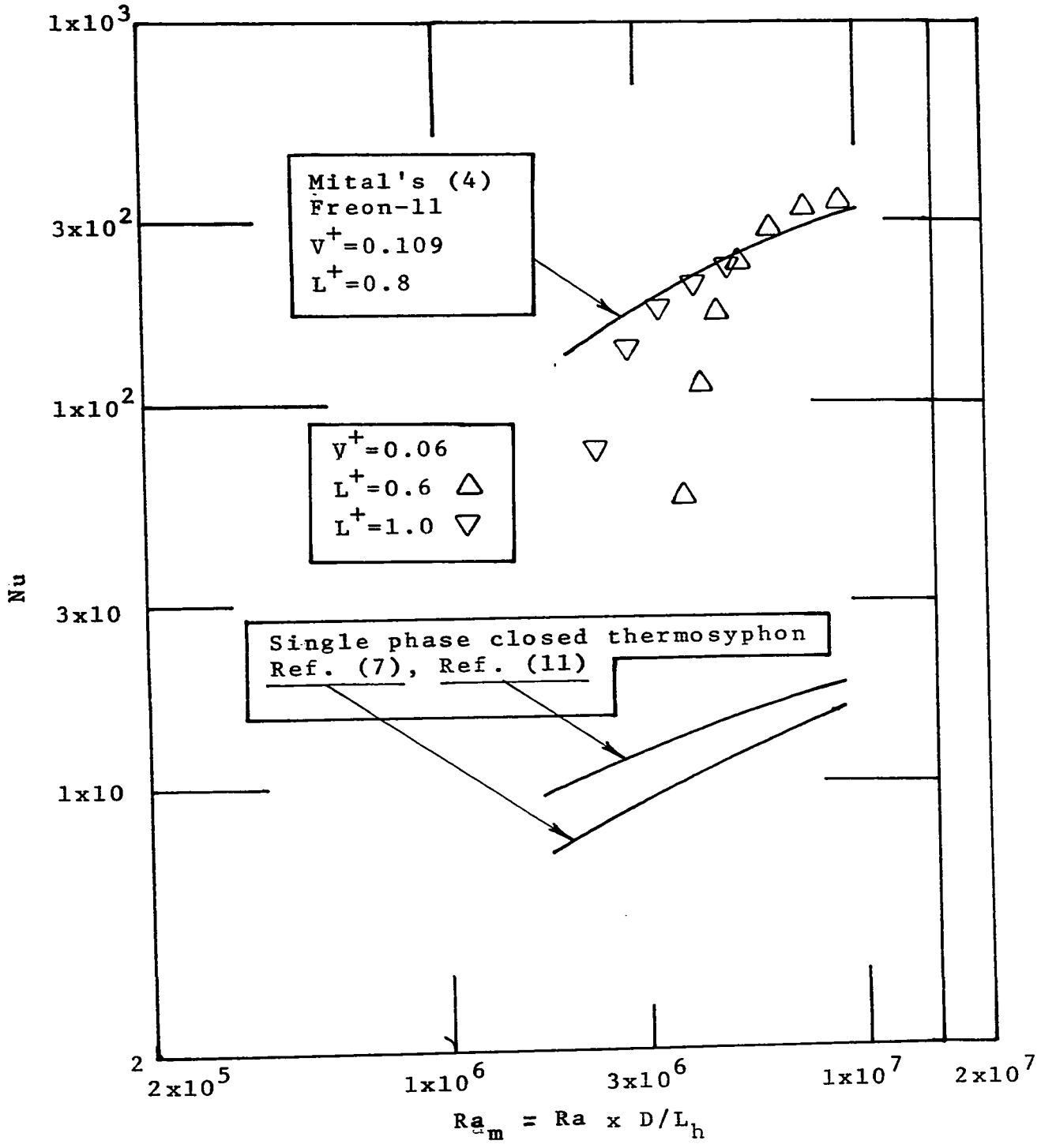

Fig. 4.22 Comparison of present experimental results of Nu vs Ra x D/L_h with those of previous investigators

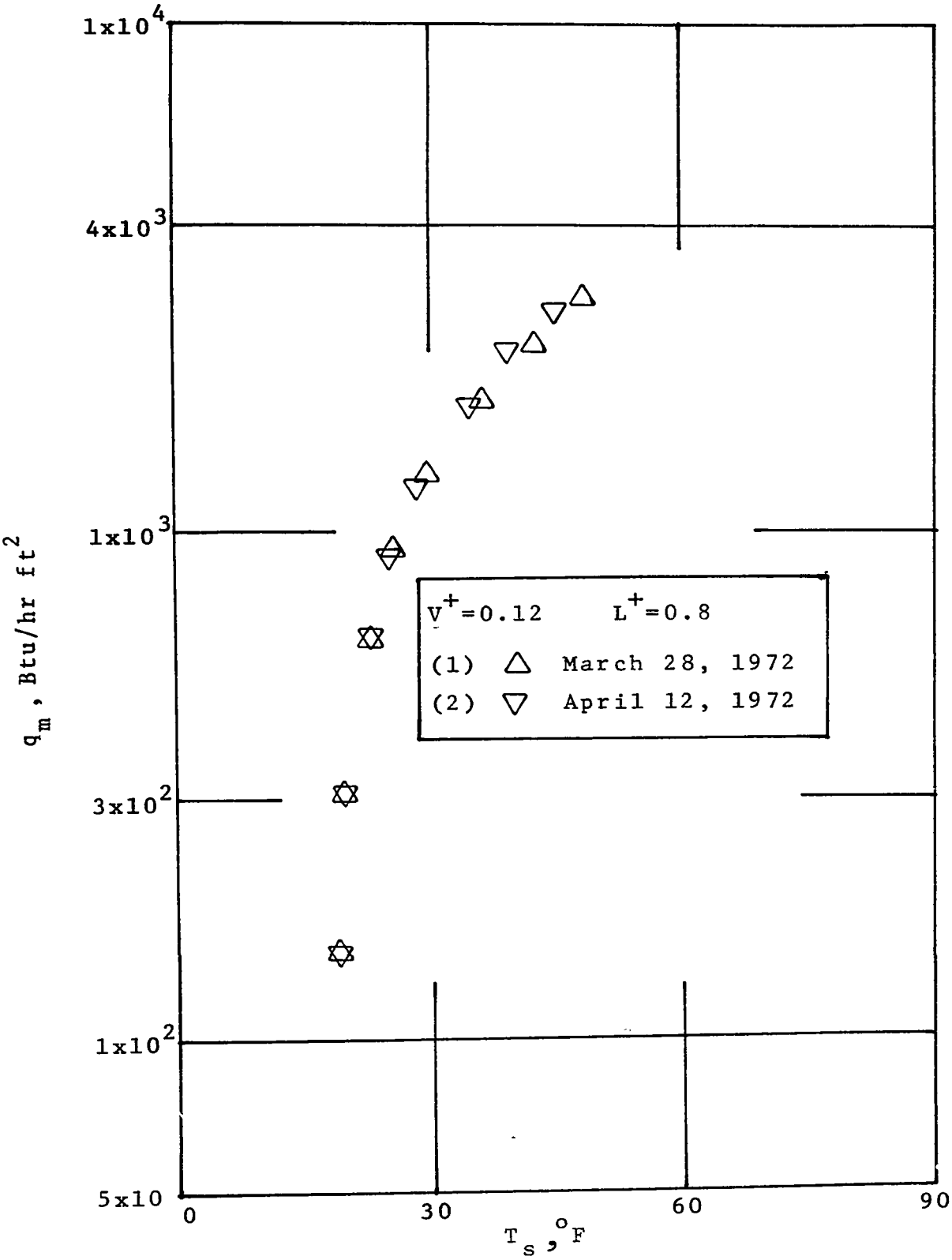

Fig. 4.23 Reproducibility test of an experimental result